वार्षिक प्रतिवेदन
Annual Report
2008-2009

भौतिक अनुसंधान प्रयोगशाला, अहमदाबाद
Physical Research Laboratory, Ahmedabad

वार्षिक रिपोर्ट

Annual Report

2008 - 2009

भौतिक अनुसंधान प्रयोगशाला, अ-मदाााद

Physical Research Laboratory, Ahmedabad

Compiled by :
The office of Dean, PRL

Published by :
Physical Research Laboratory,Ahmedabad.

Layout by :
Hari Om Computers, Ahmedabad.

Printed by :
Creative Printers Pvt. Ltd., Ahmedabad.

Council of Management

Chairman	
Professor U. R. Rao ISRO Headquarters, Bangalore	Nominee, Government of India
Members	
Dr. G. Madhavan Nair Secretary, DOS and Chairman, ISRO, Department of Space, Bangalore	Nominee, Government of India
Shri S. V. Ranganath, IAS Additional Secretary, Department of Space, Bangalore	Nominee, Government of India
Shri Sanjay S. Lalbhai Akshay, 52, Srimali Society, Navrangpura, Ahmedabad	Nominee, Ahmedabad Education Society
Shri Kartikeya V. Sarabhai Chidambaram, Usmanpura, Ahmedabad	Nominee, Karmakshetra Educational Foundation
Shri Hasmukh Adhiya The Principal Secretary, Department of Education, Government of Gujarat, Gandhinagar	Nominee, Government of Gujarat
Professor J. N. Goswami Director, Physical Research Laboratory, Ahmedabad	(Ex-Officio)
Member- Secretary	
Shri M. R. G. Murthy (April 1–June 30, 2008) Controller / Registrar, Physical Research Laboratory, Ahmedabad	(Ex-Officio)
Shri Y. M. Trivedi (July 1, 2008–March 2009) Registrar (Incharge), Physical Research Laboratory, Ahmedabad	(Ex-Officio)

Contents

Director's Foreword, Science Highlights and Events

Director's Foreword

The year 2008 was an exceptional year in the annals of the Indian Space Research Organization (ISRO) and the Physical Research Laboratory (PRL). The successful launch of the Chandrayaan-1 Mission on October 22 heralded a new era of planetary exploration backed exclusively by indigenous effort. We can now, justifiably anticipate an unprecedented growth of new science and technology in this field in the years to come.

PRL was deeply involved in the planning and execution of the scientific aspects of the Chandrayaan-1 mission from the very beginning. Additionally, PRL developed one of the payloads, the High Energy X-ray Spectrometer, flown on this mission to study transport of the volatile on the moon. PRL is now taking a leading role in analyzing data from the Chandrayaan-1 mission and is fully committed to contribute towards realizing a strong national programme on planetary exploration during the coming decade. It is both a challenge and an opportunity for PRL to ensure development of this new discipline in all its dimensions, viz, the Science, the Technology and the Human Resource.

Significant progress has been made in all the areas of research conducted at PRL that include Astronomy and Astrophysics, Solar Physics, Planetary and Geosciences, Space and Atmospheric Sciences and Theoretical Physics. Some of the salient outcomes of research done at PRL in these fields are described in the "Scientific Highlights" and additional details are also covered in this report. New activities initiated as a part of the 11th Five Year Plan period are maturing with establishment of several sophisticated experimental facilities such as the Nano-SIMS (Secondary Ion Mass Spectrometer), a Differential Absorption LIDAR (LIght Detection And Ranging System) and a Stable Isotope Mass Spectrometer for a Department of Science and Technology sponsored National Programme with more than a dozen participating institutes. Significant progress towards the realization of the Multi-Application Solar Telescope (MAST) at the Udaipur Solar Observatory, installation of a large area infrared detector at the Mt. Abu observatory and development of PARAS, an Echelle spectrograph based instrument for detection of exoplanets, was made during the year.

Efforts to induct new faculty members to strengthen various divisions and also add new areas of research are continuing. New programmes in X-ray astronomy and middle atmospheric studies with ground-based, rocket- and balloon-

borne instruments have been initiated. Plans are also underway to develop new facilities for the design and development of instruments for planetary, atmospheric and astronomy experiments using space platforms. These will offer scientifically exciting and technologically challenging avenues to PRL faculty and research scholars in the coming years.

The current faculty strength at PRL is over sixty and the number of research scholars and post-doctoral fellows has reached a healthy number of about eighty. Efforts are on to increase these numbers in the coming years. The strength of technical, administrative and other auxiliary personnel remained steady at around 220 and a significant increase in the number of project based appointments was achieved. Research during the last year resulted in more than 130 publications in peer reviewed journals, with close to hundred in high impact journals. Eight research scholars submitted their theses during the year. A good number of PRL faculty members have been invited to edit monographs, national science reports and write invited review articles.

Faculty members and research scholars of PRL received several national and international recognitions during the year for their scientific contributions in various fields. It is a matter of pride that Prof. G. S. Agarwal, past Director of PRL (1995-2005), was conferred the prestigious Fellowship of the Royal Society (FRS) in 2008 for his pioneering work in Quantum Optics. Other recognitions received by current PRL faculty include honorary fellowship of the Royal Astronomical Society of London, Fellowship of the Indian Academy of Sciences, National Academy of Sciences and Indian Geophysical Union; Ramanujan Fellowship; Special citation as lead authors for contributions to report on climate change leading to the Nobel Prize for IPCC and Editorial Board members of International journals. Several younger scientists and research scholars have also been recognized for their work and are recipient of Young Associateship of Academy and of COSPAR best paper and ASI best thesis awards. I sincerely hope that this trend will continue and PRL will make credible impact in the scientific scene both at the national and international levels in the coming years.

Several National workshops were held during the current year and PRL continued its Human Resource Development activities with specialized programmes for school students, college and M.Sc. students and training programme for engineering graduates. Over hundred such students benefited during the year from various programmes conducted at PRL. Guided visits to PRL and interactions with research scholars and faculty have now become a regular event of for school students from Ahmedabad and nearby areas. The Science Day celebrations were broadened by conducting advance lectures, tests and quizzes at five zones of Gujarat, followed by a gathering at PRL of about a hundred selected students from these zones. Five of the students were awarded scholarships based on their performance in various scientific activities and incentive awards were also given to a dozen more deserving students. The in-house journal "PRL News" continues to cover both the scientific and other extra-curricular activities taking place at PRL. Several steps were also introduced to accelerate the progressive use of Hindi in both administrative and other spheres in the laboratory.

The regular colloquium series and divisional seminars have seen participation of over twenty five prominent academicians from within the country and from abroad. Some of them have spent extended periods and had interactions with faculty and research scholars, these include, Prof. G. S. Agarwal, Prof. D. Lal, Prof. Tom Gehrels and Prof. K. I. Oyama. Prof. S. Pakvasa, visited PRL as Ramanathan Professor.

PRL administers the ISRO-RESPOND programme in Space Sciences and additionally serves as the nodal centre for the implementation of ISRO's Planetary Science and Exploration (PLANEX) and ISRO GBP programmes. Under these programmes, a large number of research scientists and teachers from various institutions and universities across the country are provided with research grants. The PLANEX group at PRL is also mandated to set up a National Facility for the analysis of planetary materials. The facility became operational during the year with the installation and qualification of three state of the art instruments. The PLANEX group also conducts thematic summer programmes and workshops in Planetary Sciences for research scholars and scientists in a sustained manner.

Several infrastructure and renovation projects were completed. The new additions included a Hostel-cum-guest house, a cafeteria and transit accommodation complex in the Thaltej campus of PRL. An exclusive facility for design and development of scientific Instruments for space platform should be ready by the end of 2010 in this campus. Plans for new infrastructure facilities for housing the Multi Application Solar Telescope at the island site in

Udaipur is nearing finalization. With these developments, we anticipate significant advancement in research activities in the coming years.

The scientific achievements elaborated in this report have been possible due to the dedication and hard work of all the members of PRL and I place on record my deepest appreciation of their sincerity and devotion. We are midway through the 11th Five Year Plan and we have to strive hard to ensure that we deliver science at the highest level that will justify the continued investment and faith reposed in us. Dedication, hard work and sincere efforts from all members of PRL will be needed for this. I request all PRL members to work in a cohesive and synergistic manner so that PRL continues to enhance its pre-eminence both at the national and international level.

Finally, I express my deep sense of gratitude to the PRL Council of Management for their wise advice, counsel and unstinting support.

J. N. Goswami
Director

Science Highlights

Astronomy and Astrophysics

- A detailed near Infrared spectroscopic study of Nova V1280 Sco has revealed that presence of spectral lines of low ionization species like NaI and MgI are markers of low temperature regions which are conducive for dust formation. The study also indicates that mass loss in a nova can begin before peak brightness is reached and can be sustained for a considerable time after the peak.
- Thermal emission in solar flares derived from SOXS X-ray spectra is in agreement with a model of evolving multi-temperature plasma governed by thermal conduction cooling. In five M class flares the emission in 6-20 KeV range was dominated by flare plasma at temperatures of 15-50 million Kelvin, while mean thermal conduction cooling time was ~1400s.
- Optical polarimetric studies of Comet NEAT C/2001 Q4 at different wavelengths and at different solar phase angles and cometocentric distances in the direction of the tail reveal that the comet could have a grain composition comprising a mixture of both silicates and organics.
- A multi-wavelength study of the solar wind disappearance event of 11th May 1999 has traced the origin of such a disappearance to a coronal hole adjacent to a large active region on the Sun. The study provided clear evidence for Sun-Earth connection via an evolving coronal hole close to an active region in the absence of coronal mass ejections.
- A study of stellar wind of a few High Mass X-ray Binary pulsars in elliptical orbits from RXTE and Beppo-SAX X-ray satellites shows a variation of absorption column density and iron line flux dependence on orbital phase. This is suggestive of clumpy stellar winds rather than a smooth symmetric stellar wind.

Solar Physics

- Detailed design review for the 50 cm aperture Multi Application Solar Telescope (MAST) was completed during June, 2008.
- The 3D evolution of a filament disappearance event, jointly observed by USO H-alpha telescope, STEREO,

THEMIS and GONG, showed plasma motions along twisted flux rope, followed by oscillations of fine structures of the filament and the eventual disappearance of the filament.

- The first study involving successful application of reconstruction techniques to the SECCHI/STEREO data for the estimation of true speed and direction of propagation of a CME suggest significant underestimations of the CME speeds in earlier studies based on single space - craft data.

- Supersonic down-flows in a sunspot light bridge are identified using measurements taken with the spectro-polarimeter on board the HINODE satellite.

- A combination of EUV images from TRACE and hard X-ray images from RHESSI were used to detect evidence for reconnection during an M-class flare near the solar limb.

- A Graphical User Interface for controlling the proto-type adaptive optics system has been developed in-house at USO.

Planetary and Geosciences

Planetary Sciences

- The High Energy X-ray spectrometer (HEX) was delivered for integration with the Chandrayaan-1 spacecraft. Post launch health checks indicated satisfactory performance. HEX will provide information on the volatiles transport on the lunar surface.

- A robust value for the solar system initial (SSI) $^{60}Fe/^{56}Fe$ has been obtained from a study of the records of the now-extinct nulcides ^{60}Fe and ^{26}Al in meteoritic chondrules; the ^{26}Al data provide the time of formation of the chondrules, relative to the first solar system solids. The inferred value of $(7\pm1)\times10^{-7}$ for SSI $^{60}Fe/^{56}Fe$ suggests a high mass ($\sim$30 solar mass) supernova as the most plausible source of this and several other short-lived nuclides, including ^{26}Al present in the early solar system.

- Moon Impact Probe (MIP) images from Chandrayaan-1 were used to identify the path it traversed before its impact point near the South pole.

- The largest chondritic meteorite fall ever in India occurred recently at Sulagiri, Krishnagiri district of Tamil Nadu on September 12, 2008. Studies of chemical composition and petrography of this meteorite revealed this to be an LL-6 chondrite.

Geosciences

- A comprehensive one-year record of atmospheric chemical constituents of $PM_{2.5}$ (fine mode aerosols) from a high-altitude site (Mt. Abu) revealed that water-soluble inorganic constituents vary from 1.0 to 19.5 $\mu g\ m^{-3}$ over the annual seasonal cycle with dominant contribution from SO_4^{2-}, NH_4^+ and HCO_3^-. A two fold increase in the abundances of SO_4^{2-} and NH_4^+ and their co-variability during winter, relative to high-dust conditions in summer, suggest dominance of anthropogenic sources and long-range transport of combustion products (biomass burning and fossil-fuel emissions) from northern India. The chemical data set also suggests near quantitative neutralization of acidic species (NO_3^- and SO_4^{2-}) by NH_4^+ in $PM_{2.5}$

- Using thermo-optical EC-OC analyzer, an analytical approach for the determination of absorption coefficient (b_{abs}, μm^{-1}) and mass absorption efficiency (σ_{abs}, m^2g^{-1}) of elemental carbon (EC) in aerosol samples has been proposed. The measured b_{abs} shows a strong linear dependence on thermal EC concentration ($R^2 = 0.75$, $n = 65$) indicating the validity of Beer-Lambert's law and hence facilitating determination of mass absorption efficiency.

- Monte Carlo simulation based calculations on radiation transport in natural mineral enabled estimation of beta particle ranges and led to a new proposition for the use of interior portion of large grains in sediments to extend their dating range. Studies on Al_2O_3:C, a phosphor proposed for space dosimetry, indicated a LET dependent OSL decay that was explained on the basis of the components of OSL decay and their saturation dose.

- Sr and Nd isotope composition of sediment samples from the Ganga Plain indicate two major excursions at $\sim$20 ka and $\sim$70 ka ago. These were attributed to decrease in contribution of sediments from the Higher Himalaya resulting from a decrease in monsoon precipitation and an increase in glacial cover. This study highlights the role of climate on erosion of

Himalaya over the past 100 ka.

- Teak trees from southern India were analyzed for their oxygen isotope variations. Tress receiving only southwest monsoon (e.g. at Jagdalpur) behaved differently from those, which received both the southwest and northeast monsoons (e.g. at Perambikkulam). Intra-annual and inter-annual oxygen isotopic variations reveal that monsoon rainfall could be reconstructed with at least 20 days resolution.

- Algal blooms transfer carbon from the atmosphere to the deep sea. The detailed study of one such spring bloom of *Noctiluca* from the northeastern Arabian Sea indicated four-fold enhancement in carbon transfer.

- A DST and PRL Sponsored multi-institutional collaborative research programme for Isotope Fingerprints of Indian Water Sources is now operational, with PRL as nodal agency. A state-of-the-art stable isotope ratio mass spectrometer laboratory is set up. Initial results suggest that oxygen and hydrogen isotopic composition of rain depends on the atmospheric moisture, and rainout processes.

Space and Atmospheric Sciences

- Effects due to the contrasting vertical (downward over Arabian Sea & upward over Bay of Bengal) transport of ozone and aerosol were inferred during pre-monsoon period across the peninsular Indian region.

- Investigation on source specific aerosol radiative forcing revealed that it is primarily governed by aerosol optical and radiative properties rather than their mass concentration.

- The effect of dust associated with the dust-storm in the Martian atmosphere is shown to considerably reduce the hydrated ion concentration up to a height of 40 km.

- Evidence for the enhancement in total electron content due to the plasma structure was obtained using optical and radio techniques. This is consistent with the prediction based on the model of equatorial spread-F.

- The bond angles and the structures of ionic fragments of methanol were determined using ion momentum spectrometer. A mechanism for the formation of the detected H_2^+ and H_3^+ ions from methanol is proposed.

Theoretical Physics

- Studies of various aspects of seesaw mechanism responsible for generating small neutrino masses, including texture zeros and renormalization group evolution of neutrino masses and mixing have been performed. These provided new insights, particularly in the scenario in which the mixing angle θ_{13}, experimentally known to be small, is radiatively generated.

- The possibility of simultaneously understanding large neutrino mixing and small quark mixing from a "mu-tau" symmetry in a model based on SO(10) gauge group is demonstrated. An interesting prediction of such a model is small CP violation in neutrino oscillations.

- The potential of large-mass liquid Argon detectors for determination of the neutrino mass hierarchy through interactions of atmospheric neutrinos was examined. A detailed analysis shows that a 100 kT magnetized detector has superior capabilities for hierarchy resolution compared to an un-magnetized detector.

- A theory to understand the observed neutrino masses and simultaneously explain the baryon asymmetry of the universe was proposed. An interesting feature of this approach is the low scale of lepton number violation, and hence, the model is testable in the next generation accelerators like the LHC. The model also predicts a stable scalar particle that could be the candidate for dark matter.

- The neutrino dark energy proposal was implemented in a left-right symmetric model with the special feature that it can be embedded into a grand unified theory.

- A novel interpretation has been given for the narrow resonance, recently discovered at Fermilab in the decay of the B meson. It is suggested that it is an exotic hybrid charmonium state, i.e., a meson with a glue component, with quantum numbers that can be tested by experiments in the near future.

- A new random matrix ensemble viz. the embedded Gaussian unitary ensemble with a non-trivial group symmetry has been proposed and analyzed. This was generated by random two-body interactions possessing spin-iso-spin super-multiplet symmetry relevant for atomic nuclei.
- The design of a compact and portable waveguide laser resonator with a quasi-Gaussian output is proposed. The resonator is closed at each end with mirrors of step-index reflectivity profiles, and is easy to fabricate even for semiconductor integrated optics technology where plane mirrors can be mimicked by cleaved facets.
- Results obtained from intensity correlation experiments for a randomized optical vortex as well as for a plane laser beam suggest that the intensity auto-correlation for an optical vortex decreases faster than that for a plane laser beam.
- A new method for determining parameters of a nonlinear dynamical system from chaotic time series data has been devised. In addition to eliminating problems of earlier methods this method is more accurate and can work in the presence of noise.

Human Resource Development

Staff Structure

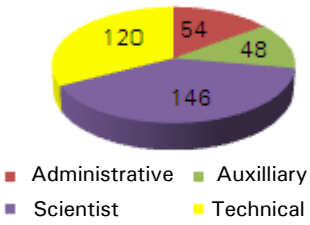

Training Programmes

Administrative and Allied Services Trainees

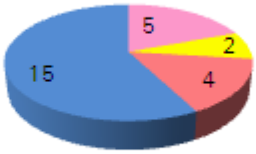

Doctoral, Post Doctoral and Other Programmes

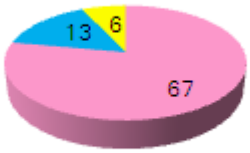

Technical Programmes

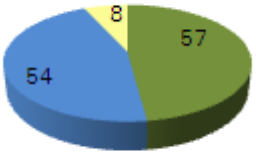

Scientific Publications

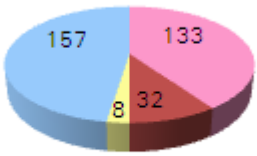

Distinguished Visitors / Colloquia

Dr. Anand Narayan
Pennsylvania State University,USA
The Origins & Evolution of week Low Ionization Quasar Absorption Systems

Dr. Ajit Kembhavi
Inter University Centre for Astronomy and Astrophysics,Pune
Super Massive Black Holes - Here, There and Everywhere

Dr. Uday B. Desai
SPANN Lab, Department of Electrical Engineering, IIT, Bombay
Wireless Sensor Networks: SenSlide and AgriSens

Dr. A. S. Kiran Kumar
Sensors Development Area, SAC, Ahmedabad
Payload Development Activities at Space Applications Centre

Prof. G. S. Agarwal, FRS
Noble Foundation Chair and Regents Professor
Oklahoma State University, Stillwater, USA
Optics in Post Laser Era and its Implication for 21st Century Quantum Physics

Prof. N. K. Mondal
Department of High Energy Physics
Tata Institute of Fundamental Research, Mumbai
Physics and Astrophysics using Neutrinos

Dr. Amritanshu Shukla
Theoretical Physics Division
Physical Research Laboratory, Ahmedabad
Double beta decay : Nuclear Structure and Neutrino mass

Dr. Y. S. Mayya
Head, Radiological Physics & Advisory Division
Bhabha Atomic Research Centre, Mumbai
Hundred Years of Langevin Dynamics: Perspectives from Aerosol Physics

Dr. B. N. Jagatap
Bhabha Atomic Research Centre and
Homi Bhabha National Institute, Mumbai
Controlling Atoms and Molecules with Photons

Dr. Archana Bhattacharya
Indian Institute of Geomagnetism, Navi Mumbai
Role of Earth's magnetic field in Space Weather

Dr. Ram Sagar
Aryabhatta Research Institute of Observational Sciences, Nainital
Progenitors of the most energetic cosmic event-GRBs

Mr. Sanjiv K. Tiwari
Senior Research Fellow Udaipur Solar Observatory(PRL), Udaipur
Helicity and the sun

Dr. Dilip Ghosh
Theoretical Physics division
Physical Research Laboratory, Ahmedabad
Physics at the Large Hadron Collider

Dr. D. P. Roy
Homi Bhabha Centre for Science Education (TIFR), Mumbai
Basic Constituents of Matter - Visible and Invisible

Dr. P. N. Vinayachandran
Indian Institute of Science, Bangalore
Exploring Indian Ocean Variability using an Ocean General Circulation Model

Prof. B. Ananthanarayan
Indian Institute of SCience, Bangalore
Vistas in Elementary Particle Physics

Dr. Malini Agarwal
Astronomy and Astrophysics Division
Physical Research Laboratory, Ahmedabad
X- ray Emission characteristics of solar flare

Dr. N. Gopalswamy
NASA Goddard Space Flight Centre, MA, USA
Interplanetary Shocks

Dr. U. C. Joshi
Astronomy and Astrophysics Division
Physical Research Laboratory, Ahmedabad
Blazars - a family of enigmatic AGNs

Dr. Jagdev Singh
Indian Institute of Astrophysics, Bangalore
Proposed visible emission line space coronagraph

Dr. Anil Bhardwaj
Vikram Sarabhai Space Centre, Trivandrum
X-ray Emission from the Solar System Bodies

Prof. K. I. Oyama
Institute of Space and Astronautical Science, Japan
Current and Future planetary exploration of Japan,Asteroid mission,Selene Moon mission,Venus Climate orbiter

Dr. R. Koul
Bhabha Atomic Research Centre, Mumbai
Ground based VHF gamma - ray Astronomy - An Overview

Prof. J. A. Klimchuk
Research Astrophysicist
NASA Goddard Space Flight Center, USA
The Angry Sun : Exploration in the Corona

Dr. B. K. Rastogi
Director General
Institute of Seismological Research, Gandhinagar
The Physics of Earthquakes

Prof. H. M. Antia
Tata Institute of Fundamental Research, Mumbai
Seismic study of Solar Structure and Rotation

Prof. D. Lal, FRS
Formar Director
Scripps Institute of Oceanography. La Jolla, San Diego, USA
Honorary Fellow, Physical Research Laboratory, Ahmedabad
Direct Measurement of Solar activity in the past 35,000 years

Dr. Suresh Govindarajan
Indian Institute of Technology, Madras
String Theory : a status report

Prof. Rohini Godbole
Centre for High Energy Physics
Indian Institute of Science, Bangalore
Glimpses of Femtoworld at the Large Hardron Collider

Prof. Tom Gehrels
Professor, University of Arizona and Fellow
Physical Research Laboratory, Ahmedabad
The History of our Universe and its Physics

Dr. A. R. Ganesan
Indian Institute of Technology, Madras
Optical Wave-front Estimation and Control for Adaptive Optics and Vision Science

Prof. Sandip Pakvasa
K. R. Ramanathan Professor, University of Hawaii, Honolulu
Neutrino : Yesterday, Today, Tomorrow

Prof. Sandip Pakvasa
K. R. Ramanathan Professor, University of Hawaii, Honolulu
HANOHANO : A Deep Ocean Antineutrino Observatory

Prof. R. V. Krishnamurthy
Department of Geosciences
Western Michigan University Kalamazoo, MI, USA
Isotopic "Score thumbs" : Implications to Geo and Cosmo chemical processes

Dr. Dipankar Banerjee
Indian Institute of Astrophysics, Bangalore
Waves in the Solar Corona

Dr. Vikram M. Mehta
Centre for Research on the Changing Earth System, Maryland, USA
Possible Influences of Atmospheric and Riverine Fresh Water on Ocean Circulation, Temperatures and Climate

Prof. J. N. Goswami
Director
Physical Research Laboratory, Ahmedabad
Chandrayaan-I : The mission thus far

Prof. B. N. Dwivedi
Institute of Technology, Varanasi
Why does the Sun matter to us?

Awards and Honours

U. R. Rao

1. A V Rama Rao Technology Award, Indian Institute of Chemical Technology, Hyderabad, May, 2008.

G. S. Agarwal

2. Elected as the Fellow of the Royal Society, London, 2008.

J. N. Goswami

3. Honorary Fellow, Royal Astronomical Society, London, 2008.
4. Associate Editor, Geochimica Cosmochimia Acta, 2009.
5. Council Member, Institute of Seismological Research, Gandhinagar, Gujarat 2008.

A. K. Singhvi

6. Goyal Prize for Applied Sciences-2006, Kurukshetra University.
7. Leader, Indian Delegation, International Geological Congress, Oslo, 2008.
8. Coordinator, National Programme on the Geological Records of Tsunamis, Ministry of Earth Sciences, Government of India.

S. Krishnaswami

9. Member, Editorial Board, Chemical Geology, Elsevier Publications.

Planeraty and Geosciences

M. M. Sarin

10. Fellow, The National Academy of Sciences, Allahabad.
11. Visiting Professor, Ocean Research Institute, Tokyo, Japan.

R. Ramesh

12. Special citation for contribution to IPCC's Nobel Peace Prize, 2007.

Sunil Kumar Singh

13. Member, Editorial Board, Chemical Geology, Elsevier Publications.

J. S. Ray

14. Member, The National Academy of Sciences, India, Allahabad.

N. Juyal

15. Member, DST Expert Committee on "Integrated program on Dynamics of Glaciers in the Himalaya", 2008.

16. Elected Fellow of the Indian Geophysical Union, 2009.

R. D. Deshpande

17. Member, Project Review and Monitoring Committee (HESCO-BARC Project), constituted by Principal Scientific Advisor to Government of India.

Neeraj Srivastava

18. "COSPAR Outstanding Paper Award for Young Scientists", COSPAR Assembly, Montreal, Canada.

Solar Physics

Nandita Srivastava

19. Co-Convener of a session at the European Geophysical Union (EGU) General Assembly, Vienna, 19-24 April, 2009.

Sanjay Gosain

20. Best thesis presentation award by Astronomical Society of India Meeting Indian Institute of Astrophysics, Bangalore, 18-20 February, 2009.

Space and Atmospheric Sciences

D. Pallamraju

21. Member, CAWSES-India Phase II Science Steering Committee.

Rajesh Kumar Kushwaha

22. Best poster award for his poster entitled "Dissociation Kinematics of CO_2^{3+}" at the DAE-BRNS SAMOP IUAC, New Delhi, February, 2009.

S. Ramachandran

23. Special Citation for contribution as Lead Author to IPCC's Noble Peace Prize 2007.

Theoretical Physics

S. D. Rindani

24. Fellow, Indian Academy of Sciences, Bangalore.

Utpal Sarkar

25. Fellow, National Academy of Sciences, Allahabad.

Srubabati Goswami

26. Ramanujan Fellowship from the Department of Science and Technology, New Delhi.

Namit Mahajan

27. Associate, Indian Academy of Sciences, Bangalore.

Conferences / Symposia / Workshops

PLANEX

1. **9th PLANEX Workshop on** "Remote Sensing of Inner Solar System Objects" Participation of more than 40 M.Sc./B.Tech students and young researchers/ teachers. Jointly organized by PRL and University of Rajasthan. at the University of Rajasthan, Jaipur, 5–9 January, 2009.
2. Discussion Meeting on "Chandrayaan-1 Data Analysis" at PRL, attended by 45 participants. Fifteen presentations by PIs of various payloads to describe the instrument capabilities and scientific objectives preceeded ageneral discussion about data analysis plans, September 26–27, 2008.
3. Review meeting of "Chandrayaan-2 Payload Proposals" at PRL, wherein 17 different payload proposals have been reviewed by an expert committee to evaluate their scientific relavance and technical feasibility on November 29, 2008.

Space and Atmospheric Sciences

1. Symposium on "Science and Exploration of Mars", Asia oceania Geosciences Society meeting held in Busan, Korea with 30 participants, 16-20 June, 2008.

Library and Information Services

1. National Workshop on "Library 2.0 : A Global Information Hub", 5–6 February, 2009.

Invited Talks

Astronomy and Astrophysics

N. M. Ashok

1. "Infrared Spectroscopic Studies of Eruptive Variables", International Conference on "Recent Advances in Spectroscopy:Theoretical, Astrophysical and Experimental Perspectives", Indian Institute of Astrophysics, Kodaikanal, 28—31 January, 2009.

B. G. Anandarao

2. "The Circumstellar Dust", IUCAA National Workshop on "Light scattering: Its applications in Astrophysics and other fields", Gujarat College, Ahmedabad, 7—8 November, 2008.

3. "New Worlds in the Universe", Symposium on Astronomy, Astrophysics and Space Science, Department of Physics, Sardar Patel University, Vallabh Vidyanagar, 22 December, 2008.

T. Chandrasekhar

4. "Angular sizes of stars and circumstellar matter", Symposium on Astronomy, Astrophysics and Space Science, Department of Physics, Sardar Patel University, Vallabh Vidyanagar, 22 December, 2008.

5. "Near earth asteroids", 9th Planet Workshop on Remote Sensing of Inner Solar System Objects, Jaipur, 5—9 January, 2009.

Rajmal Jain

6. "X-ray Emission from Solar Flares", Naval Research Laboratory, Washington, USA, 18 June, 2008.

7. "Recent Investigations from SOXS", Goddard Space Flight Center, Washington DC, USA, 23 June, 2008.

8. "Exploring Corona through Solar X-ray Spectrometer (SOXS) Mission", Mullard Space Science Laboratory (MSSL), University College London, UK, 22 July, 2008.

9. "X-ray Emission from Solar Flares", Dept. of Physics, Centre for Fusion Space and Astrophysics, University of Warwick, Coventry, UK, 24 July, 2008.

10. "The Dynamic Sun", Dept. of Physics, University of Rajasthan, Jaipur, 20 March, 2009.

Hari Om Vats

11. "Does Sun rotate?", IOWA State Star Party, Whtiterock Conservancy's Resort near Coon Rapids, Iowa, USA, 30 August, 2008.

12. "Remote sensing of solar atmosphere", National Symposium on "Advances in Remote Sensing Technology and Application", Nirma University, Ahmedabad, 18—20 December, 2008.

13. "Complexities of solar rotation", Annual meeting of Indian Science Congress, North-Eastern Hill University, Shillong, 3–7 January, 2009.

14. "A campaign of shadow band experiment during TSE of 22 July 2009", Solar Eclipse Workshop, organized by S.P.A.C.E., Delhi University, 9 January, 2009.

P. Janardhan

15. "When the Solar Wind Vanishes: Causes on the Sun, Effects at the Earth", XXVII ASI Meeting – Indian Institute of Astrophysics, Bangalore, 18—20 February, 2009.

Abhijit Chakraborty

16. "Search for Extra solar planets in India", Indo-Swiss Conference, Jaipur, November, 2008.

17. "Exo planets", ARIES, Nainital, November, 2008.

Solar Physics

Ashok Ambastha

18. "Polarization of Solar Corona", National Meeting on Solar Eclipse, IIA, Bangalore, 23 June, 2008.

19. "GONG Project of Solar Surface Observations", 10th Asian-Pacific Region IAU Meeting (APRIM2008), Kunming, China, 3–6 August, 2008.

20. "Helioseismic Characteristics of Flare Productive Active Regions", 2nd China-India Workshop on Solar Physics, Kunming, China, 7—9 August, 2008.

21. "Photo- and Polarimetric Observations of the Eclipse Corona", International Workshop on Solar Eclipses, New Delhi, 9–11 January, 2009.

Brajesh Kumar

22. "Review of Results from GONG", 27th Meeting of Astronomical Society of India, Bangalore, 18—20 February, 2009.

Shibu K. Mathew

23. "MAST update and the Back-end instruments", Magnetic coupling between the Interior and the Atmosphere of the Sun, IIA, Bangalore, 2—5 December, 2008.

Nandita Srivastava

24. "Statistical studies on CMEs", Magnetic coupling between the Interior and the Atmosphere of the Sun, IIA, Bangalore, 2—5 December, 2008.

P. Venkatakrishnan

25. "Multi Aperture Solar Telescope: An Update", 27th Meeting of Astronomical Society of India, Bangalore, 18—20 February, 2009.

Planetary and Geosciences

J. N. Goswami

26. "Space Environment and Space Missions", Invited Talk given at the Annual Meeting of the Aeronautical Society of India, Trivundrum, 9 May, 2008.

27. "Planetary Exploration : Chandrayaan-1 and Beyond", Distinguished Speaker, International Space University, Madrid, 29 July, 2008.

28. "Space Sciences and Planetary Explorations: The challenges ahead", Invited Talk on DST meeting during Inauguration of the "INSPIRE" proogramme New Delhi, 13 December, 2008.

29. "Chandrayaan-1", Invited Talk at the Special session on Indian Moon Mission at the Indian Science Congress, Shillong, 4 January, 2009.

30. "Solar System Studies: The stellar Connection", Presidential Address at the 27th Meeting of the Astronomical Society of India, Bangalore, 18 February, 2009.

31. "Chandrayaan-1: India's first planetary science mission to the Moon", Invited Talk at the 40th Lunar and Planetary Conference, 24 March, Houston, USA.

A. K. Singhvi

32. "Climate change, Earth Surface Processes and Human Impact: The relevance of paleo records towards planning the future, Climate Change forum", Beijing, China, April, 2008.

33. "Inaugural Address, International Seminar on Climate and Tectonics", Wadia Institute of Himalayan Geology, October, 2008.

34. "Aeolian record of the Thar desert : Geochronlogy of Soils, Dunes and Calcretes", International workshop on Atlas of Aeolian Sands, Oxford University, Oxford, 8—11 January, 2009.

35. "Luminescence Dating and its contribution to Indian Quaternary Studies", M.R. Sahni Memorial Lecture, 2009, Paleontological Society of India, March, 2009.

36. "Luminescence dating studies in India", Japanese National Seminar on Luminescence and Electron Spin resonance, Hamamatsu, Japan, March, 2009.

37. "Luminescence dating in Geo and Planetary Sciences-the journey, thus far", International Symposium on Material Science and the History of Earth and Sister Planets, Okayama State University, Okayama, 4—5 March, 2009.

38. "The Societal dimension of Geosciences", University Lecture, Cukurova University, Adana, Turkey, 20 March, 2009.

M. M. Sarin

39. "Atmospheric carbonaceous species (OC, EC) over Indian region: Sources, temporal variability and OC/EC ratio", International Conference on Atmospheric Chemistry, Yokohama, Japan, 29—31 October, 2008.

40. "Atmospheric sulphate, carbonaceous & mineral aerosols over Indian region", TIGERZ Workshop, IIT Delhi, 7—8 January, 2009.

41. "Determination of major ions, trace metals and carbonaceous species in atmospheric aerosols: Recent trends and analytical methods", Chemical Metrology Workshop, NPL Delhi, 16—17 February, 2009.

R. Ramesh

42. "Some outstanding problems concerning the Anthropocence", at the Workshop on "Tracking the Anthropocene and beyond: an earth system science approach to evaluate the impacts and implications of human forcing", Indian Institute of Science, Bangalore, 20 September, 2008.

43. "Constraining carbon sequestration in the oceans", IISc Centenary Conference, Indian Institute of science Bangalore, 13—16 December, 2008.

44. "Paleoclimate: outstanding problems" at "Planet earth's changing climate: critical research issues", DST Sponsored Brainstorming Meeting at CMMACS, Bangalore, 10—11 December, 2008.

45. "Ocean productivity", Foundation Day lecture, IITM, Pune November, 2008.

R. D. Deshpande

46. "Significance of IWIN National Programme for Hydrology Research in India", Xth Biennial Workshop of All India Coordinated Research Programme on Agrometeorology, Bidhan Chandra Krishi Viswa-vidyalaya, Mohanpur, West Bengal, 3–5 December, 2008.

47. "Dissolved Noble Gases in Groundwater Hydrology", International Conference on Water, Environment, Energy and Society (WEES-2009), New Delhi, 12—16 January, 2009.

48. "An Insight into the Origin and Distribution of High Fluoride in Ground Waters of North Gujarat-Cambay Region", National Seminar on Water for Future – Issues and Options, Central Water Commission (CWC), Ahmedabad, 2—3 March, 2009.

49. "Application of Isotopic Tracers for Efficient Water Resource Management", Regional Workshop on Issues related Ground Water Management and Water use Efficiency in the State of Gujarat and U.T. of Daman and Diu, Central Ground Water Board (CGWB), Ahmedabad, 4—5 March, 2009.

N. Juyal

50. "Late Glacial monsoon variability in Central Himalaya", International Seminar on Climate and Tectonics, Wadia

Institute of Himalayan Geology, Dehradun, October, 2008.

51. "Planet earth: evolution through time", Uttarakhand state council for science and technology, Dehradun, 14 October, 2008.

52. "Evolution of Gujarat alluvial Plain during the Last 130 ka", Society of petroleum geophysicist and association of petroleum geologists, ONGC, Baroda Chapter, 3 January, 2009.

J. S. Ray

53. "Understanding the Earth's mantle using isotopes", Indian Institute of Space Science and Technology (IIST), Trivandrum, 29 October, 2008.

54. "Mud Volcanoes: Geodynamic and Climatic Implications", Pandit Deendayal University Petroleum University, Gandhinagar, 18 March, 2009.

K. K. Marhas

55. "Evolution of Early Solar system", Conference (women in Science) at St. Xaviers College organized by Indian Academy of Science, 13 September, 2008.

Ravi Bhushan

56. "Sediment Provenance in the Bay of Bengal using Sr and Nd Isotopes", International Conference on "Mountain Building and Climate-Tectonic Interaction (MBCT-2008)", Wadia Institute of Himalayan Geology, Dehradun, 23—25 October, 2008.

S. V. S. Murty

57. Exploration of Moon and Mars: ISRO Plans, 37th COSPAR Assembly, Montreal, Canada, 13—20 July, 2008.

58. Meteorites and the Early Solar System, International conference on "Planetary Science 2009", Mumbai, 3—5, February, 2009.

Space and Atmospheric Sciences

S. P. Gupta

59. "Spatial and temporal variation of stratospheric conductivity – An overview", ECAR workshop at Indian Institute of Geomagnetism, Mumbai, 25—26 November, 2008.

S. A. Haider

60. "Solar wind electron and galactic cosmic rays precipitating at Mars terminator ionosphere", 5th Annual Meeting of the AOGS, Busan, Korea, 16—20 June, 2008.

S. Lal

61. Atmospheric Trace Gases and Environment, Seminar on "Current trends in environmental sciences", Vallabh Vidhya Nagar, 20 September, 2008.

62. Ozone and trace gases over the Indian region, National conference on "Geomatics and impact of climate change with specific reference to mountain ecosystem", Forest Research Institute, Dehradun, 4 February, 2009.

D. Pallamraju

63. "The response of neutral and electrodynamical variations on the oxygen dayglow emissions over low andmid-latitudes", 37th COSPAR Assembly, Montreal, Canada, 13—20 July, 2008.

64. "A combined optical and modeling approach to estimate incident particle fluxes into the earth's atmosphere", Electrodynamical Coupling of the Atmospheric Regions (ECAR) workshop, Indian Institute of Geomagnetism, Mumbai, 25—26 November, 2008.

S. Ramachandran

65. "Aerosols over continental India and surrounding oceanic regions: A review", TIGERZ data workshop, Indian Institute of Technology (IIT), Delhi, 7–9 January, 2009.

66. "Regional and seasonal variations in aerosol optical characteristics over India: Radiative impacts", Indian Centre for Climate and Societal Impacts Research (ICCSIR), Ahmedabad, 27 March, 2009.

Varun Sheel

67. "Zonal variability of Neutral Density, Temperature and Ion Production Rates in the Martian Troposphere", 5th Annual Meeting of the AOGS, Busan, Korea, 16—20 June, 2008.

R. Sekar

68. "Effects of interplanetary electric field on low latitudeionosphere", Electrodynamical Coupling of the

Atmospheric Regions (ECAR) workshop, Indian Institute of Geomagnetism, Mumbai, 25—26 November, 2008.

Som Sharma

69. "Imprint of greenhouse cooling in lidar observed stratospheric thermal structure over a sub-tropical station Mount Abu (24.5°N, 72.7°E), University of Bresia, Italy, September, 2008.

K. P. Subramanian

70. "Studies of fragmentation sequence of the precursor SF_5^{3+} photoion using momentum spectroscopy" DAE-BRN Symposium on Atomic, Molecular and Optical Physics, 10—13 February, 2009.

Theoretical Physics

R. E. Amritkar

71. "Introduction to nonlinear dynamics", (9 lectures), SERC School on Nonlinear Dynamics, Indian Institute of Science, Bangalore, 26 June—16 July, 2008.

72. "Estimating parameters of a dynamical system", National Conference on Nonlinear Systems and Dynamics, Saha Institute of Nuclear Physics, Kolkata, 5—7 March, 2009.

Angom Dilipkumar Singh

73. "Atomic electric dipole moment calculation with perturbed coupled cluster method", Symposium on "50 Years of Coupled Cluster Theory", Institute for Nuclear Theory, UW Seattle, USA, 2 July, 2008.

74. "Feshbach Resonances", (2 lectures), Workshop during the International Conference on Cold Atoms, Indian Institute of Science Education & Research, Kolkata, 12—13 December, 2008.

75. "*p*-wave phase shift and scattering lengths of alkali atoms", International Conference on Cold Atoms, Indian Institute of Science Education & Research, Kolkata, 14—16 December, 2008.

76. "Precision atomic calculations: computational challenges", DAE-BRNS Symposium on Atomic, Molecular and Optical Physics, Inter University Accelerator Centre, Delhi, 10—13 February, 2009.

77. "GRID: future of high performance computing", National Seminar on Computer Applications, L. J. Institute of Computer Applications, Ahmedabad, 20—21 February, 2009.

J. Banerji

78. "Collective excitations of a binary condensate in an axially symmetric trap", International Conference on Cold Atoms-2008, Indian Institute of Science Education & Research, Kolkata, 14—16 December, 2008.

H. Mishra

79. "Ground state structure and superfluidity in cold atoms", (2 lectures), Workshop during the International Conference on Cold Atoms, Indian Institute of Science Education & Research, Kolkata, 12–13 December, 2008.

80. "Relativistic BCS-BEC Crossover – A variational approach", International Conference on Cold Atoms 2008", Indian Institute of Science Education & Research, Kolkata, 14—16 December, 2008.

V. K. B. Kota

81. Spectral Distribution Analysis of Random Interactions with *J*-symmetry and its Extensions, International Workshop on "Nuclear Structure Physics", Shanghai Jiao Tong University, Shanghai, China, 1—7 June, 2008.

82. "Random Matrix Ensembles with Random Interactions", Homi Bhabha Centenary Conference on "Non-Hermitian Hamiltonians in Quantum Physics", Bhaba Atomic Research Centre, Mumbai, 13—16 January, 2009.

83. "Algebraic IBM-ST and mean-field DSM-T models for N = Z nuclei", Homi Bhabha Birth Centenary Workshop on "Frontiers in Gamma ray Spectroscopy (FIG09)", Tata Institute of Fundamental Research, Mumbai, 2—4 March, 2009.

S. D. Rindani

84. "Strong gauge-boson scattering at LHC", RECAPP Workshop 2008, Harish Chandra Research Institute, Allahabad, 21 September—4 October, 2008.

85. "Signatures of Top Polarization", Workshop on "Getting ready for physics at LHC", Harish Chandra Research Institute, Allahabad, 16—20 February, 2009.

R. P. Singh

86. "Optical Vortex and BEC Interaction", International Conference on Cold Atoms-2008, Indian Institute of Science Education & Research, Kolkata, 14—16 December, 2008.

87. "Vortices of Light and Matter", DAE-BRNS Symposium on Atomic, Molecular and Optical Physics, Inter University Accelerator Centre, New Delhi, 10—13 February, 2009.

88. "Spectral Engineering with a Polychromatic Vortex", Conference on laser applications in basic and in applied sciences (CLBAS-2009), Visva Bharati, Shantiniketan, 14—17 February, 2009.

Srubabati Goswami

89. "Physics Programme of India-based Neutrino Observatory (INO)", in the Working Group, NOW08, Otranto, Italy, September, 2008.

90. "Probing the Neutrino Mass Matrix", DAE-BRNS Symposium on High Energy Physics, Banaras Hindu University, December, 2008.

Subhendra Mohanty

91. "Dark Matter and Dark Energy", CRAL-IPNL Conference, Lyons, France, 7—11 July, 2008.

92. "Inflation and CMB", Field Theory and Gravity–VII Conference at IAS, Shimla, 15—19 November, 2008.

Lectures at Universities / Institutions / Workshops

Astronomy and Astrophysics

P. Janardhan

1. "When the Solar Wind Vanishes: A Multi wavelength Study of the Solar Source Regions", Max Planck Institute for Radioastronomy (MPIFR), Bonn, Germany, 26 September, 2008.

K. S. Baliyan

2. "Khagol Vigyan ke adhyayan mein remote communication evam satellites ka mahatva", at Hindi Seminar in SAC, Ahmedabad, 28 February, 2009.

Hari Om Vats

3. "Lunar Eclipse in the astronomical perspective", DMAS Ashton Observatory (USA), 26 April, 2008.

4. "Universe and the eclipses", on Astronomy day at Des Moines Science Center (USA), 10 May, 2008.

5. "Sun in Time and for us", DMAS Ashton Observatory (USA), 21 June, 2008.

6. "South Pole solar eclipse", ALCon Expo 2008, Des Moines, 18—19 July, 2008.

7. "The study of solar wind", Physics Department, Saurashtra University, Rajkot, 24 September, 2008.

Solar Physics

Brajesh Kumar

8. "Helioseismic signatures of major solar flares", at National Solar Observatory, Tucson (AZ), USA, 20 August, 2008.

Planetary and Geosciences

K. K. Marhas

9. "Nucleosynthesis of elements."*

10. "Extinct nuclides and early evolution of the solar system."*

11. "Non-destructive microanalysis of isotopes and their applications."*

*in DST Sponsored short course on Pondishery University, Pondichery, 15~20 December, 2008.

M. M. Sarin

12. "Th-234 as a tracer for carbon export from the surface ocean", LOHAFEX Workshop, NIO, Goa, 12—14 April, 2008.

13. "Climate forcing by anthropogenic aerosols", CAIPEEX Workshop, IITM, Pune, 28—29 April, 2008.

14. "Chemical characteristics of aerosols in MABL of Arabian Sea and Bay of Bengal: A comparative study", Ocean Research Institute, Tokyo (Japan), 8 October, 2008.

15. "Basic concepts in spectrochemical analysis", (2 Lectures) Refresher Course for Post Graduate Teachers, School of Chemistry, Gujarat University, Ahmedabad, 18—19 February, 2009.

R. Ramesh

16. "Advanced Mathematics Course", (35 lectures) at the Space Applications Centre, Ahmedabad, February—May, 2009.

17. "Meteorology and Oceanography", (8 lectures) at The Indian Institute of Science Education and Research, Pune, March, 2009.

J. S. Ray

18. Four lecturer on, "Fundamentals of radiogenic isotope geology", in the DST sponsored Short course on "Radiogenic isotopes and their applications", Department of Earth Sciences, Pondicheryy University, Pondicherry, 15–20 December, 2008.

A. K. Singhvi

19. "Luminescence and Dating : Principles & Possibilities", Visiting Professor to State key laboratory for Saline lakes, Xinning, China, 26 September, 2008.

20. "Paleoscismic Studies in India using Luminescence", Visiting Professor to State key laboratory for Saline lakes, Xinning, China, 27 September, 2008.

21. "The Social Dimensions of Geoscience", Visiting Professor to Cukurova University, Adana, Turkey as Tubitak Professor, 30 March, 2009.

22. "Luminescence Dating at the Physical Research Laboratory, Ahmedabad", Luminescence and ESR dating laboratory, Okayama State University, Okayama, Japan, 5 March, 2009.

23. "Luminescence Dating : An example of synergistic mutualism between physics & earth sciences", Luminescence and ESR dating laboratory, Okayama State University, Okayama, Japan, 6 March, 2009.

Sunil Singh

24. "Radiogenic isotopes in weathering processes and river systems."*

25. "Sr and Nd isotopes in oceans and its circulation."*

26. "Re-Os isotope system."*

*All in DST sponsored short course on "Application of radiogenic isotopes in geochronology and geochemistry", held at Pondicherry University, Pondicherry, 15–20 December, 2008.

S.V.S. Murty

27. "Comparative planetology: Venus, Earth and Mars."*

28. "Planetary exploration: ISRO Plans."*

29. "Current and future missions to Mars."*

*in 9th PLANEX workshop on "Remote Sensing of Inner Solar System Objects", Jaipur University, Jaipur, 5–9 January, 2009.

Y. B. Acharya

30. Chandrayaan-1: Mission profile, Spacecraft and Subsystem, 9th PLANEX workshop on "Remote Sensing of Inner Solar System Objects", Jaipur University, Jaipur, 5–9 January, 2009.

Neeraj Srivastava

31. "Remote Sensing of Moon: Clementine Examples."*

32. "Space Weathering."*

* in 9th PLANEX workshop on "Remote Sensing of Inner Solar System Objects", Jaipur University, Jaipur, 5–9 January, 2009.

D. Banerjee

33. "Remote sensing of energetic particles and photons",

9th PLANEX workshop on "Remote Sensing of Inner Solar System Objects", Jaipur University, Jaipur, 5–9 January, 2009.

Deepak Dhingra

34. "Mercury: Results from MESSENGER."*

35. "Remote sensing by HySI – Terrestrial Examples."*

    * in 9th PLANEX workshop on "Remote Sensing of Inner Solar System Objects", Jaipur University, Jaipur, 5–9 January, 2009.

M. Shanmugam

36. "Instruments for planetary exploration", 9th PLANEX workshop on "Remote Sensing of Inner Solar System Objects", Jaipur University, Jaipur, 5–9 January, 2009.

Durga Prasad

37. "Search for water on Moon and Mars", 9th PLANEX workshop on "Remote Sensing of Inner Solar System Objects", Jaipur University, Jaipur, 5–9 January, 2009.

V. K. Rai

38. "Origin of Solar System."*

39. "Exploration of Venus."*

    * in 9th PLANEX workshop on "Remote Sensing of Inner Solar System Objects", University of Rajasthan, Jaipur, 5–9 January, 2009.

Space and Atmospheric Sciences

Bhas Bapat

40. "Ion momentum spectroscopy for studying molecular fragmentation", Sardar Patel University, Vallabh Vidyanagar, 30 December, 2008.

H. Chandra

41. CSSTEAP PG Course on space science, organised by PRL, August-November, 2008 (53 lectures).

42. Space Science Course, Gujarat University, August-November 2008, (15 lectures, 2 Practical).

S. Lal

43. "Atmospheric chemistry", (2 lectures), CSSTEAP PG course in Space and Atmospheric Sciences, organised by PRL, 1—2 August, 2008

44. "Atmospheric trace gases", (2 lectures), SERC School on Atmospheric and Space sciences, Andhra University, Visakhapatnam, 21—22 September, 2008.

45. "Atmospheric chemistry", (6 lectures), CSSTEAP PG course in Satellite meteorology and global climate, Organised by SAC, Ahmedabad, 1—6, January, 2009.

46. "Atmospheric Trace Gases: Impact on Environment and Climate Change", Seminar on Climate Change, Society for Clean Environment, Vadodara, 11 January, 2009.

47. "Atmospheric Trace Gases: Their Role in Environment and Climate", Refresher Course in Environmental Science, Gujarat University, Ahmedabad, 20 February, 2009.

D. Pallamraju

48. "Climate and Weather of the Sun-Earth System", (2 lectures), SERC School on Atmospheric Studies, Andhra University, Vishakhapatnam, 27—28 September, 2008.

49. "Space Weather: Science and Applications", 3 lectures, SERC School on Aviation Meteorlogy with special reference to Modern Observational Techniques and Nowcasting, Air Force Administrative College, Coimbatore, 1—20 December, 2008.

50. "Techniques for the Exploration of Planetary Atmospheres", 9th PLANEX workshop on Remote Sensing of Inner Solar System Objects, University of Rajasthan, Jaipur, 5—9 January, 2009.

S. Ramachandran

51. "Atmospheric aerosols", Gujarat University, 16 December, 2008.

R. Sekar

52. "Upper atmospheric airglow techniques", (4 lectures)

to the Post-graduate students, Department of Physics, Gujarat University, December, 2008.

H. S. S. Sinha

53. Three lecturer on, "Space Science", to the Post-graduate student, Department of Physics, Gujarat University, October, 2008.

Som Sharma

54. "Space & Atmospheric Sciences Studies at PRL", a Lecture to Gujarat Battalion NCC, NCC regional office, Ahmedabad, July, 2008.

Theoretical Physics

A. C. Das

55. "Solar-Terrestrial Physics", (9 lectures), Space Science Course, Gujarat University, Ahmedabad, October-December, 2008.

56. "Introduction to Solar Physics, Magnetospheric Physics and Space Weather", (50 lectures), Sixth Post Graduate Course in Space and Atmospheric Sciences of CSSTEAP, organized by Physical Research Laboratory, Ahmedabad, December, 2008 – February, 2009.

H. Mishra

57. "Relativistic BCS-BEC crossover in fermionic matter", Astrophysics Group, Institute for Theoretical Physics, University of Frankfurt, June 2008.

58. "Superfluidity in quark matter and ultracold atoms", Academic Staff College, Jawaharlal Nehru University, New Delhi, February 2009.

V. K. B. Kota

59. "Shell model based SDM and DSM methods for beta and double beta decay", SNOLAB, Sudbury Canada, 10 October, 2008.

R. Rangarajan

60. "Gravitino production in an inflationary Universe and implications for leptogenesis", Harish-Chandra Research Institute, Allahabad and Jamia Millia Islamia, New Delhi, December, 2008.

R. P. Singh

61. "Optical vortices: light beams with orbital angular momentum", Laboratory for Electro-optics Systems, ISRO, Bangalore, 27 June, 2008.

62. "Optical Vortices: Light Beams with Helical Wavefront", Indian Institute of Science Education & Research, Mohali, 5 November, 2008.

R. K. Varma

63. "Nurturing Science Talent: A challenger requiring a paradigm shift", (INSA lecture under the series: "Excitement and Anticipation in Basic Sciences") at the K. R. Ramanathan Auditorium, Physical Research Laboratory, Ahmedabad, 27 March, 2009.

Computer Centre

Jigar Raval

64. "IT Security and Linux", during Student Technical Awareness Conference (S-TAC) under agesis of IEEE Student Branch at G. H. Patel College of Engineering and Technology, Vallabh Vidyanagar, 15 March, 2009.

Library and Information Services

Nishtha Anilkumar

65. "Technology enabled library services", UGC Refreshers Course, Gujarat University, Ahmedabad, 3 September, 2008.

Theses submitted

1. **Amit Misra**

   "Study of Satellite Derived Aerosol Properties and Validation with Ground Truth Data", (April, 2008), Gujarat University, Ahmedabad.

2. **Ravi Bhushan**

   "Geochemical and Isotopic studies on waters and sediments of the northern Indian Ocean", (June, 2008), M. S. University of Baroda, Vadodara.

3. **Sanat Kumar Das**

   "Observational and theoretical estimation of the contribution of anthropogenic and natural aerosols to radiative forcing of the atmosphere", (October, 2008), Gujarat University, Ahmedabad.

4. **Santosh K. Rai**

   "Isotopic and Geochemical Studies of Ancient and Modern Sediments", (September, 2008), M. S. University of Baroda, Vadodara.

5. **Satya Prakash**

   "Role of the Ocean in the Global carbon Cycle", (April, 2008), M. S. University of Baroda, Vadodara.

6. **Shilpy**

   "Study of the vertical distribution of ozone in the lower atmosphere", (November, 2008), Gujarat University, Ahmedabad.

7. **Shreyas Managave**

   "High resolution monsoon reconstruction using oxygen isotopes in teak trees", (February, 2009), M. S. University of Baroda, Vadodara.

8. **Uma Kota**

   "Rocket-borne studies of mesosphere and airglow emissions", (July, 2008), Gujarat University, Ahmedabad.

Astronomy & Astrophysics

The research activities of the Astronomy and Astrophysics Division encompasses a variety of topics – Dust formation in explosive events like novae, Activity in young stellar objects, energetics of Active Galactic nuclei, grain formation in comets and galactic centre region studies. Most of these activities involve the use of optical and Infrared instruments attached to the I.2m telescope at Mt. Abu Infrared Observatory (MIRO). In addition research on some aspects of the sun like solar flares, solar rotation and solar wind is also being carried out in the division. Studies in X-ray astronomy and extra-solar planets are new activities of the division.

Dust forming properties of novae: a nova V1280 Sco

Why do only some novae form dust while others fail to do, is an unsettled question that is debated extensively. This issue is important because novae can be prolific dust producers. By generalizing results from the dust-forming nova V1280 Sco, we can now predict as to which novae will form dust. Infrared spectra of this source was modelled assuming thermal equilibrium and it was shown that spectral lines arising from the presence of low-ionization species like NaI and MgI indicate low temperature regions that are conducive to dust formation. A detailed examination of several novae indicated that dust formation was invariably associated with such lines in a nova's spectrum. Studies of V1280 Sco also indicate that mass loss began before the maximum light was reached and that,the mass loss was sustained for a considerable time after its maximum brightness. The angular size of the nova remnant during the fire-ball expansion phase was also derived. At this time the ejecta behaved like a black body. We also participated in a novel international collaboration that recorded and studied the expansion of a dust shell around a classical nova for the first time.

This work was done in collaboration using interferometric techniques from the 8.2m Very Large Telescope Interferometer, Chile.

(R. K. Das, D .P. K. Banerjee and N. M. Ashok)

Near Infrared Observations of the novae V2491 Cygni and V597 Puppis

A white dwarf in a nova binary system in the post-outburst stage has a photosphere at a high temperature. This can be a source of super-soft X-rays. Two novae viz. V2491 Cyg and V597 Puppis have recently been shown to be the source of such super- soft X-rays. It is, therefore,

desirable to correlate the infrared and optical properties of these objects with their X-ray properties during the post-outburst phase. We obtained near-infrared JHK spectroscopic observations of V2491 Cyg and V597Pup during the early phases of the decline of their outbursts during November 2007 and April 2008 respectively. Both novae were detected in the post-outburst super-soft X-ray phase. Being bright in X-rays, V2491 Cyg has been extensively observed. Infrared observations using the 1.2 meter, Mount Abu infrared telescope indicated emission lines of HI, OI, HeI and NI in both objects. In V597 Pup, the HeI line intensity increased rapidly with time. Based on spectral characteristics, both objects were classified as He/N novae. The possibility of V2491 Cyg being a recurrent nova was also investigated. Temporal evolution of the line widths in V2491 Cyg indicated that, it is unlikely that the binary companion is a giant star with heavy wind as in recurrent novae of the RS Oph type. Significant deviations from the recombination case B conditions were inferred from the strengths of HI lines. This indicated that in both novae, the HI lines were from optically thick regions. In both cases, the slope of the continuum spectra had a dependence that deviated from a Rayleigh-Jeans spectral distribution. Infrared observations were also correlated with the X-ray properties of these novae.

(Sachindra Naik, D. P. K. Banerjee and N. M. Ashok)

Multi-wavelength study of accretion in high mass proto-stellar objects

It is hypothesized that stars of all masses manifest accretion disks and exhibit mass outflows during their proto-stellar evolution. However mass outflows in the case of high mass stars is not yet established. Resolution of this issue makes it necessary to examine possible correlation between the outflow and accretion parameters in the high mass proto-stellar objects (HMPOs) and deduction of the central source parameters. Toward this, multi-wavelength photometry of about 30 HMPOs was initiated and relevant near- and far-infrared data from IRAS / 2MASS / MSX / SPITZER archives was analyzed. A spectral energy distribution model was used to extract physical parameters relating to the HMPO central star, the accretion disk and the envelope. These were correlated with outflow mass derived from molecular diagnostic surveys in the radio and mm wave regions. The outflow rates correlated with the HMPO mass, age and envelope mass accretion. The results show similarities with such studies on low mass stars, and indicate that the high mass stars (at least up to about 25 solar masses) also can form by accretion.

This work was done in collaboration with M.S.N. Kumar of CAUP, Porto, Portugal.

(Lokesh Dewangan and B.G. Anandarao)

Outburst recurrence in the McNeil's object

It is known that V1647 Orionis (or the McNeil's object) a low mass young stellar object (YSO), has undergone at least two outburst episodes since 1966; the more recent being during 2005—2007 that lasted for ~2 years. The duration and other characteristics such as amplitudes and rise and fall times indicate the object to be of EXOrs class rather than FUOrs. EXOrs undergo long lasting episodes with larger amplitudes. It is considered that the outburst phenomenon is linked with a thermal instability in the accretion disc that gives rise to a substantially enhanced mass accretion rate for an extended period. It is therefore important in the pre-main-sequence evolution of YSO. After a year long quiescence the object exhibited another outburst phase. We were the first group to report the outburst in the infrared and made regular JHK' photometry with MIRO-NICMOS infrared array and provided the outburst amplitudes viz., J = 3.8; H = 2.8; and K' = 2.0 over the magnitudes in the quiescent period. It appears that V1647 Ori may be a prototype of its own class, with recurrence time scales different from EXOrs

(V. Venkata Raman and B. G. Anandarao)

A new wide-field near-infrared camera for photometry and spectroscopy

A new wide-field near-infrared camera and spectrograph (NICS) was developed and commissioned at MIRO. NICS uses a f/6.5 focal ratio at the 1.2 m telescope to give an un-vignetted field of view of 8×8 arc min^2, with a sky angle resolution of 0.5 arc sec/pixel. The instrument uses a HAWAII-1 1024×1024 HgCdTe detector array with 18.5 μm pixel size. It has capability for MKO standard broad-band imaging photometry (in Y, J, H, K, and K' bands); narrow band imaging (centred on H2 and Br gamma lines); and for spectroscopy at a resolving power of 1000 in 0.85-2.5 μm region . It covers two consecutive bands (IJ, JH and HK) in a single exposure. NICS has been tested for its photometric capability and the images of standard stars show that the sensitivities are 15.6 mag in J band; 14.4 in H band; and 13.5 in K band at S/N = 3 with an 10 sec integration. The uncertainities for all the bands are <0.1 mag. Figure 1 shows the NICS and Figure 2 shows the JHK color composite of the spiral galaxy M51 (exposure times: 30 sec in each band). The spectroscopic capability is to be tested soon.

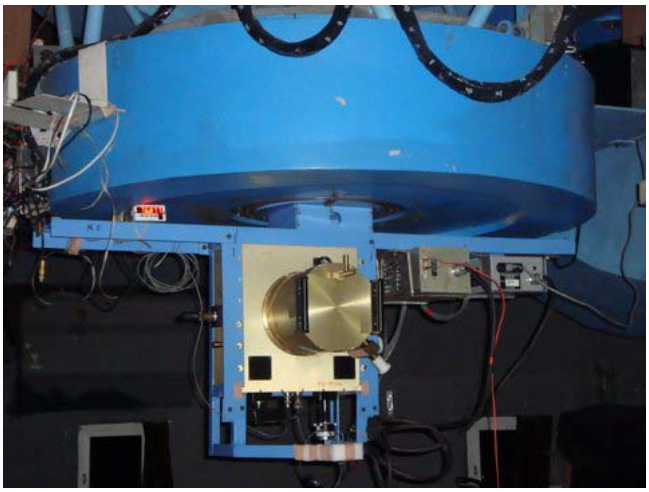

Fig. 1 Near-Infrared Camera and Spectrograph (NICS) mounted at the Cassegrain focus of the 1.2 m IR telescope in Gurushikhar Observatory, Mt. Abu.

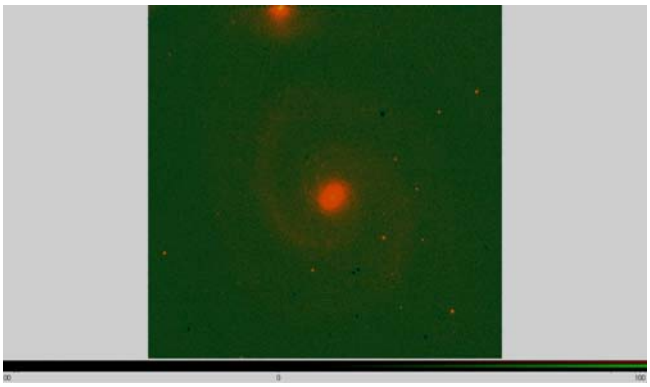

Fig. 2 A JHK colour composite of the spiral galaxy M51 - blue represents J, green H and red K bands. One can see that the galaxy is predominantly bright in K band (red), especially in the spiral arms where one expects on-going star formation. An exposure time of 30 sec was given in each of the three bands using the new NICS.

The optical design of NICS was made by Dr. E. Harvey Richardson of University of Victoria, Canada.

(B. G. Anandarao, A. Chakraborty, R. R. Shah, F. M. Pathan, V. Venkata Raman and S. N. Mathur)

Near Infrared Lunar Occultations of Sources in the Galactic Center region from Mt. Abu and ESO (Paranal)

The rare passages of the moon's disk over the heavily obscured central regions of our galaxy enable studies of occulted objects with high angular resolution of a few milliarcsec in the near-infrared. This is the lunar occultation technique. During one such lunar passage, over a dozen events were successfully observed in the K band using the NICMOS IR Camera in a fast sub-array mode. One of the observed sources, 2MASS 17341641-290835 is particularly well resolved with a circumstellar envelope and a uniform disk angular size of 14.5 ± 2.3 milliarcsec.

In an earlier event observed at ESO, Paranal, Chile, the very large telescope (8.2m, Antu) was used for the first time to record Lunar Occultations of the highly reddened sources in the K band in a region near the Galactic Center. In the present study, 51 sources were observed in 4 hours. Thirty sources had good Signal/Noise and a detailed analysis indicated two binary detections at sub-arcsec projected separations. Three barely resolved stars at 2 milliarcsec were also inferred. In one of the objects (2MASS 17453224-2833429) it was possible to detect circumstellar emission. This extended emission indicates an optically thin shell with an inner radius of 10-15 milliarcsec corresponding to about 40 AU.

The work involving VLT was done in collaboration with the ESO team led by Dr. A. Richichi, ESO Garching.

(T. Chandrasekhar and Tapas Baug)

Polarimetry of Comet NEAT C/2001 Q4

Linear polarization studies on Comet NEAT C/2001 Q4 using an optical polarimeter at MIRO were conducted through IHW narrow band (continuum) and BVR broad band filters. The phase angle during observation ranged from 85.6° to 55°. In this phase angle range, the polarization increased with wavelength. Polarization colour in the narrow bands changed at different epochs, possibly due to cometary activity or contamination by molecular emission. Polarization was also measured in the cometary coma at different locations along a line, in the direction of the tail. A minor decrease in the polarization as the photocenter (nucleus) is traversed was observed. The brightness decreased sharply away from the nucleus. These studies suggest that Comet NEAT C/2001 Q4 has high polarization and cometary grains comprise silicates and organics..

(S. Ganesh, U. C. Joshi and K. S. Baliyan)

Photometry and polarimetry of Blazars

A selection of blazars (viz 3c66a, 3c279, 3c454, PKS1510, PKS0716, Mrk 421, Mrk 501, OJ287, 1ES2344, Wcom, H1426) were observed in optical and near-infrared domain using the optical polarimeter, CCD and NICMOS camera at MIRO. Additional polarization observations for the VERITAS collaboration were carried out to study the structure of 1ES1218 and W com.

PKS1510 varied significantly in brightness with intraday and day-to-day timescales. PKS0716 showed brightening during November and December 2008. A similar behavior was also noticed with GeV Gamma-rays by AGILE while no enhancement in the X-rays was seen. This behavior of the blazar PKS0716 suggested that in this case synchrotron self Compton (SSC) model was applicable, where in low energy synchrotron photons serve as seed photons for emission at high energy.

(K. S. Baliyan, S. Ganesh and U. C. Joshi)

Study of Gamma-Ray burst GRB060526

Gamma-Ray bursts (GRB) are highly energetic events in universe, but these decay rapidly. Thus to understand their nature, it is necessary to quickly localize them and capture their counterparts at other wavelengths. Counterpart of one such burst, GRB 060526 was observed using 1k x 1k CCD array. This bright GRB could be observed for several hours. We also investigated the light curve of highly variable afterglow and environment in which this GRB occurred at a high redshift of $z = 3.221$. This observational campaign along with other collaborators resulted in a comprehensive photometric dataset on a GRB afterglow. The set added 218 data points to the literature. Furthermore, low-resolution, high signal-to-noise spectra of the afterglow was modelled using an analytical model with broken power-law fits and with a broadband numerical energy injection model.

The work was carried out in collaboration with Theone C.C., Neils Bohr Institute, Copenhagen and other co-workers.

(K. S. Baliyan and S. Ganesh)

Study of white dwarfs

Inadequate understanding of the convective zone physics leads to large errors in stellar models. It is, therefore, important to study the convection zone layers in large amplitude pulsating white dwarfs (DAV). The information helps us to understand the internal structures of white dwarfs, the age of galactic disk using astero-seismology, and the depth of the convective layer. With this in view,several DA and DB white dwarfs were observed to get a continuous light curve to test the models. The observations were made under whole earth telescope (WET) campaign. We analyzed the data on EC14012-1446 and other observed white dwarfs. This source was remarkably well behaved during the run and 13 independent frequencies distributed in 8 modes, and over 60 combination frequencies could be identified.

This work was done in collaboration with the WET team comprising over 50 astronomers from 30 countries.

(K. S. Baliyan, H. O. Vats, S. Ganesh and U. C. Joshi)

Interstellar extinction towards the Inner Bulge from Spitzer survey results

An understanding of the distribution of interstellar extinction is cardinal to the understanding of stellar populations and structure in the inner regions of the Milky Way. Earlier work with near-infrared data from the DENIS and 2MASS surveys indicated that the extinction in these regions was large (25 magnitudes). And in many regions this was only a lower limit. At mid-infrared wavelengths the extinction is less than at shorter wavelengths. We therefore used the mid-infrared survey data from the GLIMPSE-II and GALCEN programs on the Spitzer Space Observatory to map the interstellar extinction towards the Inner Bulge of the Milky Way Galaxy. The area covered spans 20° in longitude and 2°- 4° in latitude around the Galactic Center (Figure 3).

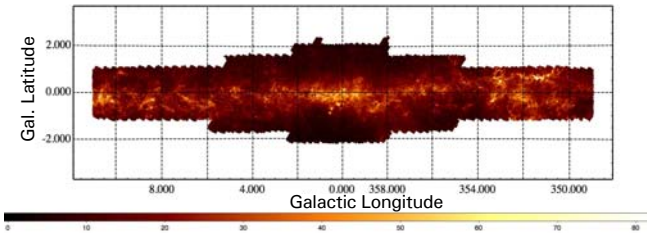

Fig. 3 Map of the interstellar extinction towards the Galactic Bulge derived from Spitzer IRAC data.

We used the mid-infrared photometry of the red giants at two wavelengths-3.6 and 5.8 μm.The data were compared to theoretical models for the red giants and the extinction coefficient for small, regular areas was derived, tiling the entire area surveyed. The spatial distribution of extinction indicated a clumpy and filamentary nature. Relatively uniform regions with moderate extinction and regions with. extinctions exceeding 80-100 visual magnitudes were also identified. Some of the highest extinction regions exhibited signatures of star forming activity. The spatial variability of the extinction coefficients for near and mid-infrared wavelengths was also studied.

This work is done in collaboration with Mathias Schultheis (Obs. de Besancon, France) and Kris Sellgren (Ohio State Univ., USA)

(S. Ganesh, U. C. Joshi and K. S. Baliyan)

Orbital phase spectroscopy of high mass X-ray binary pulsars to study the stellar wind of the companion

Pulse-phase and orbital-phase resolved X-ray spectroscopy of accretion powered X-ray pulsars can be used to understand distribution of matter around the neutron star. The energy spectra of these pulsars can be described by a power-law with a high-energy cutoff. As most of the binary pulsars are located in the Galactic plane, their spectra are usually modified by strong soft X-ray absorption. However, some binary X-ray pulsars outside the galactic plane show the presence of a marginal excess over the extended power-law component in the hard X-ray region. Apart from the hard and soft spectral components, features of iron emission line, cyclotron resonance etc. are also seen in several X-ray pulsars. It is, therefore, important to study the spectral (pulse-phase average, pulse-phase resolved, and orbital-phase resolved) properties of the pulsars to understand the system and the surrounding medium.

We have been investigating the stellar wind of some High Mass X-ray Binary (HMXB) pulsars such as 4U 1538-52, Cen X-3, GX 301-2, OAO 1657-415, Vela X-1 etc., with a focus on a comprehensive orbital phase dependent spectroscopy of four HMXB pulsars viz. 4U 1538-52, GX 301-2, OAO 1657-415 and Vela X-1. Measurements of the variation of the absorption column density, iron-line flux along with other spectral parameters over the binary orbit for these pulsars in elliptical orbits were carried out using the RXTE and BeppoSAX satellites. A spherically symmetric wind profile was used as a model to compare the observed column density variations.Of the four pulsars, only in 4U 1538-52, the model accorded with the observations and in the remaining three, the stellar wind appeared. clumpy and the smooth symmetric stellar wind model could not explain the data. In GX 301-2, neither the presence of a disk nor a gas stream from the companion could be validated. Furthermore, the spectral results on OAO 1657-415 and Vela X-1 were similar to that of GX 301-2.

This work was carried out in collaboration with U. Mukherjee (B. P. Podar Institute of Management and Technology, Kolkata), B. Paul (Raman Research Institute, Bangalore) and C. S. Choi (Center for Astrophysics, KASI, Korea).

(Sachindra Naik)

Indian X-ray Polarization Explorer

Indian X-ray Polarization Explorer is a collaborative project between the Physical Research Laboratory, Raman Research Institute and SAID/ISRO Satellite Centre and was proposed as a 400 kg class mini satellite platform.Polarization is an important property of radiation from astrophysical sources and carries unique information regarding the emission mechanism, physical conditions and emission geometry at the origin. Importance of polarization measurements of X-rays is well realized. We propose to develop a polarimeter based on Thomson scattering.This will have a collecting area of ~ 800 cm^2 and will be sensitive in the energy range of 8–30 keV. Bright Galactic X-ray sources will be examined. The expected sensitivity is ~1% MDP (Minimum Detectable Polarization) at a 3σ level from a unit crab source with about I million sec exposure. PRL's contribution in this experiment would include a Si-PIN detector based monitoring cum spectroscopy detector and GEANT4 based Monte-Carlo simulations of the scattering geometry of the experiment.

A dedicated laboratory for X-ray polarimetery experiment is being established. The Si-PIN detectors and other basic components have been procured and single detector prototype has been successfully demonstrated. Optimization of the detector energy resolution and energy range is under progress. A potential candidate for the custom designed large area (~100 cm^2) pixellated (8x8 pixels) Si detector has been identified and procured. This will be caliberated using a low noise single channel prototype electronics. ASIC based multi-channel front-end electronics (MFE) for this detector is being designed. Field Programmable Gate Array (FPGA) based MFE control, data acquisition and real-time spectrum generation, back-end electronics design and development is in progress.

(S. V. Vadawale, Sachindra Naik, A. B. Shah, S. L. Kayasth, J. Pendharkar and N. M. Ashok)

X-ray polarimeter simulations:

A Monte-Carlo simulation code based on the GEANT4 toolkit is being developed for simulations for the X-ray polarimeter. This code enables simulation of the sensitivity of the X-ray polarimeter for different geometries. Initial results from this simulation are now being refined to optimize the experiment design

(S. V. Vadawale, J. Pendharkar and Sachindra Naik)

Radiation Dosimeter onboard Space capsule Recovery (SRE) Experiment

The second version of SRE, SRE-2 will be launched by ISRO during late 2009. It is planned have a space radiation monitor and dosimeter onboard this mission. With the SRE-

2 and HSP (Human Space Program) teams at VSSC development of an active radiation monitor / dosimeter using Si-PIN detectors is underway. Design details and Preliminary Design Review document for the scientific objectives and data processing requirement along with identification of detectors, low noise pre-amplifier and amplifier chips was completed. Additionally Monte Carlo simulations were carried out to assess the feasibility of identifying incident particle types and their energy spectra using the the data from this experiment.

(S. V. Vadawale and J. Pendharkar)

Time Varying Thermal X-ray Emission in Solar Flares

The temporal evolution of spectra of the medium to hard X-ray flux (F_t) from an evolving multi-temperature plasma is governed by thermal conduction cooling. This aspect was modelled and found to agree with Solar Xray Spectrometer (SOXS) observations. Theoretical brems-strahlung spectrum of an isothermal plasma with temperature T as a function of photon energy is shown in Figure 4 (upper panel). Figure 4 (Bottom panel) shows the hard X-ray spectra of the flare on 19 November 2003 observed by Si detector. A multi-temperature power-law function was used to fit the data. This provided peak temperature and differential emission measure (DEM) of the flare plasma. We investigated 5 M-class flares. The measured DEM power-law index for these five flares shows that the emission in the 6-20 keV energy range is dominated by temperatures in the range (5-50) x 10^6K, and the power-law index of the thermal spectrum γ varies in the range 2.2-6.1. The cooling time in solar flares was measured using the SOXS X-ray time profiles and Hiraso Hα observations.

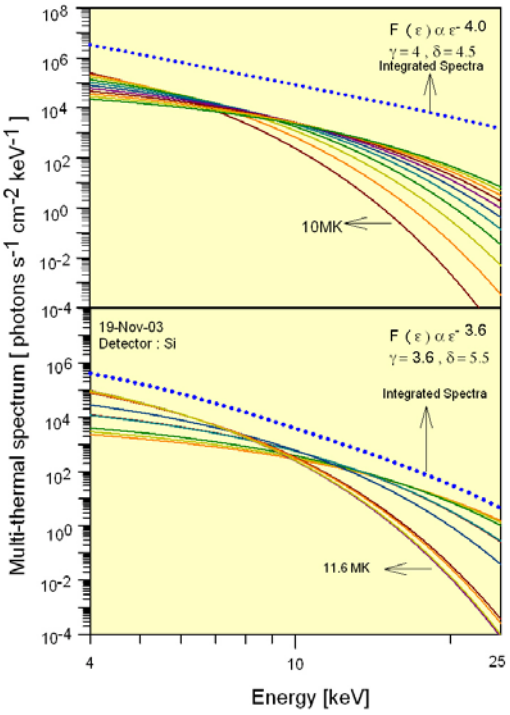

Fig. 4 Upper panel - Theoretical X-ray bremsstrahlung spectra for temperature T = 10-30 MK in steps of 2 MK (thin curves) and their sum (blue dotted line). Lower panel - Modeled bremsstrahlung spectra of 19 November 2003 flare with contribution from peak temperature and DEM distribution measured from the spectra observed by the Si detector.

The calculated cooling time for all flares varied from 20 to 100 s. The analysis of time-varying thermal emission permitted a comparison of the observations with theoretical models involving physical timescales and their scaling law.

(Rajmal Jain, A. S. Rajpurohit,
Arun K. Awasthi and Malini Aggarwal)

Solar Coronal Plasma Diagnostics

The physical process of coronal heating has been an outstanding problem in solar physics. Micro/nano flares versus wave (acoustic and Magneto Hydro Dynamical) heating mechanisms have been proposed but none of them is completely satisfactory. The temperature of the solar corona ranges from less than 10^5 to 10^8 K. The X-ray telescope (XRT) on board Hinode satellite has enabled an improved understanding of the temperature structure in the corona by providing observations in nine different X-ray wavebands. These wavebands correspond to different temperatures. Using the Hinode data, coronal temperature around the entire sun can be derived using the filters-ratio method. We have developed a software tool to estimate the temperature on the entire Sun as well as in the localalized regions, using emission intensity and the temperature dependant response function of a filter. The ratio of intensities through their Al and Ti poly filters on the XRT along with reverse mapping of the filter response provides a handle on the temperature of the observed solar plasma. From the data taken on 22 February 2007 the average temperature of the corona is found to be 2 x 10^6 K and active region temperatures reach upto 6 x 10^6 K.

This work was done in collaboration with Meet Shah of Nirma Institute of Technology, Ahmedabad.

(Arun K. Awasthi and Rajmal Jain)

Study of High-energy Flare Event associated with CME

We carried out the spectral analysis of solar flare (GOES class M6.4) of 25 August 2005, in the energy range 4-

100 keV, (Figure 5). Spectral analysis using OSPEX tool in *SolarSoft* suggested that the photon spectra in the energy range 4-20 keV can be better approximated to a multi-thermal power-law function. A triple power law provides a better fit for energies in the range 20-100 keV. In this flare event, plasma up to 40 keV was dominated by thermal emission at temperatures in excess of 30 x 10^6K, while for energies >40 keV RHESSI spectra indicated the dominance of non-thermal emission. The spectral fit enabled us to measure plasma parameters such as emission measure temperature, photon index, and elemental abundance. Figure

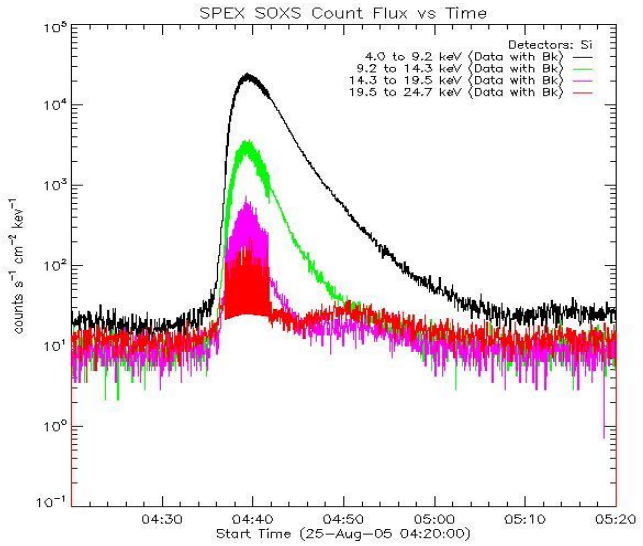

Fig. 5 Light curve of 25 August 2005 solar flare as recorded by Si detector of the SOXS mission.

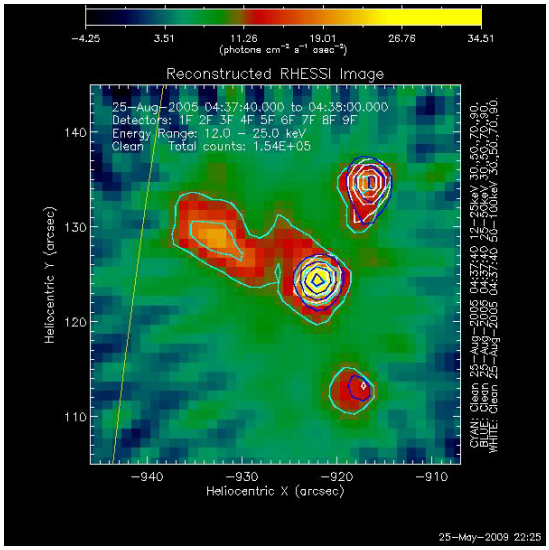

Fig. 6 High resolution X-ray image of 25 August 2005 solar flare observed by the RHESSI satellite in 12-25, 25-50 and 50-100 keV energy bands.

6 gives RHESSI satellite image reconstructed using "clean iterative algorithm". The displayed image in the energy range 12-25 keV is overlaid with 25-50 and 50-100 keV contour images The image reveals the foot-points on the disc and that the non-thermal, hard X-ray emission originates from these foot-points. The coronal flare plasma at the loop top is generally hotter than at the foot-points of the loop producing thermal bremsstrahlung.

This work was done in collaboration with Nipa Bhatt of C.U. Shah Science College, Ahmedabad.

(Rajmal Jain)

Dynamics of Small-scale Network

The mechanism for physical coupling among various layers of the solar *atmosphere* is currently a key issue. High spatial resolution is required to address this question. The granulation network on Sun is considered to be due to an interplay between convective magnetic processes beneath observable photosphere. Understanding physical characteristics and dynamics of granulation with highest possible spatial resolution is of importance in the investigation. The Filtergram and the associated Stokes vector polarimetric data from Solar Optical Telescope (SOT) onboard Hinode mission are being analyzed using a SolarSoft software developed by us. The SOT provides 0.2" resolution on the photosphere. The intensity of the granules is directly proportional to their temperature and hence the their intensity variation is of interest. Inversion of four Stokes vectors (*I, Q, U, V*) observed by spectro-polarimeter (SP), an associated instrument of SOT, provided the spatial variation of physical parameters viz. intensity, magnetic flux and line of sight velocity. We have successfully constructed Stokes line profiles.These will be analyzed by Stokes inversion techniques viz. Stokes Inversion through Response function (SIR), and Milne-Eddington Inversion Technique (MALANIE).

This work was done in collaboration with Meet Shah of Nirma Institute of Technology, Ahmedabad.

(Arun K. Awasthi and Rajmal Jain)

Energy-dependent Timing of X-ray emission in Solar Flares

A study of a sample of ten M-class flares observed by the Si detector of the SOXS experiment revealed energy-dependent timing of X-ray emission in solar flares. We measured the initiation, peak and end time of the flares as a function of energy, and found that they vary with energy. This permitted measurement of the flare plasma cooling

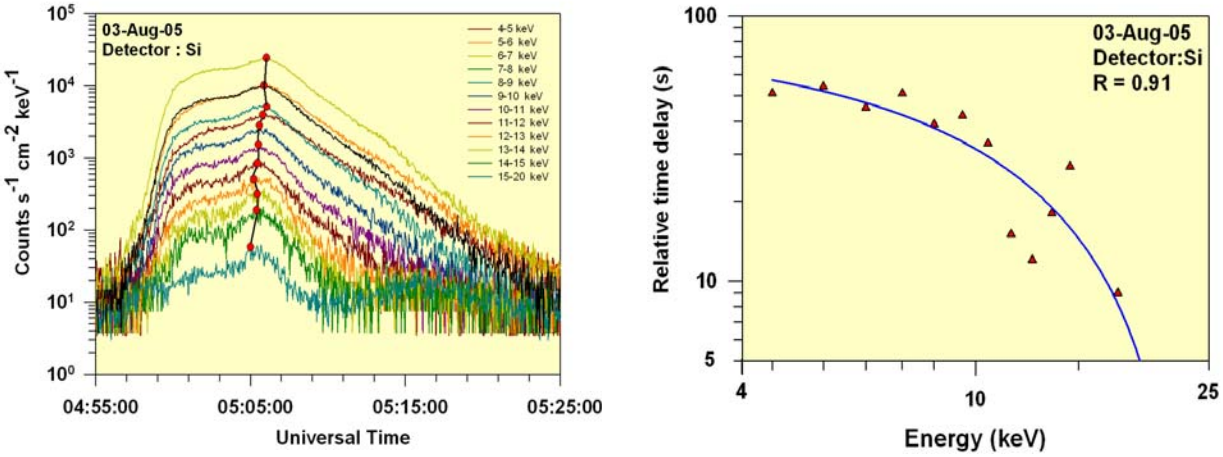

Fig. 7 (Left panel) Temporal profiles in 12 energy bands (ε = 8-5, 5-6 ... 14-15, 15-20 keV) of the 03 August 2005 flare. Each peak time is shown by circle. The curve connecting these circles illustrate the delay between successive profiles. (Right panel) Relative time delays between two consecutive energy bands as a function of energy for 03 August 2005 flare.

time and demonstrated the Neupert effect in X-ray emission. Characteristic times for heating and cooling of the X-ray emitting plasma in solar flares were estimated from the time profile as in Figure 7 (left), the temperature and the emission measure of the thermal X-ray burst, and the over-all length scale of the flare-heated plasma at thermal X-ray maximum. The temporal evolution of the 03 August 2005 flare in 12 different energy bands reveal that this flare evolved rapidly in the beginning via non-thermal transport of energy, and then through a slow heating, most likely from chromospheric evaporation and plasma collision. Figure 7 (left) also reveals delay of the onset of flare at higher energies while peaking earlier relative to the previous energy channels.

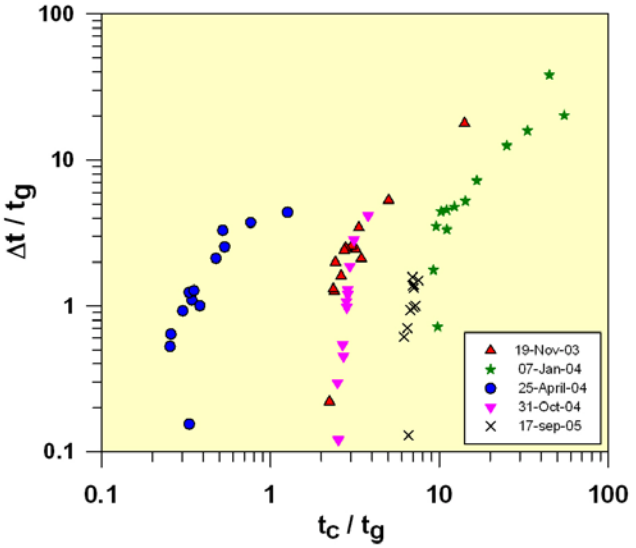

Fig. 8 Time delay Δt obtained by convolving a Gaussian profile with half width t_g with an e-folding time t_c for each flare. The time scale are normalized by t_g

It is assumed that the heating is due to magnetic reconnection and the cooling is due to conduction and radiation. Since the conductive losses increase rapidly with temperature, we consider that thermal conduction cooling dominates in high-temperature X-ray loops, while radiative cooling dominates in the later phase of the flare, seen as post-flare loops observed at EUV and Hα wavelengths. Figure 7 (right) depicts a relative delay in the peak time measured from temporal evolution in each energy band with respect to 15-20 keV energy band. We found that in all of the ten flares relative delay increased towards lower energy bands initiating of multi-temperatures in the flare plasma. Therefore our observations provide a direct evidence of multi-temperature plasma in the flare, and suggest that hard X-ray spectra is better fit with multi-temperature rather than isothermal function.

Figure 8 shows that the logarithmic increase of time delay (Δt) with cooling time suggests the dominance of Neupert effect in flares. The time delay is obtained by convolving the Gaussian time profile with an e-folding cooling time (t_c).

(Rajmal Jain, A. S. Rajpurohit, Arun K. Awasthi and Malini Aggarwal)

Predicting the amplitude of Solar Cycle-24

Precursor techniques, such as geomagnetic indices, are often used in the prediction of the maximum amplitude for

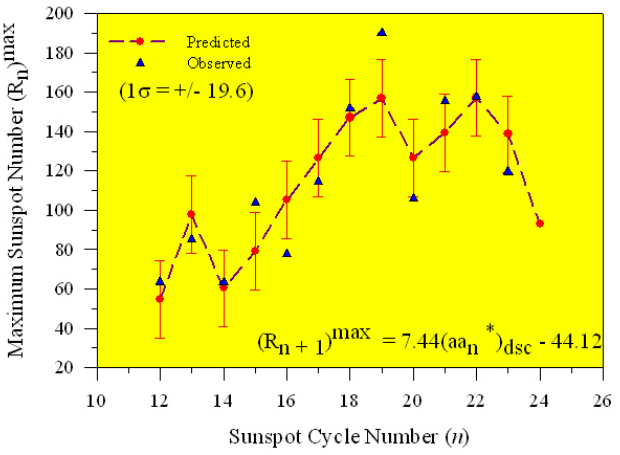

Fig. 9 Variation of predicted (red circle) and observed (blue triangle) maximum annual mean sunspot number $(R_n)_{max}$ as a function of sunspot cycle number (n). The predicted $(R_n)_{max}$ are connected with dashed line. Presuming a smoothed monthly mean sunspot number minimum in August 2008, the smoothed monthly mean sunspot number maximum is expected around October 2012 ± 4 months (1-sigma accuracy).

a sunspot cycle. Here, the year 2008 is taken as the sunspot minimum year for cycle 24. Based on the average Geomagnetic activity index value for the sunspot minimum year and the preceding four years, we estimated the expected annual maximum amplitude for cycle 24 to be about 92.8 ± 19.6 (1-sigma accuracy), indicating a somewhat weaker cycle 24 as compared to cycles 21-23 (Figure 9).

This work was done in collaboration with Nipa J. Bhatt of C U Shah Science College, Ahmedabad.

(Rajmal Jain and Malini Aggarwal)

Study of solar X-ray flares on Earth's Atmosphere

The data on Xray flares from GOES satellite during 1996-2000 was selected as representative cases of solar minimum and maximum. The impact of X-ray flares on Earth's atmosphere was investigated. The study indicates that the sudden enhancements in the X-ray emission during a solar flare produce excessive ionization in the D region of the Earth's atmosphere below 100 km. This is inferred from the temporal variations of the minimum frequency reflected from the ionosphere. The effect is more pronounced in the solar minimum than that in the solar maximum.

This work in being done in collaboration of K N Iyer and Niraj Pandya of Saurashtra University, Rajkot.

(Hari Om Vats and Som Kumar Sharma)

Rotation of solar atmosphere

Over the years, efforts have been made to understand the temporal and spatial variations in the rotational properties

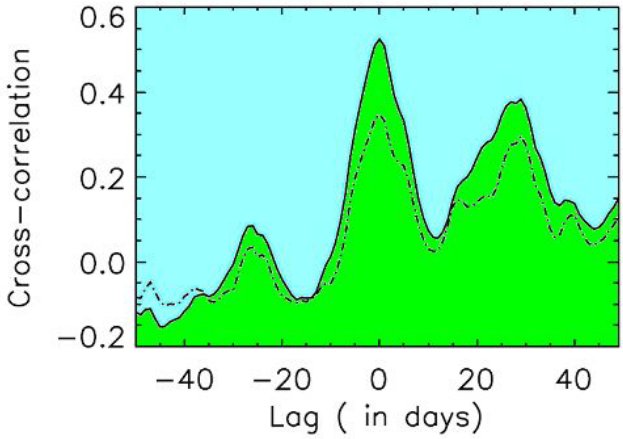

Fig. 10 Cross correlation of X-ray emissions at 1-8 A° (continuous line) and 0.5-4 A° (dot dash line) with the sunspot number for the year 1999.

of the solar corona. This work uses radio emissions up to 2.8 GHz. This study was extended to emissions at 34 GHz and X-ray emissions from solar corona at 1- 8 Å and 0.5-4 Å. Figure 10 shows that the cross correlation of solar emission in the 1- 8 Å region is greater than that in the 0.5-4 Å region. However, the temporal variation of cross correlation with lag of few days is similar for both the emissions. The correlation curves also show that the source region of X-ray emission rotates with a period of about 28 days. Similar study for the year 2000 indicates a rotational period of 34 days. The difference could be due to dominance of high latitude emission with the increasing solar activity.

This work is being done in collaboration with K N Iyer (Saurashtra University, Rajkot) and Satish Chandra (PPN College Kanpur, UP).

(Hari Om Vats)

Source Region Evolution of the Disappearance Event of 11 May 1999: A Multi Wavelength Study

Detailed study of the well known solar wind disappearance event of 11 May 1999, traced its origin to a coronal hole (CH) adjacent to a large active region (AR) complex AR8525 in Carrington rotation 1949. The AR was located at central meridian on 05 May 1999 when the flows responsible for this event began. In this study we examined the evolution of the AR-CH complex during 5-6 May 1999

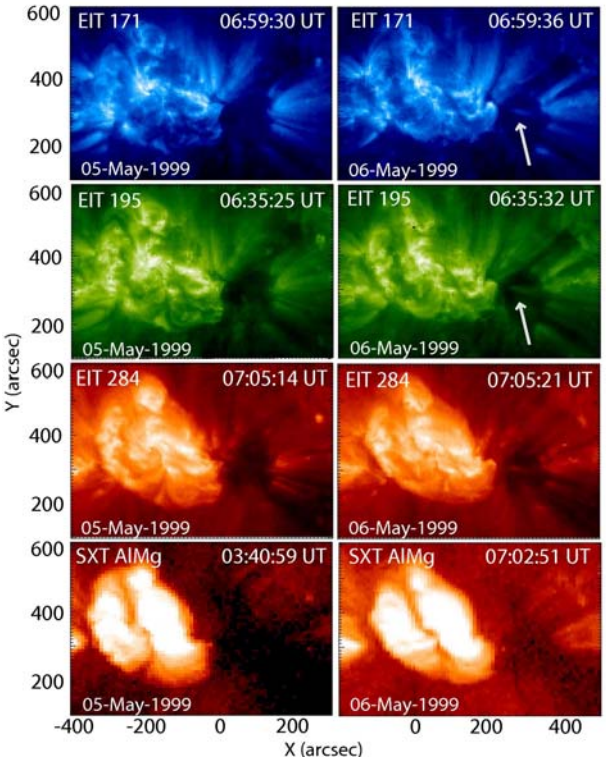

Fig. 11 A portion of the solar disk centered on the active region AR8525 and coronal hole that was the source of the disappearance event of 11 May 1999. The images shown are 05 May 1999 (left column) and 06 May 1999 (right column).

to study the changes that were responsible for this disappearance event. The study was carried out using images from the Soft X-ray Telescope (SXT), the Extreme-ultraviolet Imaging Telescope (EIT) and the Michelson Doppler Imager (MDI). These enabled a detailed elucidation of the evolution of the CH and AR complex AR8525.

A dynamic evolution in the CH-AR boundary was seen. This evolution was accompanied by the formation of new loops in EUV images that were spatially and temporally correlated with emerging flux regions as seen in MDI data. These observations provide clear evidence for Sun—Earth connection: between an evolving coronal hole close to an active region; during quiet solar conditions and, in the absence of CME's. With the exception of co-rotating interacting regions (CIR), these observations provide the first link between the Sun and space weather effects at 1AU, arising from non-explosive solar events. (Figure 11).

This work was carried out in collaboration with Dr. Helen Mason and Colleagues at the Department of Applied Maths and Theoretical Physics (DAMTP), University of Cambridge, Cambridge CB3 OWA, UK.

(Janardhan P.)

Synthesis Imaging of the Quiet Sun by Combining GMRT and Nancay Radioheliograph Observations

To exploit the complementary UV coverage and capabilities of the Giant Meterwave Radio Telescope (GMRT) and the Nancay Radio Heliograph (NRH) coordinated observations of the sun were carried out. The aim was to combine the visibilities produced by the GMRT and the NRH and thereby produce synthesis images for the quiet sun and snapshot images for noise storms and bursts. The resulting images will have a high dynamic range and resolution. The resultant possible studies would concern quiet sun structures (in particular coronal holes), radio noise storms, bursts and propagation effects in the inhomogeneous corona. Observations of small sources can constrain parameters of the turbulent spectrum in the corona. Faint non-thermal sources in the quiescent corona can contribute towards the overall heating of the corona. The procedure for combining GMRT and NRH visibilities has already been used to produce high dynamic range, high resolution snapshot maps of the whole sun while the procedure for the composite synthesis observations of the quiet sun has recently been tested, using existing common observations. Since the start of solar cycle 24, the sun has been quieter than usual, with hardly any sunspots and active regions on the solar disk. Such a situation is ideal to produce quiet sun maps, taking full advantage of the synthesis technique. Coordinated GMRT and NRH observations were carried out in November 2008 and more observations are scheduled in June-July 2009. The data obtained is being reduced and analyzed.

This work is being carried out in collaboration with Dr. Claude Mercier and Colleagues at the Paris Observatory, LESIA, NRH Group, Meudon, France and Dr. Prasad Subramanian at the Indian Institute of Science Education and Research, Pune.

(Janardhan P.)

Solar Physics

The research and development activities of the Udaipur solar observatory revolve around the central theme of solar activity and solar eruptive processes. Helioseismology is used as a tool to dig into the sub-surface origins of eruptions. Surface magnetic field is measured to monitor magnetic energy storage and evolution of the potential triggers of the eruptions. Above the surface, chromospheric and coronal phenomena are used to predict the geo-effectiveness of these eruptions. A combination of analyses of archived data, mathematical modeling and construction of sophisticated instruments is employed to achieve the desired goals.

Transient Magnetic and Doppler Features Related to the White-light Flares in NOAA 10486

Rapidly moving transient features in magnetic and Doppler images of super-active region NOAA 10486 were detected during the energetic white-light events, X17/4B flare of 28 October 2003 and the X10/2B flare of 29 October 2003. These flares occurred at topologically separated locations within the same active region. The transient features appeared during impulsive phases of the flares and moved with speeds ranging from 30 - 50 kms^{-1}(Figure 12). There are some interesting questions related to these observed transients: What kind of physical process caused the moving magnetic and Doppler velocity transients? Is there any relationship between moving transients, HXR sources and flare kernels?

In the case of the X17/4B flare of 28 October 2003, we found that the two locations of magnetic transients were associated with sign reversals in magnetic polarity. These features differed in their basic characteristics as follows: (i) the location of sign reversal that occurred in strong magnetic field of the leading (negative) umbra was nearly stationary. Both HXR source and WLF kernel were associated with this feature, (ii) The other location of sign reversal, observed in the weak field area near the neutral line, moved rapidly toward the following (positive) polarity umbra, and exhibited a better association with HXR compared to the WLF kernels (Figure 13).

On the other hand, magnetic and Doppler transients observed on 29 October 2003 were nearly stationary during the course of the X10/2B flare. The locations of magnetic transients, where sign-reversal anomaly appeared, did not conform to the HXR sources. Interestingly, we observed a strong HXR source (and WLF kernel) in weak field region without the corresponding sign reversal anomaly. On the

other hand, there was a WLF kernel but no HXR source associated with the magnetic transient observed in strong field location of the positive polarity umbra. This is in contrast with the HXR-magnetic anomaly relation observed for the white-light flare of 28 October 2003, and also in contradiction with the earlier suggestions about the association of HXR sources with polarity sign reversal phenomenon.

The observed flare kernels and moving transients associated with these events possessed large velocities. This is expected due to the large magnetic energy stored in the magnetically complex active region giving rise to these exceptionally energetic super-flares.

La
fo

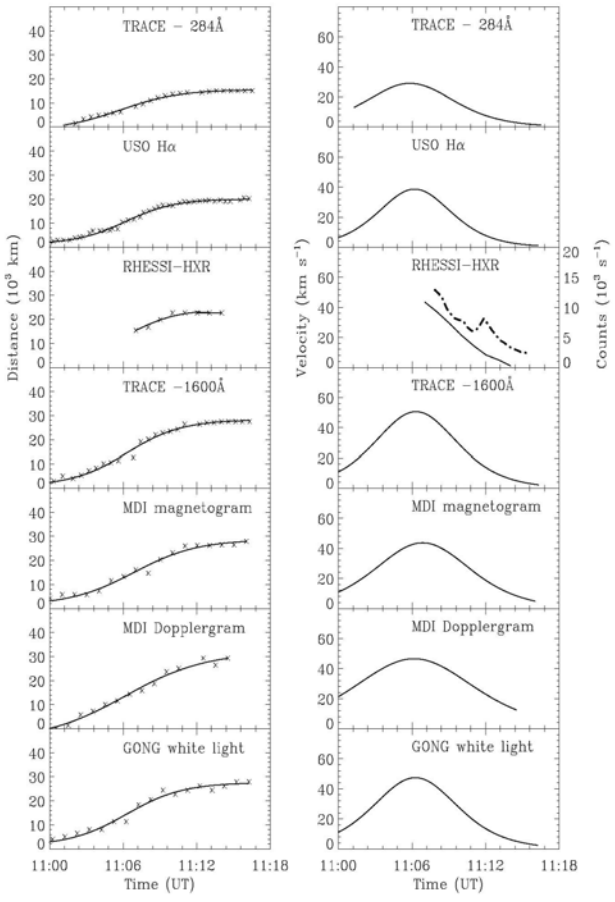

Fig. 12 Left panel: Distances of flare kernels and magnetic/ Doppler transients from a reference line during 11:00-11:15 UT using different observations: TRACE UV 284Å, Hα, RHESSI HXR, TRACE UV 1600Å, magnetogram, Dopplergram and white-light (from top to bottom rows). Measured distances are marked by "×", while the solid profiles represent the Boltzmann sigmoid fitting through these points. Right panel: Separation velocities derived for various features from the fitted distances corresponding to the left panel. The dash-dotted line in RHESSI velocity panel shows the HXR light curve.

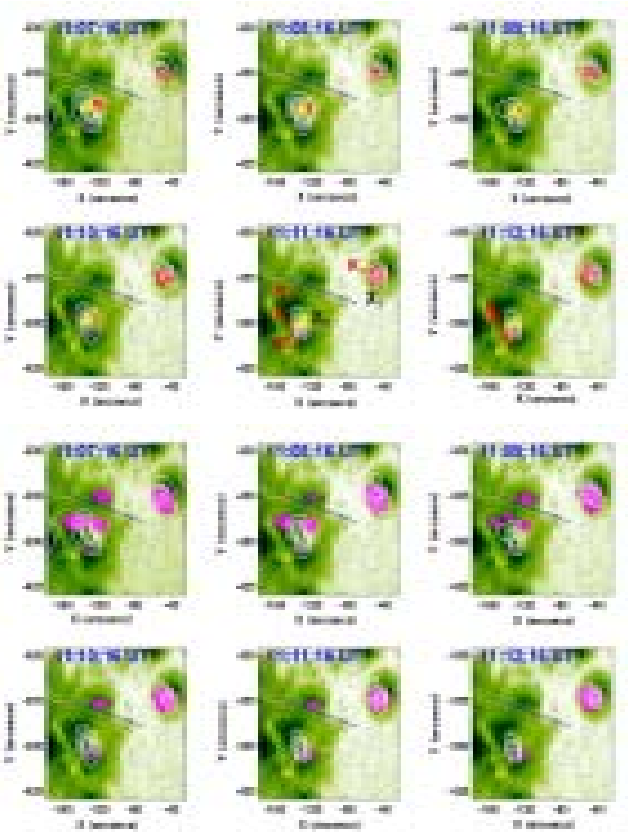

Fig. 13 Time sequence of white-light intensity maps (background green half-tone image) during the impulsive phase of the X17/4B flare - 11:07:16-11:12:16 UT on 28 October 2003. Superimposed dashed (solid) contours represent negative (positive) flux at ± 800, ± 1500 gauss levels, while the dotted contours mark the magnetic neutral lines. RHESSI HXR fluxes (white contours) in the energy range 100–200 keV are overlaid at the levels 20, 40, 60, 80% of the maximum value. Red patches mark the enhanced WLF kernels (top rows 1-2) and magenta patches represent the enhanced magnetic transients (bottom rows 3-4).

magnetic field lines at higher levels of corona. Finally, the answer to the question of characteristics of the moving magnetic transients (or magnetic anomaly) still remain ambiguous, as a clear and consistent correlation of these features with HXR sources (or WLF kernels) did not emerge from the study of the two white-light flares.

(R. A. Maurya and Ashok Ambastha)

Supersonic Downflows In A Sunspot Light Bridge

We report the discovery of supersonic downflows in a sunspot light bridge using spectropolarimeter measurements on board the Hinode satellite. The downflows occur in small patches close to regions where the vector magnetic field rapidly changes orientation (Figure 14), and are

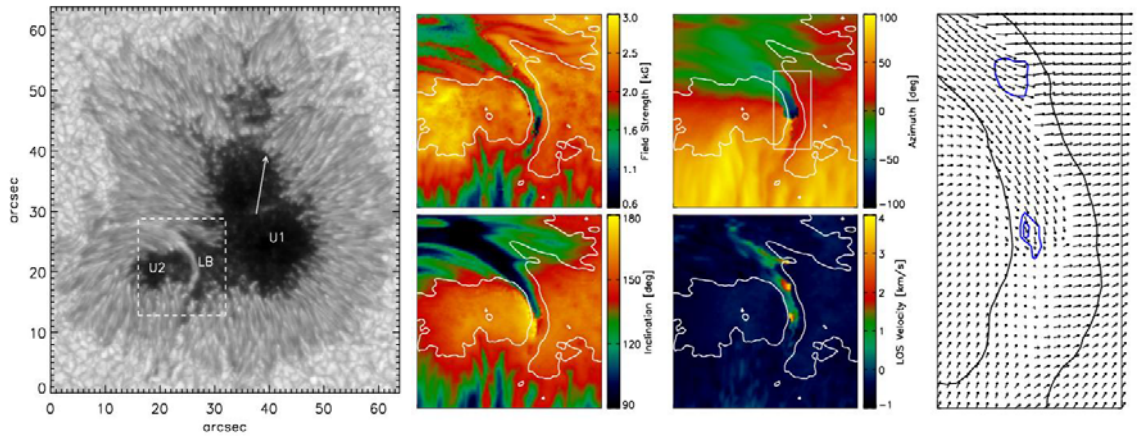

Fig. 14 First column: Continuum image of NOAA AR 10953 at 630nm. The white box represents the region containing the light bridge (LB), while U1 and U2 are the sunspot umbrae adjacent to the LB. North is up and West to the right. The arrow indicates the direction to disk center. Second and third columns: Magnetic field strength, field inclination, field azimuth, and LOS velocity in the 16'' x 16'' sub-region containing the LB, as deduced from the inversion. The angles are expressed in the local reference frame. Azimuths increase counterclockwise, with zero representing fields pointing to solar West. Positive velocities indicate redshifts. The mean umbral velocity is zero. Fourth column: Transverse component of the vector magnetic field in the LB. The blue contour lines mark LOS velocities of 2.5 and 4 km/s.

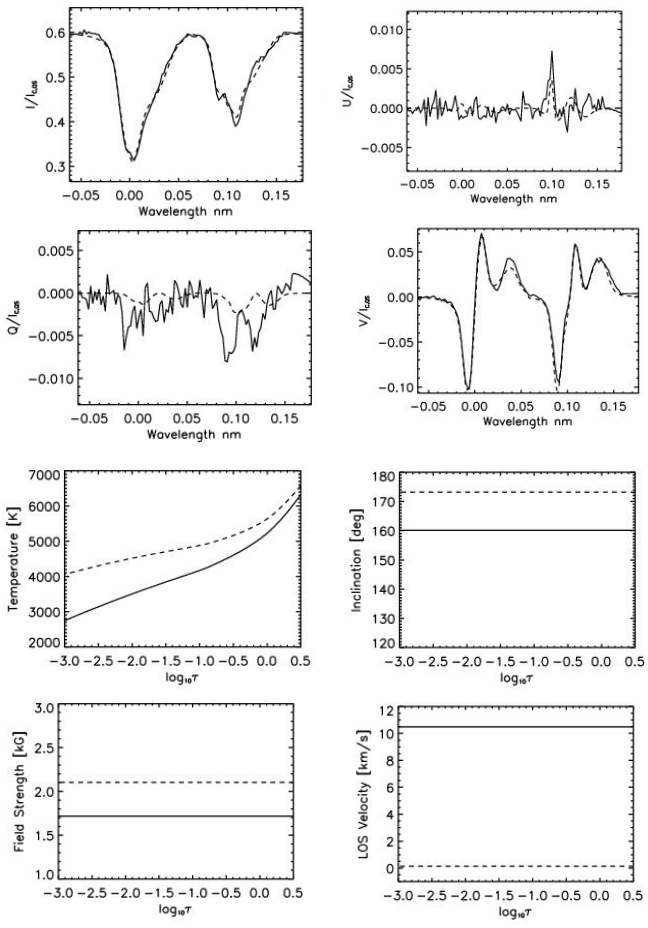

Fig. 15 First and second rows: Observed (solid) and best-fit (dashed) Stokes profiles using a simple two-component atmosphere. Third and fourth rows: Atmospheric stratifications for the two components (solid and dashed lines, respectively).

associated with anomalous circular polarization profiles (Figure 15). An inversion of the observed Stokes spectra reveals velocities of up to 10 km/s, making them the strongest photospheric flows ever measured in light bridges. Some of the downflowing patches are co-spatial and -temporal with brightness enhancements in chromospheric Ca-II H line-core filtergrams. We interpreted the supersonic downflows and the Ca II H brightenings as being due to magnetic reconnection in the upper photosphere/lower chromosphere. For the first time, our results link observations of chromospheric activity over light bridges with their photospheric counterparts.

This work is in collaboration with Dr Luis R. Bellot Rubio, of IAC, Spain.

(Rohan E. Louis, Shibu K. Mathew and P. Venkatakrishnan)

3D evolution of a filament disappearance event observed by STEREO

During a recent campaign JOP 178, a filament disappearance event was observed on 22 May 2008 (Figure 16). Situated in the southern hemisphere, the filament, showed a sinistral chirality consistent with the hemispheric rule. The event was observed by several observatories in particular by THEMIS and USO, Udaipur. A day before the disappearance H-alpha observations, show up and down flow in adjacent locations along the filament were seen (Figure 17) and these suggested plasma motions along twisted flux rope. THEMIS and GONG observations show shearing photospheric motions leading to magnetic flux canceling

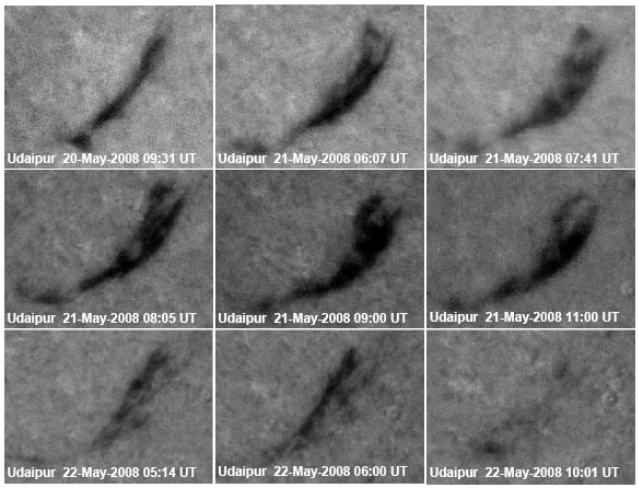

Fig. 16 The evolution of the disappearing filament from 20 to 22 May 2008, as seen in H-alpha filtergrams from Udaipur Solar Observatory. The date and time of the images are mentioned in the bottom of the corresponding panel. The filament is vanishing on May 22 in bottom right image.

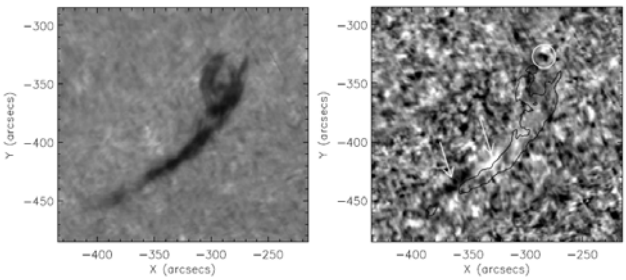

Fig. 17 Intensity and velocity images in H-alpha line observed using MSDP instrument at Meudon Solar Tower during 21 May 2008, 09:00 UT. The left photo shows the line center intensity while the right photo shows the dopplergram overlaid by contours of the filament. The maximum (most white) and minimum (most black) velocities are +800m/s and −200m/s respectively (positive is redshift). The white circle indicates up and downward flows at the end of one foot of the filament. Elongated areas of blue and redshifts suggest some twist along the filament body.

around barbs. STEREO A, B satellites with separation angle 52.4 degrees, gave different views of an untwisted flux rope in He II 304 Å images. We reconstructed the 3D geometry of the filament during its eruption phase using STEREO EUV He II 304 Å images and found that the filament was highly inclined to the solar normal.

He II 304 Å movies show individual threads to be oscillating and rising to an altitude of about 120 Mm with apparent velocities of about 100 km/s during rapid evolution phase. The filament finally disappears (by becoming optically thin to undetectable levels), as the flux rope expands into the corona. However, no CME was detected by STEREO and only a faint CME was recorded by LASCO at the beginning of the disappearance phase during 02:00 UT. This may be due to a partial filament eruption. Further, in Fe XII 195 Å images, bright loops appear beneath the filament prior to the disappearance phase which could be due to magnetic reconnection below the flux rope.

This work is in collaboration with Brigitte Schmieder, Ramesh Chandra and Guy Artzner of Observatoire de Paris, France.

(Sanjay Gosain and P. Venkatakrishnan)

Flare-Associated Decay of Penumbra-Like Structure Near Polarity Inversion Line: Hinode, TRACE and MDI Observations

Photometric decay of photospheric features like sunspot penumbrae have so far been reported only in association

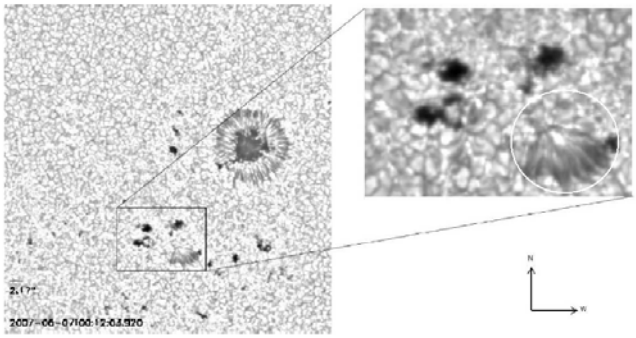

Fig. 18 A sample image taken in G-band filter from Hinode/SOT. The boxed region shows the region of interest. A magnified view of the region of interest is shown on the right side of it. The penumbra-like-feature (PLF) in white circle decays during the flare.

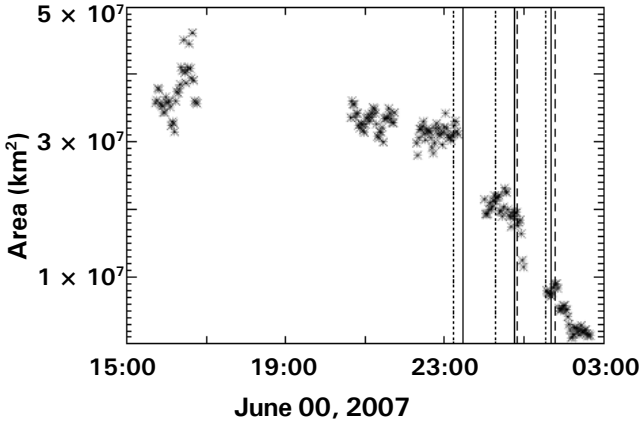

Fig. 19 A plot showing the area of PLF as a function of time. The start (dotted vertical lines), peak (solid lines) and end (dashed) time of the flare are also shown.The first 3 bars are for the C1.7 flare, the next 3 are for B7.6 and the last 3 bars are for the B6.6 class flares occurred at different times. The PLF area decreases at an increased rate during these flares.

with X and M-class flares. Using high-resolution space based observations, provided evidence that such photometric changes are also associated with smaller B-class flares. A rapid photometric decay of a penumbra like feature (PLF) following C1.7 and B7.6 class flares as seen in high-resolution HINODE observations, was identified (Figure 18).

The PLF was located close to a polarity inversion line. The photometric area of the PLF evolves slowly prior to C1.7 class flare and rapidly after the C1.7 and B7.6 class flares (Figure 19), which suggests clearly a relationship between PLF decay and the flare. We notice bright filament and its apparent slow rising motion close to the location of the PLF decay in chromospheric Ca II H images, suggesting a possible relationship between them. The TRACE 171 Å images obtained simultaneously shows a brightening of filament over the PLF. Further, the evolution of magnetic field during PLF decay is studied using the high-resolution line-of-sight (LOS) magnetograms from SOHO/MDI and vector magnetograms derived from Hinode/SOT-SP. The MDI/LOS flux over the PLF region decreased rapidly after the C1.7 class flare. The flux increased marginally after the B7.6 class flare till about 30 minutes followed by a continuous decrease in flux at a rate of 1.4×10^{19} Mx/h. The SOT/SP vector magnetic field in the PLF region before and after the flares show that in addition to the longitudinal field the transverse field component also decreased significantly after the flares, possibly due to decay of PLF.

This work was in collaboration with B. Ravindra of Indian Institute of Astrophysics.

(Sanjay Gosain)

Effect of Polarimetric Noise on the Estimation of Twist and Magnetic Energy of Force-Free Fields

The force free parameter α (also known as helicity parameter or twist parameter), bears the same sign as the magnetic helicity under some restrictive conditions. The single global value of α for a whole active region gives the degree of twist per unit axial length. We have investigated the effect of polarimetric noise on the calculation of global α value and magnetic energy of an analytical bipole. The analytical bipole was generated using the force-free field approximation with a known value of constant α and magnetic energy. The magnetic parameters obtained from the analytical bipole were used to generate Stokes profiles 'from the Unno-Rachkovsky solutions for polarized radiative transfer equations. We then add a random noise $\sim 10^{-3}$ of the continuum intensity (I_c) to these profiles to simulate real profiles as obtained from modern spectropolarimeters such as Hinode (SOT/SP), SVM (USO), ASP, DLSP, POLIS, and SOLIS etc. These profiles with their noise, were then inverted using a Milne Eddington inversion code to retrieve the magnetic parameters. Typically a hundred realizations of this process of adding random noise and polarimetric inversion was repeated to study the distribution of error in global alpha and magnetic energy values. The results suggested that: (1) the sign of α is not influenced by the polarimetric noise and accurate values of global twist can be calculated, and (2) under the force-free conditions, accurate estimation of magnetic energy with uncertainty as low as 0.5% is possible.

(Sanjiv Kumar Tiwari, P. Venkatakrishnan, Sanjay Gosain, and Jayant Joshi)

Helicity at Photospheric and Chromospheric Heights

In the solar atmosphere under certain conditions, the twist parameter α has the same sign as magnetic helicity. It has been observed using Photospheric magnetograms that negative/positive helicity is dominant in the northern/southern hemisphere of the Sun. Chromospheric features show dextral/sinistral dominance in the northern/southern hemisphere and sigmoids observed in X-rays also have a dominant sense of reverse-S/forward-S in the northern/southern hemisphere. It is of interest to establish as to whether individual features have one-to-one correspondence in terms of helicity at different atmospheric heights. We used UBF H_α Images from the Dunn Solar Telescope (DST),and H_α data from Udaipur Solar Observatory and Big Bear Solar observatory. Near simultaneous vector magnetograms from the DST were used to establish one-to-one correspondence of helicity at Photospheric and

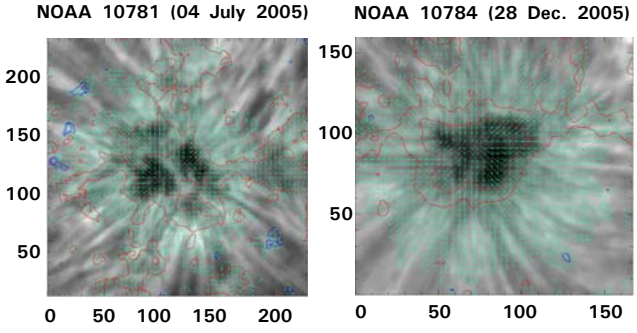

Fig. 20 Two examples of the chromosphere above sunspots, with the photospheric transverse vectors of the same field of view over-plotted on them. The axis divisions are pixel numbers. The contours and vectors show longitudinal and transverse magnetic fields, respectively.

Chromospheric heights. It was concluded that the sign of helicity (positive/negative) derived from global twist present around sunspots in the photosphere has one-to-one correspondence with the (Sinistral/dextral) sense of chirality observed in the associated chromospheric data (Figure 20).

This work was done in the collaboration with Dr. K. Sankarasubramanian of ISAC/ISRO, Bangalore.

(Sanjiv Kumar Tiwari and P. Venkatakrishnan)

Magnetic reconnection during the two-phase evolution of a solar eruptive flare

A detailed analysis of the evolution of an M7.6 flare that occurred near the south-east limb on 24 October, 2003 utilizing a multi-wavelength data set, was carried out. X-ray and EUV observations of the flare from Reuven Ramaty High Energy Solar Spectroscopic Imager (RHESSI) and, Transition Region and Coronal Explorer (TRACE) respectively define two phases of the flare evolution (Figure 21). The first phase was characterized by the altitude decrease of a loop-top (LT) source for about 10 minutes. This was clearly observed in X-ray images below 25 keV and in EUV images at 195 Å. During the second phase, high energy X-ray emission between 25-300 keV originated from two distinct foot-points (FP) sources which correlated with

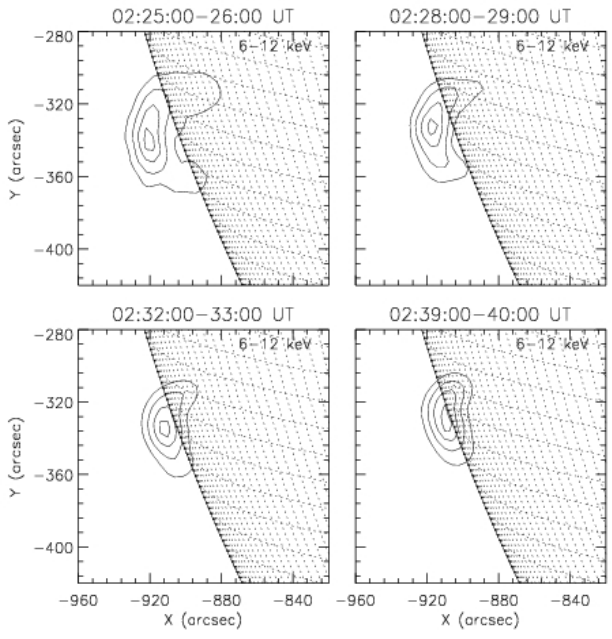

Fig. 21 Sequence of RHESSI 6-12 keV images during the first phase of the flare showing the altitude decrease of the flare loop-top source. The integration time for each image was 1 min. The contour levels are 40%, 60%, 80%, and 95% of the peak flux in each image. The solar limb and heliographic grids are also drawn in the images.

chromospheric flare ribbons in TRACE UV (1600 Å) images and Hα filtergrams. The LT source now shows an upward expansion while the two FP sources separate from each other. The first phase seems to be mostly dominated by hot thermal emission from flaring loops with temperatures T > 25 MK while the second phase is dominantly non-thermal in nature. Observations of the second phase are mostly consistent with the standard flare model while the results of the first phase contains evidence for the "collapsing magnetic trap" effect in solar flare.

This work was carried out collaboration with Astrid Veronig, K-S. Cho, and B.V. Somov.

(Bhuwan Joshi)

Coronal mass ejections and hard X-ray emissions associated with the kink instability

A morphological study of the 2004 August 18 solar eruption that occurred in the active region NOAA 10656 near the west limb using (E)UV data from the Transition Region and Coronal Explorer (TRACE); H_α filtergrams of Big Bear Solar Observatory (BBSO); white light images of Mouna Loa Solar Observatory (MLSO); hard X-ray data of the Reuven Ramaty High Energy Solar Spectroscopic Imager (RHESSI), and microwave data of the Owens Valley Solar Array (OVSA). These provided an excellent set of observations for tracing the early evolution of the coronal mass ejection (CME) from a flux rope emergence to its propagation into space and connected series of events. This was made possible due to the coronameter's field of view down to 1.1 solar radius that overlapped with that of TRACE. This dataset revealed continuously evolving (E)UV, H_α, and WL features that suggested the rise of a small, low-lying loop, its writhing motion, break of the kinked loop at its crossing point, and transformation of the ejecta to the CME. Hard X-ray and microwave sources were found in varying locations with complicated temporal dependence. This was interpreted as being due to two successive flares. During the second flare, a hard x-ray coronal source was detected at the crossing point of the kinked loop. More intriguingly, the kinked loop was apparently broken at the crossing point of the two legs, that indicated a magnetic reconnection at the X-point configuration. After the break of the kinked UV loop, a CME structure shows up in the MLSO field of view, and propagated away from the sun. It was concluded that this CME occurred due to the kink instability.

This work was done in collaboration with K. S. Cho of Korea Astronomy and Space Science Institute, Daejeon, South Korea.

(Bhuwan Joshi)

Estimation of true speed and direction of propagation of CME using SECCHI/STEREO observations

The launch of SECCHI coronagraphs on the twin spacecraft STEREO has made CME observations possible from two vantage points.These observations are useful in reconstructing the 3-D structures and in measuring the true speeds of CMEs. These can lead to improved understanding of the initiation and propagation of CMEs. We applied two techniques to obtain 3-D reconstruction of leading edge of a partial halo CME of 20 May 2007 observed by SECCHI coronagraphs,. Using the 3D height-time technique and the tie-pointing technique based on epipolar geometry. The true speeds and direction of propagation of the CME were estimated. The estimated true speeds were compared with the projected plane-of-sky speeds of the leading edge of the CME derived from LASCO aboard SoHO as well as from STEREO A and B images individually (Figure 22). It was found that true speeds are approximately 1.8 times that of the projected speeds of the CME. A comparison of the two reconstruction techniques show a good agreement, within the measurement errors.

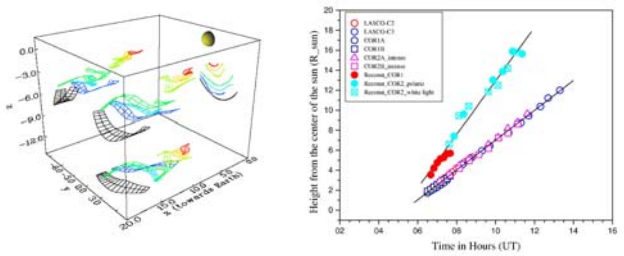

Fig. 22 Left panel: The reconstructed leading edge of 20 May 2007 CME as seen in the COR2 field of view. Here, the strips of the CME surface are colour coded for the different times (viz. 07:37, 08:10, 08:37, 09:37, 10:07, 10:37 and 11:07 UT) from an oblique direction and also projected onto the walls of the coordinate system walls. The coordinate system used is HEEQ.
Right Panel: Height-time plot for a selected feature on the leading edge of the CME of May 20, 2007, in the field of view of different coronagraphs. The lower line denotes the projected path of an identified feature on the leading edge in various coronagraphic fields of view. The upper line represents linear fit to the reconstructed coordinates plotted with time.

From the estimated true speeds, the arrival time of the CME was computed which is close to the actual arrival time inferred from the in-situ measurements with an error of 12 hours. These were compared with the arrival times obtained by various other methods. These also show that the projected speeds measured from single spacecraft (no STEREO) can yield large errors (~70 hours) in arrival time. Our results clearly established that a better estimation of the true speeds of the CME in the Sun-Earth direction is achieved from the 3D reconstruction and therefore has an important bearing on the prediction of the Space Weather. This was the first study involving successful application of reconstruction techniques to the SECCHI/STEREO data for the estimation of true speeds and direction. The implication space weather prediction formulae was also examined.

This work was done in collaboration with Bernd Inhester of Max-Planck Institute for Solar System Research, Germany and Marilena Mierla of Royal Observatory of Belgium, Brussels.

(Nandita Srivastava)

Large photospheric downflows in localized regions of active regions observed during major flare events of solar cycle 23

Solar flares, associated with the active regions, release a large amount of energy within few minutes to hours. Apart

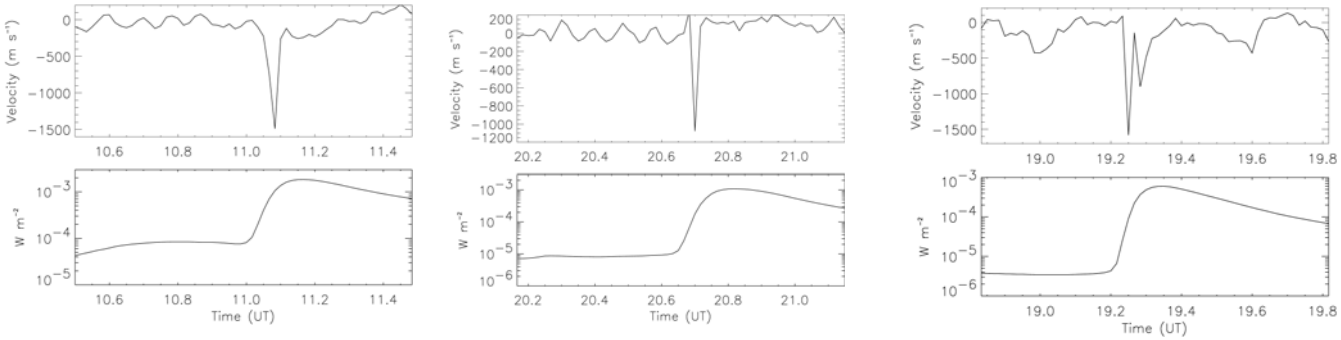

Fig. 23 Plots showing the large solar photospheric downflows appearing during the rise time of soft X-ray flux from the Sun as observed with the X-ray detector onboard the GOES satellite. These plots are for the major flare events of solar cycle 23 which are as follows: (left panel) 28 October 2003 (X17.2 class), (middle panel) 29 October 2003 (X10 class), and (right panel) 6 April 2001 (X5.6 class).

from the high intensity radiations, these produce a large flux of energetic particles which moving at high speeds. We examined the impact of these energetic particles on the solar photospheric flows during flares of different X-ray intensity that occurred in the solar cycle 23. The flare events of 28 October 2003 (X17.2 class), 29 October 2003 (X10 class), and 6 April 2001 (X5.6 class) were used for this study. Analysis of Dopplergrams from SOHO/ MDI and GONG indicate large photospheric downflows (magnitude in the range of 1-2 Km/s) occurring in the localized regions of the active regions during the aforesaid flare events. Figure 23 shows the large velocity flows that appeared during the rise time of soft X-ray flux from the Sun (as observed with the X-ray detector onboard the GOES satellite). It is believed that these large velocity flows are the response of the solar photosphere towards the impact of a shock wave launched ahead of the energetic particles produced during the flare. However, a contamination in the velocity signals obtained from MDI and GONG is expected due to the distortion of the line profile accompanying major flares. Absence of line-profile information, make a definitive statement about the actual magnitude of these flows appearing during the major flares, difficult. However, the future solar missions like MAST (multi aperture solar telescope) and HMI are expected provide quantitative explanations of these events.

(Brajesh Kumar and P. Venkatakrishnan)

Fast MHD Surface/Body Waves In The Solar Corona With Steady Flows: Heating By Viscous And Thermal Dissipation

The effect of steady-flows on the amplitude and the heating rate profile of the fast MHD surface and body waves was examined in inhomogeneous corona. We assumed the equilibrium magnetic and plasma configuration of solar corona as a slab-geometry such that the z-axis of the slab was along the uniform background magnetic field. We allowed for density stratification perpendicular to the direction of background magnetic field. This study evaluated the extent to which fast waves could be collisionally dissipated. Their dissipation by viscosity and heat conduction in the solar corona was evaluated by invoking the presence of steady flow and by comparing the results with minimum required optically thin radiative cooling rate. Only body waves existed for the field-aligned propagation. However, surface wave was present along with body waves for oblique propagation. It was seen that the steady-flows had negligible effect on surface waves. However, it modulated the wave amplitude and thereby the heating rate profile of body waves. The steady flow indicated opposite behaviour for the field-aligned propagating fast body waves as compared to the obliquely propagating body waves. In the case of field-aligned propagation, the anti-parallel flows increased the relative wave amplitude and therefore heating rate, as compared to parallel flows. However, for the oblique propagation an opposite trend was observd. Further, the obliquely propagating body waves were more effective in coronal heating as compared to field-aligned propagating body waves. We also examined the wave amplitude and heating profile of shear waves propagating almost normal to the interface.It was seen that the transverse components (i.e.,u_x and u_y) of shear surface waves were equal and larger than the longitudinal component (i.e.,u_z) by 3 orders of magnitude. The heating rate associated with shear surface wave was several orders of magnitude smaller than the required heating rate. On the other hand, the heating rates associated with shear body waves could provide sufficient energy to balance the coronal radiative losses provided the wave amplitude is of the order of observed non-thermal broadening values.

This work is in collaboration with A. Satya Narayanan of the Indian Institute of Astrophysics.

(V. S. Pandey and P. Venkatakrishnan)

Automatic Detection of Filaments and their Disappearance using Full Disc H_α Images

Filaments are cool and dense regions in the solar chromosphere suspended between regions of opposite

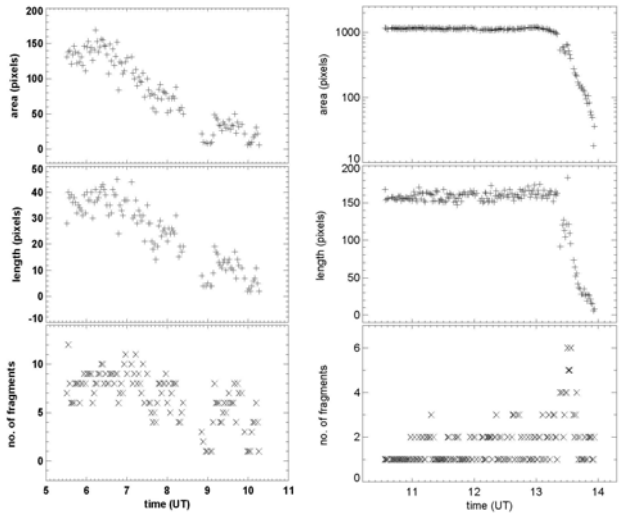

Fig. 24 Total area (top panel), total length (middle panel), and number of fragments (bottom panel) of the filament observed on 2008 Apr 26 (left column) and of the filament observed on 2005 Jan 05 (right column).

photospheric magnetic polarity, and supported by magnetic field. Their lifetimes range from a few hours to several weeks, and they may either disappear slowly or erupt rapidly at the end of it. Such filament disappearance events are now accepted to be associated with coronal mass ejections (CMEs), transients during which mass from the corona is ejected into the interplanetary space. We developed a new algorithm capable of providing a near real-time signal of a disappearing filament observed through the broad-band H_α filter.

As a test of the algorithm, we used H_α full-disc images of filament disappearance for two events: 2008 April 26 from Udaipur Solar Observatory and 2005 January 05 from Kanzelhöhe Solar Observatory. The results of use of the algorithm to the filament disappearance of the two events are shown in Figure 24. We found that the filament on 2008 Apr 26 decreased in area steadily from about 150 pixels to <10 pixels. Correspondingly, its length also decreased from 40 pixels to a few pixels. The numbers of fragments also decreased. On the other hand, the filament eruption on 2005 Jan 05 was rapid. The area as well as length of the filament was almost constant up to 13:06 UT, after which both quantities decreased rapidly. The number of fragments of this particular filament did not change till the filament area was constant. However, as the filament started to disappear, it break up into several fragments could be seen. This number then went down as rapidly as it had risen. At the end only 1 or 2 fragments were left behind.

This study demonstrated that this algorithm can detect filaments and their disappearances. The time for each image to complete the entire sequence of operations is around a minute on a on desktop computer with a 3 GH_z CPU & 2 GB RAM. This implies that the program is suitable for real-time observations on the upcoming instrument at USO.

(Anand D. Joshi, Nandita Srivastava and Shibu K. Mathew)

A Technique for Automated Determination of Flare Ribbon Separation and Energy Release

We present a technique for automatic determination of flare-ribbon separation and energy released during the course of two-ribbon flares. We have used chromospheric H_α filtergrams and photospheric line-of-sight magnetograms to analyze flare ribbon separation and magnetic field structures, respectively. Flare ribbons were first enhanced and then extracted by the technique of 'region growing', i.e., a morphological operator to help resolve the flare ribbons. Separation of flare ribbons was then estimated from the magnetic neutral line using an automatic technique implemented into Interactive Data Language (IDL) platform. Finally, the rate of flare energy release was calculated using photospheric magnetic field data and the corresponding separation of the chromospheric H_α flare ribbons. This method can be applied to measure the motion of any feature of interest (e.g., intensity, magnetic, Doppler) from a given reference point. We applied this technique to the X17/4B flare of 28 October 2003, and found that: (i) Entire ribbon did not move with the same velocity; but different parts of the flare ribbon move with widely varying speeds and directions, (ii) In the areas with stronger fields, the flare ribbon separation got decelerated; because the high magnetic field posed a barrier to the motion of the ribbons, (iii) The magnetic field reconnection (i.e., electric field strength) and energy release rate (i.e., Poynting flux) increased with increase in separation velocity.

(R. A. Maurya and A. Ambastha)

Stray light correction and contrast analysis of Hinode broad band images

The contrasts of features in the quiet Sun are studied using filtergrams recorded by a Broad-band Filter Imager on the Hinode/Solar Optical Telescope. In a first step, the scattered light originating in the instrument was modeled using Mercury transit data. Combinations of four two-dimensional Gaussians with different widths and weights were employed to retrieve the point-spread functions (PSF) of the instrument at different wavelengths. These also describe the instrumental scattered light. The PSF parameters at different wavelengths were tabulated and the observed images were deconvolved using the PSFs. Figure 25 left and Figure 25 right show the observed and deconvolved images, respectively. The corrected images were used to obtain contrasts of features such as bright points and granulation

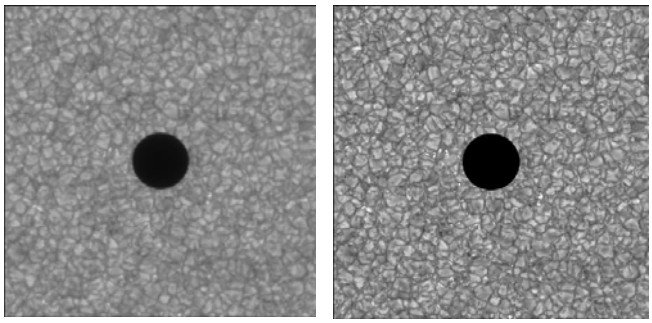

Fig. 25 left and right: Observed left and corrected right G-band images. Each tick mark corresponds to around 2.7 arcsec, the Mercury is at the center of the FOV. Both the images are plotted on the same gray scale.

in different wavelength bands. After correction, RMS contrasts of the granulation of between 0.11 (at 668 nm) and 0.22 (at 388 nm) were obtained. Similarly, bright point contrasts ranging from 0.07 (at 668 nm) to 0.78 (at 388 nm) were determined, which are a factor of 1.8 to 2.8 higher than those obtained before PSF deconvolution. The mean contrast of the bright points is found to be somewhat higher in the CN-band than in the G-band, which confirms theoretical predictions.

This work is in collaboration with Sami K. Solanki and Vasily Zakharov of Max-Planck institute of Solar system Research, Germany.

(Shibu K. Mathew)

GUI based Software for Adaptive Optics system at Udaipur Solar Observatory

The software for operating the Adaptive Optics system essentially comprises 2 programs, written in C.These run simultaneously and communicate with each other through shared memory. The main program called the "Correlation Tracker" determines the local/global tilts of the wavefront from the images acquired by the wavefront sensing camera (Figure 26). These are subsequently converted to suitable voltages and fed to the wavefront correcting elements in a closed loop operation. The second program is called the "control Program" that permts the user to feed various system and performance parameters to the Correlation Tracker. A Graphic User Interface (GUI) for the Control Program allows the user to suitably change system

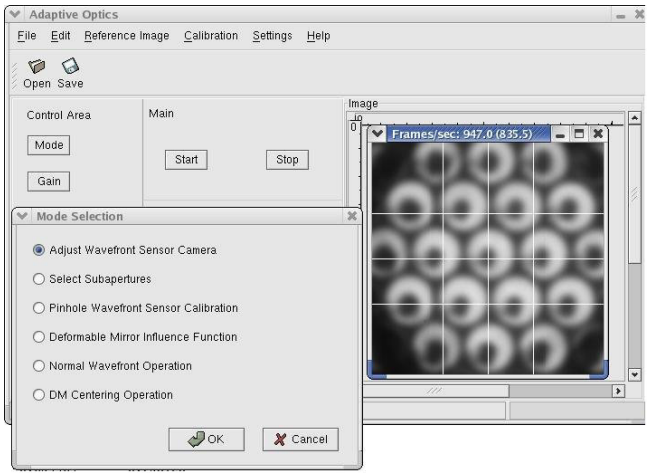

Fig. 26 Snapshot of the GUI based control program for AO system at Udaipur Solar Observatory.

parameters at will (Figure 26). The GUI utilizes the GTK library and allows a more convenient layout of control options in comparison to the previous existing command line mode. The procedure for making a general purpose visualization interface along with the event initiation signals is also developed. The Possibility of improving the system band width by parallelization of the correlation estimation code, utilizing the exiting multi-core processor technology, is being explored.

This work was done in collaboration with Vikram Bhogayta, and Maulik Vadodariya, engineering trainees from Dharmsingh Desai Institute of Technology, Nadiad.

(Adaptive Optics Team at USO)

PLANEX

The main achievement during the year was to place HEX payload onboard Chandrayaan-1. Analysis of the data from Chandrayaan-1 payloads HEX, TMC and HySi are in progress. Laboratory investigations of meteorites, simulation studies to understand natural and induced nuclear radiations from planetary surfaces are other areas of planetary sciences research conducted under the PLANEX program. Design and development of payloads based on nuclear techniques, for future planetary missions of ISRO is the new activity.

Chandrayaan-1 mission: High Energy X-ray (HEX) Spectrometer

Chandrayaan-1 spacecraft was successfully launched from the Satish Dhawan Space Centre, SHAR, Sriharikota by PSLV-XL (PSLV-C11). It carried the High Energy X-ray Spectrometer (HEX) payload that was designed and developed jointly by PRL and ISAC. In the lunar orbit, HEX was successfully commissioned on December 5-6, 2008. The HEX spectrometer has been designed to study natural X-rays from the lunar surface in the energy range 30—270 keV using pixilated Cadmium Zinc Telluride detector arrays. The HEX payload comprises the HEX detector package (HEXDEP) and the HEX Data Interface Package (HEXDIP). HEXDIP interfaces with spacecraft mainframe systems such as, power, telemetry, telecommand and the solid state Recorder (SSR).

The fabrication, testing and environmental checks of the flight Model (HEX-FM) were successfully completed in May 2008.Calibration of the HEX-FM was carried out during its thermovac test in late May 2008. Radioactive calibration sources (^{241}Am, ^{133}Ba and ^{57}Co) were placed inside the thermovac chamber (two at a time in two separate runs). An attempt was made to acquire data from all nine CZT detector modules at temperature step of every 5 °C in the range of 20 °C to –20 °C. Analysis of this data indicated that a significant fraction of pixels was shadowed by the collimator and hence adequate calibration was not available for these pixels. Consequently, a second round of calibration was carried out in August 2008, in which four separate runs were taken at different positions to expose all the pixels to the source and have adequate calibration data for all pixels. Based on these data, a final calibration data base comprising pixel-wise gain, offset and resolution for all pixels with requisite temperature dependent data was prepared.

HEX data processing pipeline software

HEX data processing pipeline software is intended to run automatically whenever the freshly downloaded data is available. Various processing steps involved in pipeline processing are: error checking and filtering of the raw data, extracting data from the HEX binary format, tagging each X-ray event with UTC, fetching the temperature of the particular detector module from the house keeping telemetry data, fetching temperature dependent calibration data for the particular pixel and applying the calibration to obtain the absolute energy for the event, determine the spacecraft ephemeris and attitude using both spacecraft and instrument SPICE kernels and calculating longitude and latitude of the particular event. Finally the software writes the data in standard formats and stores the file in the data archive to be used during later higher level analysis. Level-0 data is written in the PDS format whereas Level-1 data is written in both FITS and PDS formats to facilitate further analysis. The complete data processing pipeline software was developed at PRL and deployed at the ISSDC (Indian Space Science Data Center).

HEX flight data analysis

Regular science operations of HEX started from 22nd February 2009 due to thermal consideration. This was as per the schedule. The ambient temperature was unsuitable for HEX operations during the prime imaging season of December 2008 to February 2009. HEX science data was acquired till 20th April and after that the science operations were stopped again due to thermal issues with the start of the second prime imaging season. Preliminary analysis of the HEX flight data shows that even though the instrument performance is as expected, the background count-rate is more then expected, which required a longer integration period for obtaining significant science data.

This work was done in collaboration with ISAC group.

(Y. B. Acharya, S. Vadawale, M. Shanmugam, D. V. Subhedar, S. Purohit, V. Shah, S. L. Kayastha and J. N. Goswami)

LABNET- A WSN Based Lab Monitoring and Control Network

Wireless Sensor Networks (WSN) are amongsts the exciting and most promising technologies for computing and communications. These comprise a large number of autonomous, tiny, battery-powered computing devices called nodes. As an initiative to develop WSN for Lunar and Planetary Exploration experiments to examine the basic feasibility of the concept, a smart and tiny lab environment monitoring network, LABNET, using wireless sensor network was developed. Wireless sensor nodes with different environmental sensors were placed at vantage points. These permitted remote access of the data to the user and information in real time on the environmental conditions in the laboratory. The focus of this work is to utilize the portability, reliability, flexibility and robustness of the wireless sensor networks to design a system with intelligent sensing for monitoring, control and predictive instrumentation in laboratories. The PLANEX laboratory at PRL houses a number of sophisticated analytical instruments like Electron Probe Micro Analyzer, X-Ray Fluorescence Spectrometer and Inductively Coupled Plasma Mass-Spectrometer and Sample Processing labs that require continuous monitoring and control of ambient temperature and humidity. Sensor nodes of WSN deployed in each of these laboratories act as the end device/routers which collect the data measured by its sensor at specified intervals of time and transmit the data to a coordinator node connected to a remote computer that logs all the data. This data collected from all the nodes enables the remote user to know about the current environmental status in the laboratory. Each sensor node is also equipped with certain switches/actuators to take preventive action in the case of occurrence of an undesired event. In the case of an unpredicted failure or breakdown, the instrument shuts down safely and generates an alert signal to the user. The results clearly show that the onboard sensors are able to detect even fine variations in the parameters temperature and humidity. The results also showed that even smallest of the perturbations is communicated to the remote computer in real time. Further, the communication was continuously established without any failure during the entire observation period which shows the reliability of the sensor network for such an application. Integrating LABNET with internet and GSM grid would be able to provide continuous real-time information and alerts to the user.

(K. Durga Prasad and S. V. S. Murty)

Spectral Reflectance studies of Lunar Swirls:

Lunar swirls are bright sinuous markings on the moon associated with high magnetic field. These are sufficiently strong to prevent solar wind from reaching the surface. Clementine UV-VIS data (~200 m) was used to study two of the known swirls Reiner Gamma (7.9^{0}N, 301^0) in basalt and the Airy crater (18^{0}S, 5.7^0) in the highland region, with an objective to understand soil maturation process due to

micro-meteoritic bombardment only. In both the cases, it was seen that the soils within the swirl region follow a maturity trend different from normal in the adjacent regions that are devoid of magnetic field (Figure 27). This suggested the relevance of solar wind in the space weathering process. Further, the trends merge with the usual trend at high R_{950}/

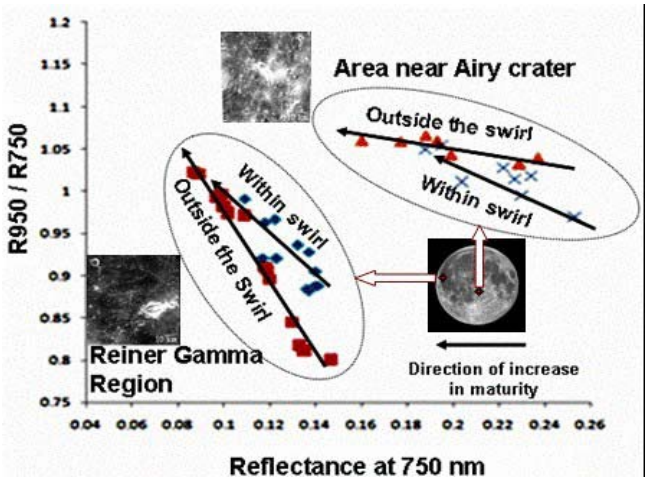

Fig. 27 Scatter plot of NIR ratio (R950 / R750) Vs R750 for soils of Reiner Gamma, swirl near Airy crater, and their nearby regions devoid of appreciable magnetic field, showing differences in maturity trends.

R_{750} and low R_{750} values. This implied the possibility of the presence of soils within the swirl area that have experienced different environmental conditions (possibly due to recent cometary/meteoroid impact) during maturation.

(Neeraj Srivastava)

Identification of new lithologies

A new Approach for Lithological Mapping of Lunar Surface has been formulated, which involves Formulating criteria for discriminating between lithologies on the lunar surface; and Implementation of the adopted criteria in the form of a mathematical code and its validation.

The first aspect was addressed by integrating diverse parameters like mineralogy, elemental composition, maturity, albedo etc. Such a combination (hybrid approach) allowed reliable identification of wide variety of lithologies and in some cases, sub-classes within known lithological classes. The adopted criteria are able to discriminate most of the rock types cited in literature. Such an integrated approach has not been used so far in discriminating among various lithologies.

The second aspect was implemented by writing mathematical code in image processing software ENVI. The code is written in a hierarchical fashion where each output is based on a binary decision. After applying the criteria, the target dataset gets divided into two classes: one for which applied criterion/condition holds true and the other, for which it is false. One can further divide each of the generated classes by applying additional conditions and hence obtain subclasses.

This approach has been tested on two lunar targets: central peaks of crater Tsiolkovsky and Bullialdus for which broad lithological set-up is known. Results from the new approach match with the interpretations of earlier workers. In addition, it was possible to identify lithology of gabbroic affiliation on Tsiolkovsky central peak which has not been reported earlier.

(D. Dhingra)

Analysis of Moon Impact Probe (MIP) Images

Images from the Moon Impact Probe onboard Chandrayaan-1 were analyzed to trace the spacecraft path on the lunar surface. Using available Clementine albedo images and Earth based radar images, part of the covered area was identified. Analysis established that the spacecraft crossed over the limb of Malapert Mountain. Using Clementine images, the scale of various features seen in MIP images was also ascertained.

(D. Dhingra)

Theoretical Modelling of X-ray fluorescence signals for Apollo 12 mare basalt composition in different solar conditions

From the earliest days of space exploration, remote sensing X-ray and gamma ray spectroscopy have been used to obtain elemental composition maps of planetary bodies. Determination of the major elements abundance (such as Mg, Al, Si, Ca and Fe) in the lunar crust (particularly at the far-side highlands, far-side mare basalts, and the ~12 km deep South Pole Aitkin Basin) are considered crucial to understand their evolution. X-ray fluorescence (XRF) is a well established technique for quantitative elemental analysis of samples. The X-ray spectrum of a planetary surface measured from satellite orbit is dominated by a combination of fluorescence X-rays excited by incident solar X-rays, and coherently and incoherently scattered solar X-rays from the lunar surface. Using the forward modelling technique of Jenkins and DeVries in the late sixties, we determined the X-ray signals from prominent K_α lines observable by a collimated 14 cm^2 X-ray detector from a 100 km lunar orbit with ~20 km spatial resolution.

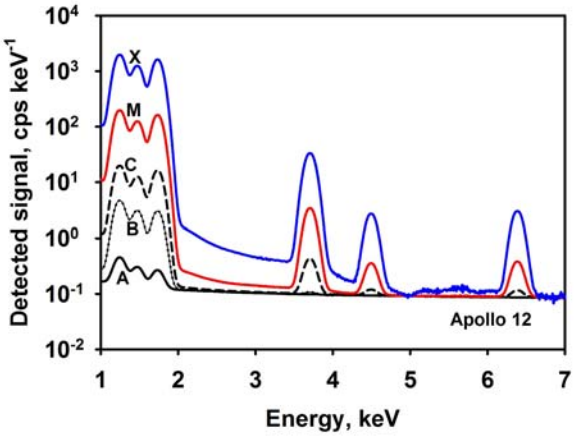

Fig. 28 Expected lunar X-ray spectra for an Apollo 12 basalt composition for different solar activity levels.

The solar models exhibit hardening of the solar X-ray spectrum with increase in solar activity.

Figure 28 shows the expected lunar X-ray spectra for an Apollo 12 basalt composition for different solar activity levels. Our results show that Mg, Al and Si characteristic K_α lines can be observed under all conditions. The Ca line (~3.7 keV) can be differentiated from a fixed background (assumed as ~0.1 cps keV^{-1}) for more energetic solar conditions such as C, M and X flares, whereas Ti (4.5 keV) and Fe (6.4 keV) lines are identifiable only during M and X flare conditions for Apollo 12 basalt composition.

(D. Banerjee)

Sulagiri, the largest meteorite fall in India

On Sept. 12, 2008, around 8:30 hrs. local time, a meteorite fell in the Krishnagiri district of Tamil Nadu, now known as the Sulagiri meteorite. The meteorite fragmented at least once during the transit and led to multiple fall around a cluster of villages near Sulagiri, defining an elliptical shaped strewn field of 3 km along NW—SE direction and 1 km across. The size of the collected fragments increased from W to E. Seven pieces of the meteorite were collected, totalling ~110 kg, making Sulagiri the largest meteorite to have fallen in India. The largest fragment weighed 50 kg and made a crater of ~1.5 m on impact, on the main road (see Figure 29).

Petrological investigation using optical and electron microscopy shows that Sulagiri meteorite comprises orthopyroxene (Opx) and olivine. Chondrules in varying shapes, sizes (200—500 μm) and textures are present, but chondrule boundaries are mostly poorly defined and are often homogenized with coarse to moderately recrystallised matrix. This indicated highly equilibrated petrologic type.

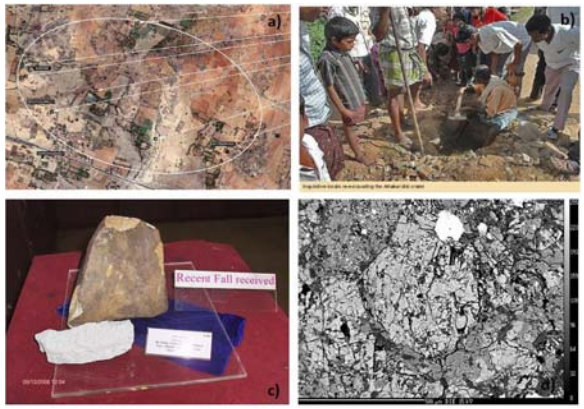

Fig. 29 (a) The strewn field of the Sulagiri meteorite is shown on a Google Map, indicating the direction of fall and location for the collected pieces; b) The crater made on the main road by one of the pieces. Curious villagers are re-exavating the filled crater; c) One of the collected pieces with fusion crust, as well as an interior piece are displayed; d) A back scattered electron (BSE) image of a thin section, shows a chondrule (in the centre) and a metal particle (white) at the edge of chondrule.

EPM studies of thin sections gave average Fa content of olivine as 25.4 and Fs content of Opx as 21.9, which fall at the extreme end of L-chondrites. The bulk chemical composition was estimated using wet chemistry of a homogenized sample gave Ni = 0.72% and Co = 340 ppm. This places Sulagiri in LL class. Uniform Fa content of olivine in matrix and chondrules and the poorly defined chondrule boundaries suggest the metamorphic grade as 6. Radioactivity of a 96 g piece was counted using a 148 cm^3, low background, high purity germanium gamma ray spectrometer in a 10 cm thick lead shield. The specific activities of the radionuclides ^{26}Al, ^{60}Co, ^{22}Na, ^{54}Mn, ^{57}Co, ^{46}Sc, ^{56}Co and ^{58}Co have been calculated using ^{40}K as internal standard (determined against a lab standard, counted in the same geometry) and have been decay corrected to the time of fall. Assuming a spherical shape, the recovered radius is ~20 cm and the pre-atmospheric radius is expected to be ~ 42 cm (for about ~90% mass ablation). ^{26}Al (58.5 ± 3.1 dpm/kg) also suggests the meteoroid radius to be >40 cm. The activity ratio $^{22}Na/^{26}Al$ is nearly unaffected by shielding and expected to anti-correlate with solar activity (with a phase shift). Lower value of this ratio for Sulagiri (1.17) as compared to the values of 1.4 for Innisfree (LL5, fell in Feb. 1977) and 1.6 for Alta'ameen (LL5, fell in Aug. 1977) which fell at solar minimum, suggest a complex exposure history for Sulagiri.

This work has been carried out in collaboration with Geological Survey of India, Kolkata.

(S. V. S. Murty, Suruchi Goel, R. R. Mahajan, P. N. Shukla, K. Durga Prasad, A. D. Shukla and J. N. Goswami)

Planetary and Geosciences

Atmospheric aerosols over India: Chemical characteristics

As a part of an ongoing study, efforts were continued for systematic sampling and characterization of size-segregated ($PM_{2.5}$ and PM_{10}) aerosols from selected sites in India (Mt Abu; Patiala, Kanpur and Shillong). This programme aims to establish the spatial and temporal variability in the abundances of carbonaceous species (EC, OC), water-soluble organic compounds (WSOC), polycyclic aromatic hydrocarbons (PAHs), water-soluble inorganic constituents (WSIC), S-ratio (SO_4^{2-}/ SO_x) and crustal elements (Fe, Al, Mg, Ca). The dominance of agricultural waste burning was evident in aerosols over Patiala based on the concentrations of EC, OC, PAHs and OC/TSP ratio (varying from 0.1 to 0.5). Highest OC and EC concentrations (~10 μg m^{-3}) occurred during 1 to 5 Nov 2008 coinciding with higher $PM_{2.5}$ mass (~250 μg m^{-3}). The contribution of both biomass burning and fossil-fuel emissions is significant over Kanpur and exhibits large temporal variability. The ratio of OC/EC ranges from 3 to 24 and that of WSOC/OC from 0.2 to 0.7. The cause for such large variability is attributed to enhanced secondary organic aerosols (SOA) formation. The *S*-ratio and SO_4^{2-} concentration over Shillong suggests long-range transport of anthropogenic constituents arising from biomass burning.

A comprehensive one-year record of atmospheric chemical constituents from a high-altitude site (Mt. Abu), was documented using measurements of $PM_{2.5}$ (fine) and $PM_{10\text{-}2.5}$ (coarse) aerosols. The WSIC in fine mode aerosols varied from 1.0 to 19.5 μg m^{-3} over the annual seasonal cycle, with dominant contribution from SO_4^{2-}, NH_4^+ and HCO_3^-. A two-fold increase in the abundances of $SO_4^{2-}$and NH_4^+ and their co-variability during wintertime, relative to high-dust conditions in summer, suggests higher contribution from anthropogenic sources in northern India and long-range transport of combustion products (biomass burning and fossil-fuel emissions). In the coarse mode, WSIC ranged from 0.1 to 24.8 μg m^{-3} and its contribution to aerosol mass was consistently low (annual average = 21 %). The predominance of Ca^{2+} and HCO_3^- indicates contribution from carbonate rich mineral dust. The chemical data set also suggests near quantitative neutralization of acidic species (NO_3^- and SO_4^{2-}) by NH_4^+ in $PM_{2.5}$ and mineral dust in $PM_{10\text{-}2.5}$. These chemical transformation process occurring in high-dust, semi-arid regions is crucial for better paramerization of sulphate in atmospheric radiative forcing. Under ICARB-phase II (National Integrated Campaign for Aerosols, Gases and Radiation Budget), intense sampling was also carried out during Jan 2009 on board Sagar Kanya (cruise #254) to assess the atmospheric deposition

of nutrient species (Fe, P and N) and anthropogenic constituents. Preliminary results suggest the dominance of anthropogenic constituents (SO_4^{2-}, Pb and Cd) in the marine atmospheric boundary layer and that the solubility of aerosol Fe is enhanced by the chemical processing during long-range atmospheric transport.

(A. Kumar, K. Ram, T. Francis, P. Rajput, B. Srinivas, R. Rengarajan, M. M. Sarin and A. K. Sudheer)

Atmospheric absorption properties of carbonaceous aerosols

Black carbon (BC) is a primary constituent of ″soot″ and is a major absorbing aerosol species in the atmosphere. BC is also considered as driver of the global warming due to the increase in anthropogenic emissions on a regional to global scale. The mass of the light absorbing carbon (LAC) in atmospheric aerosols is either assessed optically (as BC mass) or thermally (as elemental carbon, EC). Using a thermo-optical EC-OC analyzer, we developed a unique approach to determine the absorption coefficient (b_{abs} Mm^{-1}) and mass absorption efficiency (σ_{abs} m^2g^{-1}) in aerosol samples analyzed from Manora Peak (29.4°N, 79.5°E, ~1950 m amsl). Optical properties (b_{abs} and σ_{abs}) were simultaneously assessed using optical-attenuation (ATN) at 678 nm from a laser source. Measured b_{abs}(equivalent to ATN) indicated a strong linear dependence on thermal EC concentration ($r^2 = 0.75$, $n = 65$) indicating the applicability of Beer-Lambert's law (Figure 30). Further, b_{abs} exhibit a temporal variability with higher values during Sept-Feb and lower during Apr-Aug. Furthermore, the slope (10.4 m^2g^{-1}) of the linear plot (Figure 30) provides a direct estimate of σ_{abs} at Manora Peak. A large temporal variability in σ_{abs} was observed during the sampling period (range: 6.1–18.8 m^2g^{-1}), attributed to the differences in the source regions of aerosols, their composition and mixing state of BC in aerosols. So far, the use of 'site-specific σ_{abs} (as well as associated temporal variability) for BC determination with the optical instruments is not a common practice as it requires two independent measurements of absorption (from optical methods) and EC concentration (from thermal methods). The analytical approach used in this study uses a single instrument (thermo-optical EC-OC analyzer) to infer b_{abs} and 'site-specific' σ_{abs} values.

(K. Ram, M. M. Sarin)

Modulation of atmospheric radiative forcing during dust storm events

A detailed study of optical, physical and chemical properties of aerosols was conducted from Mt. Abu in order to assess

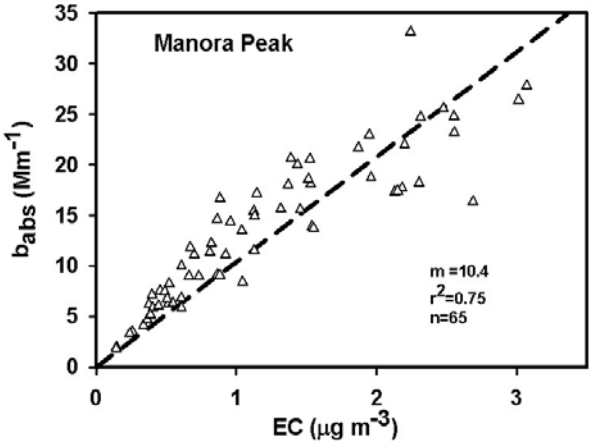

Fig.30 Linear regression plot of absorption coefficient (b_{abs} Mm^{-1}) vs. EC concentration.

the modulation in atmospheric radiative forcing during dust storm events as compared to normal days. Dust storms originating in the Great Thar desert (as identified from the aerosol index (AI) images of the Total Ozone Mapping Spectrometer (TOMS)), modifies the aerosol properties in western India. Measured chemical composition of aerosols indicates that dust loading in the atmosphere increased by a factor of 8; whereas the columnar AOD increased up to 0.29 during the dust events compared to its maximum value of 0.23 during normal days. The Angstrom parameter exhibits negative values up to –0.5 as coarse aerosols are increased significantly during the storm event. This is also reflected by a three fold increase in the scattering coefficient and a net increase in the mean absorption coefficient. Therefore, single scattering albedo decreases from 0.80 during normal days to 0.75 during storm events and the

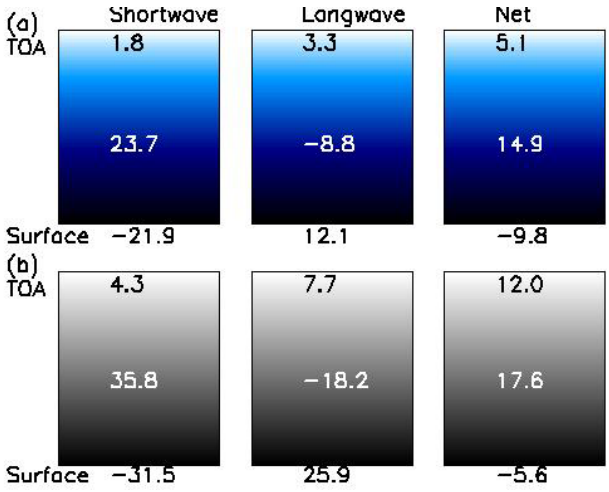

Fig. 31 Modulation in regional atmospheric forcing during (a) normal days and (b) dust events.

shortwave atmospheric forcing increases from 24 to 36 Wm^{-2}. However, the long-wave radiative forcing during the dust events is significantly modulated from -9 to -18Wm^{-2}. Though the dust storm events are episodic in nature, their impact could be significant on the regional atmospheric forcing (Figure 31).

(S. K. Das, A. Jayaraman and M. M. Sarin)

New Instrumentation : Spatially resolved luminescence system

A system for spatially resolved luminescence analysis for the dating of rock surfaces and samples with complex mineralogy, is being developed at PRL. The system comprises an Electron Multiplier CCD camera coupled to a programmed thermal and optical stimulation system, data acquisition and controls. The contol system comprises a micro-controller with a firmware programmed for sensing, controlling and generating two driver signals to control sample temperature and the lightflux incident on it. These signals can be generated individually or in combination and provide six different modes of operations. These operations are executed by firmware that provides for programmable parameters like intensity and duration of stimulation, ramp rate, end point temperature, stimulation temperature etc. The system generates synchronization pulses for activation and de-activation of gas purge valve and trigger the EMCCD camera luminescence image acquisition. In addition the system controls a motorized sample positioning and lifting mechanism. A LabVIEW based application software has also been developed to communicate with the hardware via RS-232 link. The software provides user-friendly operations including sample sequence-editing for automated sample analysis and Excel based file saving facility. A prototype consisting of detection optics for 1:1 imaging of the sample onto EMCCD has been completed and is being tested.

This work was a part of engineering training of Mr. A. Patel and Ms. K. Gandhi, Nirma University and Ms. D.H. Patel and D. Joshi of Charotar Institute of Technology, Changa.

(P. Adhyaru, N. Chauhan, M. S. Shah and A. K. Singhvi)

Extension of Age upper limits of Luminescence Dating

The prospect of extending the upper dating limits of Luminescence Dating using large cm sized quartz grains was explored. So far, Luminescence dating has used 100-200 μm grains that received full quantum of beta and gamma doses from the environment. In this study, the premise, that the interior of these grains receives only the gamma dose and hence approaches saturation over several fold longer time scales, was examined. Towards this end, the variation of beta dose vs. radial depth from naturally occurring ^{40}K, ^{212}Bi (^{232}Th-series) and ^{234}Pa and ^{214}Bi (U-series) was computed using code Monte Carlo n-Particle (MCNP) simulation code. Simulations suggested that at a depth of 2 mm the beta dose is 0.1% of the surface dose. This implies that the removal the external 2 mm skin of the grain can grain interiors that experience only the gamma dose Hence the use of samples from the interior of large grains can extend of the dating range by three to four, as typically gamma dose is about 20-30% of the total environmental dose. Presently, examination of various methodological aspects such as the optical transparency of large grain in respect of their photo-bleaching, etching time and measurement schemes for the interior using the EMCCD system are being examined.

This work was done in collaboration with Dr. P. Selvam and Dr. Y.S. Mayya of the Bhabha Atomic Research Centre, Mumbai.

(N. Chauhan and A. K.Singhvi)

Space Dosimetery

For radiation dosimetry in space, the use of optically stimulated luminescence of Al_2O_3:C has been advocated. To assess its suitability for use in the proposed manned mission, the properties of Al_2O_3:C were examined in respect of charge particle irradiation.The OSL decay shape change with dose and could be explained by de-convoluting the OSL decay in terms of components with different photo ionization cross—sections. The components different dose saturation behaviour that leads to a dose dependent OSL decay. Thus the OSL decay shape of high beta dose sample corresponded to high LET dosed sample. This study has important ramification in the use of Al_2O_3:C in space dosimetry and suggests the need to use only the signal with high photo ionization cross section.

(R. H. Biswas, M. K. Murari and A. K. Singhvi)

Thermal modeling of faults: Insights into thermal resetting of luminescence

In case of faulting event, resetting of luminescence signal takes place by frictional heat generated during slip of rock. To simulate the temperature conditions resulting from fault, temperature profiles were generated using transient thermal modeling. Thermal effects of various slips ($d = 2$ to 8cm) for different values of vertical distances ($z = 1$ and 3mm) from fault plane at fixed depth ($H = 1000$m) and pore pressure factor ($\lambda = 0.35$-0.40), were computed. The time duration of slip was assumed to be 0.3s, typical for low

magnitude earthquakes. Numerical simulation suggested that a minimum total slip of about 2 cm is needed to generate temperature in the range 300—400^{0}C at depth of 1000m. At higher depths even lower slips can provide similar temperature. The thermal profiles indicate that even for the values of the fault parameters corresponding to weak faults, the temperatures at the fault plane can reach 400^{0}C thereby ensuring that the thermal resetting of luminescence signal occurs. This work now provides for development for field criterion for the dating of fault gouges using luminescence.

This work was done in collaboration with Prof. R.N. Singh, National Geophysical Research Laboratory, Hyderabad.

(M. K. Murari and A. K. Singhvi)

Luminescence Applications

Morava River—basin (Czech Republic): Analysis of luminescence ages of Morava river basins sediments was carried out to understand the erosion processes in response to natural and anthropogenic factors. Deposits of ages between 0.3 ka and 4 ka along with historical records enabled delineation of extreme flood events of Morava river basin and its correlation with the climatic evolution of the region.

This work was done in collaboration with Prof. J. Kadlec of Charles University, Prague, Czech Republic and Prof. G. Kocurek, University of Texas, USA.

(D. P. Shinde, M. K.Murari and A. K. Singhvi)

Dating of samples Schirmacher oasis in Antarctica: The moraine sediments of a circular sandy lake in the eastern part of Schirmacher oasis in Antarctic region were studied using OSL. Single Aliquot Regeneration (SAR) and single grain analysis of these highly heterogeneous moraine deposits showed a large dispersion in optical ages. The SAR ages varied from 0.8±0.06 ka and 4.8±0.4 ka to 56.6 ± 5.2 ka to 121.5 ± 17.2 ka. The physical disposition of these samples suggested a weaker ice sheet growth in the Antarctica during the Last Glacial Maximum and a larger extend during the Marine isotopic stage 4.

This work was carried out in collaboration with Dr. R. Asthana of Geological Survey of India, Faridabad and Dr. Rasik Ravindra of the National Centre for Antarctic Research, Goa.

(D. P. Shinde and A. K. Singhvi)

Dating of Paleoseismic events in Himalaya: Paleosesimic investigations around Janauri anticline in NW Himalaya using trench logs, GPR and geomorphic studies indicated two low angle thrust fault strands with displacements of 7.5 m and 1.5 m. Optical dating of displaced stratigraphic units indicated two faulting events, bracketed to between 2600—800 yrs and 400—300 years. This data along with the data on the recent Kangra earthquake enable deduction of the convergence rates in the region.

This work was done in collaboration with Prof. J. Malik, IIT Kanpur.

(D. P. Shinde, N. Juyal and A. K. Singhvi)

Dating of Paleolithic site in South India: Attaripakkam near Chennai has yielded a large suite of Upper and middle Paleolithic artifacts. The artefact bearing horizons and the horizons capping them were dated using OSL of quartz. The ages ranged from 1ka — 40ka, providing first chronometric constraints to these cultures. These ages establish relationship of sediments with archaeological material and facilitate paleo-environmental reconstruction.

This work was done in collaboration with Dr .S. Pappu of Sharma Heritage Centre of Pune.

(D. P. Shinde and A. K. Singhvi)

Dating of Volcanic Ash: The methodology of dating volcanic ash in Indian context has been hotly debated. A volcanic ash at Tejpur in Madhumati river basin, Southern Gujarat was reported recently and the designated as the youngest Toba Tuff (YTT). Dating of Ash layer using ITL MAAD protocol yielded an age of 52±9 ka with ages of 49±4 ka and 68±5 ka for the over and underlying horizons. These ages with a sensitivity correction procedure for athermal fading suggested that the age of the age of volcanic ash was 80±10 ka. This age accords well with the YTT ash date from the Indian peninsula. Ash Horizons from other localities in India are now being examined evolve a routine methodology for the dating of volcanic ashes in the Indian context.

This work was done in collaboration with Dr. R. Raj of M.S. University of Baroda.

(R. H. Biswas, N. Juyal and A. K. Singhvi)

Chronology of fluvial terraces in the Alaknanda basin: Field stratigraphy, sedimentology and luminescence chronology was used to reconstruct the history of sedimentation processes in the Alaknanda basin of Central Himalaya. This fluvial sedimentary processes in the region are influenced, both by the monsoon and by tectonics. The study indicated that the Alaknanda basin witnessed three phases of fluvial sedimentation that are differentiated by vertical offsets during the last 30 ka. Luminescence chronology on the fill sediments bracketed these events between 26 ka-18 ka

(phase-I), 15 ka -7 ka (phase-II) and <6 ka to 0.2 ka (phase-III). The intervening periods witnessed surface uplift which are expressed by the strath surfaces and accelerated incision. Sedimentary architecture of the basin indicates gradual improvement in hydrological condition and is attributed to the strengthening of the summer monsoon after the ice age. Further, a progression in age of the fill terraces was seen. Fluvial sediments >10 ka were not observed proximal to the Main Central Thrust (MCT) whereas, the lesser Himalaya has preserved older fill sediments (~>25 ka). This age progression is attributed to the seismicity and focused rainfall in the vicinity of the MCT. Further analysis is in progress to develop a regional picture of geomorphic response to the Late Quaternary climate and seismicity in the Alaknanda basin.

This work was done in collaboration with Prof. Y.P. Sundriyal and Dr. S.P. Sati of the HNB Garhwal University, Srinagar.

(N. Juyal and A. K. Singhvi)

Inferring microphysical processes in mesoscale convective systems using radar measurements and isotopic analysis

A first attempt was made to exploit the potential of a synergistic use of multiple approaches that inform on microphysical processes underlying precipitation. This was to elucidate short term variations in Mesoscale Convective Systems (MCSs). In a campaign rain samples were collected during the passage of MCSs over Gadanki (a tropical station).Simultaneous use of a powerful VHF radar and disdrometer was made to characterize the vertical structure and drop size distribution (DSD) of precipitation. Besides the convection and transition rain, two distinctly different phases of the stratiform rain are identified with the initial phase characterized by no significant variation in rain integral parameters with time, and dominance of smaller rain drops. Strong radar backscatter, presence of a considerable number of bigger drops, and a gradual increase in rainfall parameters (rapid in the case of mass weighted mean diameter) marks the second phase of stratiform rain. Evaporation of rain drops seems to be significant in both convection and stratiform portions of MCS observed over Gadanki. Observed changes in the temporal variation of the stable oxygen isotope ratios ($\delta^{18}O$) of precipitation are interpreted in terms of microphysical processes leading to isotopic fractionation. The pattern of variability in isotopic abundance is found to be different from convection to transition and to stratiform rain. The rate of isotopic depletion is more (4‰ per 30 min) in convection and in the initial phase of transition rain, which is attributed to amount effect. The present analysis clearly shows that the height (or temperature) and the rain regime of condensation are of paramount importance in determining $\delta^{18}O$. A correlation of $\delta^{18}O$ with rainfall integral parameters stresses the need for caution in interpreting the depleted isotopic ratios as indicative of high rainfall and/ or bigger drops.

This work was done in collaboration with Drs T. N. Rao and D. N. Rao, NARL, Gandaki.

(R. A. Jani, R. Ramesh and R. Srivastava)

Quantification of new production during winter *Noctiluca scintillans* bloom in the Arabian Sea

New data on the nitrate, ammonium, rates of urea uptake and *f*-ratios for the eastern Arabian Sea (10° to 22°N) were generated during the late winter (northeast) monsoon. These included regions of green *Noctiluca scintillans* bloom. A comparison of N-uptake rates of the *Noctiluca*— dominated northern zone to the southern non-bloom zone indicated the presence of two biogeochemical regimes during the late winter monsoon: highly productive north and less productive south. Conservative estimates of photic zone-integrated total N-uptake and *f*-ratio are high in the north (~19 mmol.Nm^{-2} d^{-1} and 0.82, respectively) during the bloom, and low (~5.5 mmol.$Nm^{-2}d^{-1}$ and 0.38 respectively) in the south. The total data implied persistence of high N-uptake and *f*-ratio during blooms year after year. This quantification of the enhanced seasonal sequestration of carbon is an important input to global biogeochemical models.

This work was done in collaboration with Drs. M. Raman and R. M. Dwivedi, SAC, Ahmedabad.

(S. Prakash and R. Ramesh)

Centennial rainfall variations in the southern Western Ghats

Studies of rainfall variations usually focus on large regions that not useful for agricultural purposes in smaller regions of extreme rainfall variability. With this view, non-IMD time series obtained from private farms in the southern Western Ghats, where cardamom and vanilla are grown, were analysed. These species are sensitive to moisture availability and atmospheric humidity. The semiarid cardamom hill slopes showed a statistically significant decreasing trend of ~3 mm per year during the last three decades. Unless conservation and mitigation efforts are undertaken this will have an adverse effect on cardamom and vanilla cultivation. It has been reported earlier that the southwest monsoon-El Nino relationship has weakened in the recent past. The opposite is observed by us for the north-east monsoon dominated regions. In the earlier decades there is no significant effect of El Nino, but the relationship has become stronger in the recent years.

This work was done in collaboration with Dr. M. Murugan, NIAS, Bangalore.

(R. Ramesh)

High resolution monsoon reconstruction using oxygen isotopes in teak trees from southern India

From the intra-ring analysis of teak trees from central India, it can be concluded that $\delta^{18}O$ of rainfall and relative humidity during growing season are important parameters deciding $\delta^{18}O$ of teak trees. During the main growing season, $\delta^{18}O$ of rainfall alone, and during the early and late growing season, relative humidity along with $\delta^{18}O$ of rainfall plays a crucial role in deciding $\delta^{18}O$ of tree rings. The observed and the model calculated intra-ring $\delta^{18}O$ values of teak tree from southern India appear to suggest that $\delta^{18}O$ values associated with the main season and the end of the growing season can be related to the SW and NE monsoon rainfall. This offers new possibility of reconstructing both monsoons by high-resolution intra-ring isotope analysis. As the trees can store signatures of rainfall with seasonally varying $\delta^{18}O$, care in the interpretation of inter-annual variation in $\delta^{18}O$ from such areas, is called for. Varying amounts of isotopically different rains are likely to affect the bulk tree ring isotope ratios. For interpreting inter-annual variation in $\delta^{18}O$ and using it for reconstructing past rainfall, issues like photosynthates carried over from the previous year, enriched $\delta^{18}O$ values of tree ring due to rainfall in the late growing season and rainfall with seasonally varying $\delta^{18}O$ should be considered and deconvoluted. Past rainfall was successfully reconstructed for central and south India for a time up to 1824 AD and 1743 AD, respectively.

This work was done in collaboration with Dr. A. Bhattacharyya, BSIP, Lucknow, H. Borgaonkar, IITM, Pune, and M.S. Sheshshayee,UAS, Bangalore.

(S. Managave and R. Ramesh)

Carbon isotopic variations in fluid-deposited graphite

Carbon isotopic composition of fluid-deposited graphite in a metamorphic terrain can be used as a tracer for the sources of fluids, their compositions and temperatures of graphitization. Due to isotopic fractionation during precipitation, invariably the $\delta^{13}C$ of graphite shows a large spread. This makies it necessary to understand these processes. Using a novel quantitative approach, involving Rayleigh isotope fractionation during formation of graphite from a realistic multicomponent metamorphic fluid, we could simulate the observed $\delta^{13}C$ spread in fluid-deposited graphite. Results reveal that most graphite crystallize from a mixed CO_2–CH_4 fluid that acquires its isotopic composition from a variety of sources like organic matter, carbonate, mantle degassing or variable mixtures of these.

(J. S. Ray)

Volcanological studies of Barren Island, India

Barren Island is the only active volcano of India, located in the Andaman Sea. Extensive volcanological work during three field trips (2007-2009) provided new results.The volcano is built of prehistoric lava flows that are dominantly basalt and basaltic andesite, with minor andesite. These flows are intercalated with volcaniclastic deposits comprising tuff breccias, and ash beds deposited by pyroclastic falls and surges, exposed along a roughly circular caldera wall. There are indications of a complete phreatomagmatic tephra ring around the exposed base of the volcano. A polygenetic cinder cone has existed at the centre of the caldera and produced basalt-basaltic andesite *aa* and blocky *aa* lava flows along with tephra, during historic (1787–1832) and four recent eruptions (1991, 1994–95, 2005—06, 2008—09). The recent *aa* flows include a toothpaste *aa* flow, with tilted and overturned crustal slabs carried atop an *aa* core, as well as locally developed tumuli-like elliptical uplifts with corrugated crusts. Multiple evidence suggest that this belongs to either of the 1991 or 1994–95 eruptions. The volcano is currently active, erupting lava and tephra. We suggest significantly different interpretations of several features of the volcano as compared to previous workers. Volcanology and eruptive styles of the Barren Island volcano lays the ground for a detailed geochemical-isotopic and petrogenetic work, and provides clues to clues to the future activity of the volcano.

This work was done in collaboration with H.C. Sheth of IIT Bombay and R. Bhutani of Pondicherry University.

(J. S. Ray, Alok Kumar)

Climate Control on Erosion: Evidences from the Ganga Plain and the Bay of Bengal sediments

Impact of climate on erosion in Himalayan region was studied using Sr and Nd isotopic composition of sediments from cores in Ganga Plain and the Bay of Bengal. $^{87}Sr/^{86}Sr$ and ε_{Nd} of sediment samples from a 50m core from near Kanpur (spanning past ~100 ka of sedimentation) ranged between 0.72701 and 0.76708 and −14.4 and −16.6 respectively. Sediment sources to the core site are Higher and Lesser Himalaya and the observed variations in the isotope compositions result from the variations in their mixing proportions. The Sr and Nd isotope compositions exhibit two significant excursions,at ~20 ka and at ~ 70 ka (Figure 32). These excursions coincide with periods of

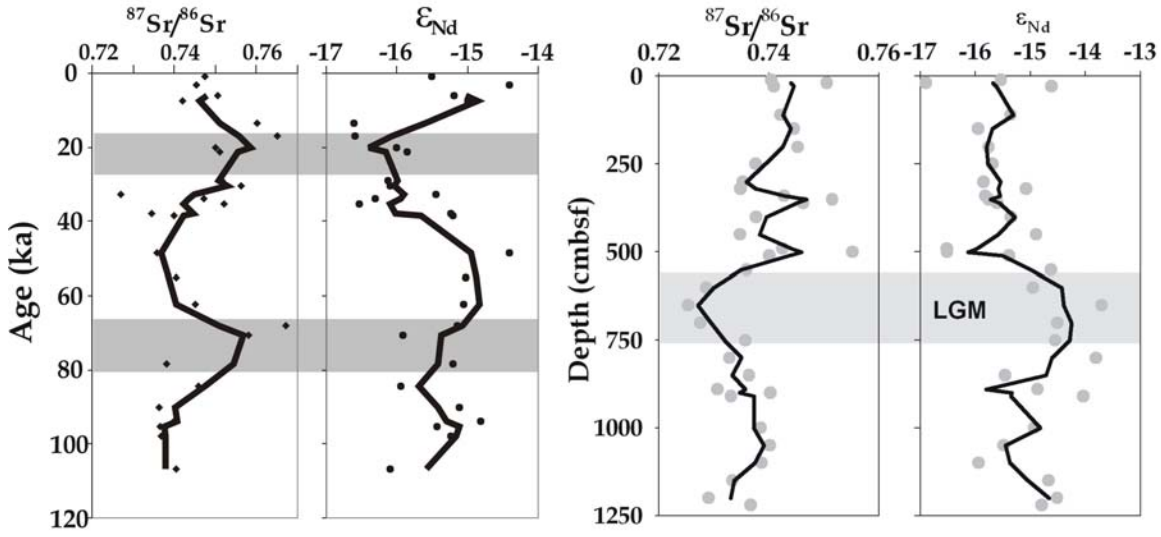

Fig. 32 Nd and Sr isotope variation in sediment core from Ganga Plain (left) and the Bay of Bengal (Right)

minimum precipitation with larger glacial cover over the Himalaya indicating the direct influence of climate in reducing the proportion of sediments from the Higher Himalaya at the core site. Further, this study indicates that the time lag, between transfer of sediments from Himalaya to the Plain is short.

Similar to the Ganga Plain, samples from a 12m sediment core from the Bay of Bengal also show significant variations in Sr and Nd isotope composition with depth (time) indicating a variability in their provenance. Lower $^{87}Sr/^{86}Sr$ ratio and higher ε_{Nd} of sediments during the Last Glacial Maximum (LGM) suggest decreased sediment contribution from the Himalaya to the Bay of Bengal. This could be due to combined influence of reduced SW monsoon coupled with larger extent of glaciation over the Higher Himalaya during LGM. This is analogus to the inferences from the Ganga Plain. These studies indicate that climate had controlled erosion in the Himalaya.

This work was done in collaboration with Profs. S.K. Tandon and R. Sinha and that from the Bay of Bengal with Dr. V. Ramaswamy.

(Waliur Rahaman, Sunil Kumar Singh and Gyana Ranjan Tripathy)

Isotopic, geochemical and mineralogical studies of alkaline/saline soil in the Ganga Plain: Impact of their dissolution on silicate weathering rates in the Ganga basin

Silicate erosion and associated CO_2 consumption rates were estimated using Na* (chloride corrected Na) as a proxy under the assumption that Na* is exclusively derived from silicates. This approach could be prone to uncertainties in the Ganga Plain as it contains alkaline/saline soils. The importance of these soils in contributing to Na* is not fully evaluated and if found important, the estimates of silicate weathering and CO_2 consumption for the Ganga basin could be over estimated. A detail study of these alkaline/saline was initiated to characterise their chemical and isotopic composition and to evaluate their role on the major ion budget of the Ganga. Soil samples from the Plain and Peninsular drainage of the Ganga along with surface waters draining them were analyzed. Several water samples had high pH (up to 9.6) and high conductivity, indicating significant concentration of dissolved salts, most likely from these soils. These soils have 0.1 to 4 wt% of water leachable Na and 0.4 to 12 wt% of HCO_3. $^{87}Sr/^{86}Sr$ ratio of the soils ranges between 0.720898 and 0.722966 and is similar to the values (0.721246 – 0.722364) in waters draining them. This suggest that these soils can be a source of Na, Sr and HCO_3 etc to the Ganga river. The impact of this on earlier estimates of silicate weathering rate and associated CO_2 consumption is being assessed.

(Jayati Chatterjee and Sunil Kumar Singh)

Dissolved $^{87}Sr/^{86}Sr$ in the Tapi and Mandovi Estuaries: Role of Submarine Groundwater Discharge

Sr concentrations and isotope composition of the Mandovi and Tapi estuaries along the salinity gradients were measured using TIMS, ISOPROBE-T. Sr concentration in these estuaries varies linearly with salinity indicating its conservative behaviour. However, a more precise Sr isotope measurements on these waters show that Sr behaves as a non-conservative tracer. In both the estuaries, the $^{87}Sr/^{86}Sr$ deviates from the linear trend on a mixing plot in the higher salinity region. In the Mandovi estuary, the departure

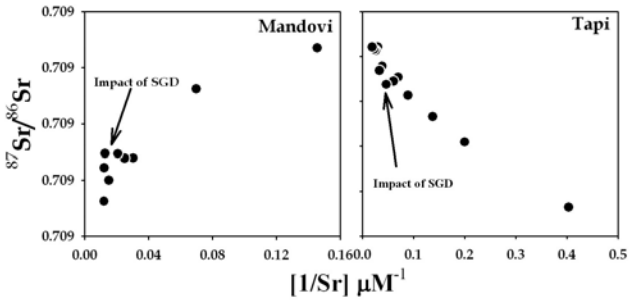

Fig. 33 $^{87}Sr/^{86}Sr$ vs Sr in the Mandovi and Tapi Estuaries

of the $^{87}Sr/^{86}Sr$ is positive whereas in the Tapi it is negative (Figure 33). These trends can result from a supply of submarine groundwater. Continental Sr in the Mandovi is more radiogenic compared to seawater and hence the deviation is positive, whereas in Tapi the deviation is negative as the continental Sr is less radiogenic compared to seawater. This study, for the first time, shows the direct evidence of SGD on Sr budget of seawater. It is planned to extend this study to other elements and isotopes to evaluate the role of SGD in these estuaries.

(Waliur Rahaman and Sunil Kumar Singh)

Biogeochemistry of trace elements and isotope in the Arabian Sea, Bay of Bengal and the Southern Ocean

Trace elements and isotopes (TEIs) play vital roles as nutrients and as tracers of the contemporary and the past oceanic processes. A knowledge of the diverse sources and sinks of micronutrients, their transport and chemical form in the ocean are needed to understand their biogeochemical cycling. Due to its geographical setting and the Southwest monsoon, Arabian Sea is one of the highly productive basins of the world. It has a perennial water column anoxia and related denitrification. The Bay of Bengal receives large amounts of freshwater and particulate matter. Water stratification in the Bay of Bengal inhibits productivity. Productivity in the Southern Ocean is limited due to inadequate supply of trace elements. A comprehensive study to understand the various aspects of biogeochemistry of the TEIs in the Indian and the Southern oceans has been initiated. Many seawater profiles have been sampled in the Arabian Sea and in the Bay of Bengal onboard *Sagar Sampada* during 2007 and 2008. Preliminary results from the Arabian Sea and Bay of Bengal for Re, Mo, U and Ba indicate conservative behavior in the Arabian Sea.

Some of the cruises taken as part of this study are :

1. *Sagar Sampada*: Arabian Sea and Bay of Bengal during November 10 to December 2, 2008; Participants: Ravi Bhushan (Chief Scientist), J.P. Bhavsar, Vineet Goswami, Satinder Pal Singh, Jayati Chatterjee and B. Srinivas

2. *Akademik Boris Petrov*: Southern Ocean during Feb 12 to April 14, 2009 Participants: Rohit Srivastava (Deputy Leader), Navin Gandhi, Amzad H. Laskar, Vineet Goswami and Jayati Chatterjee.

Fig. 34 Cruise Track and sampling in the Southern Ocean.

Cruise track is shown in Figure 34. Surface and depth profile samples were collected all along the cruise for Trace Elements and Isotopes measurements. These waters were filtered and one aliquot was acidified onboard for TE measurement. Large volume samples were processed onboard using either iron co-precipitation or C18 cartridge for REE separation.

(Ravi Bhushan, Jayati Chatterjee, Vineet Goswami, Satinder Pal Singh and Sunil Kumar Singh)

Sulphur isotope compositions of volcanic sulphate in Antarctic ice cores

Reconstruction of past volcanism from glaciological archives uses measurement of sulphate concentrations in ice. This however does not allow a proper evaluation of the climatic impact of an eruption because of the uncertainty in classifying if the influence of the event extended to stratosphere or troposphere. We used anomalous sulphur isotope composition of volcanic sulphate to identify stratospheric eruptions over the last millennium. Theappplicability of this new approach was validated using 10 intense volcanic signals in ice cores from Dome C and South Pole, Antarctica. Of the 10, the sulfur isotopes results classified seven as stratospheric eruptions. Of these seven, three are kown to be stratospheric (Tambora, Kuwae, the 1259 Unknown Event). Identification of three unknown events (circa 1277, 1230, 1170 A.D.) and the Serua eruption as stratospheric eruptions, for the first time suggests that they could have had significant climatic impact. Further the sulphur isotope compositions records of the Kuwae and the 1259 evet was different at South Pole and Dome C samples.

Differences in sulphate deposition and preservation patterns between the two sites can explain these discrepancies. This study shows that an anomalous sulphur isotope composition of volcanic sulphate in ice core indicates a stratospheric eruption, but the absence of such composition does not necessarily lead to the conclusion of a tropospheric process because of differences in the sulphate deposition on the ice sheet.

This work was done in collaboration with M Baroni, J Savarino (Laboratoire de Glaciologie et Géophysique de 1'Environnement, Université Joseph Fourier, CNRS, Saint Martin d'Héres, France), J Cole-Dai (South Dakota State University, Brookings, South Dakota), M H Thiemens (University of California San Diego, La Jolla, CA, USA).

(Vinai K Rai)

***In-situ* Iron fertilization experiment in the Southern Ocean**

The Indo-German ocean iron fertilization experiment (LOHAFEX) was carried out from the German research vessel "Polarstern" in the southwest Atlantic from January to March 2009. A 300 km^2 patch of ocean inside an eddy was fertilized with 4 tons of dissolved iron and its effect on the plankton and on ocean chemistry including concentrations of carbon dioxide and other radiatively important gases was followed continuously for 39 days.

An essential parameter of the progress of the induced plankton bloom is the rate at which particulate matter, especially POC is exported from the surface mixed layer to greater depths. Repeated measurements of the integrated ^{234}Th depletion in the surface waters allow quantifying the

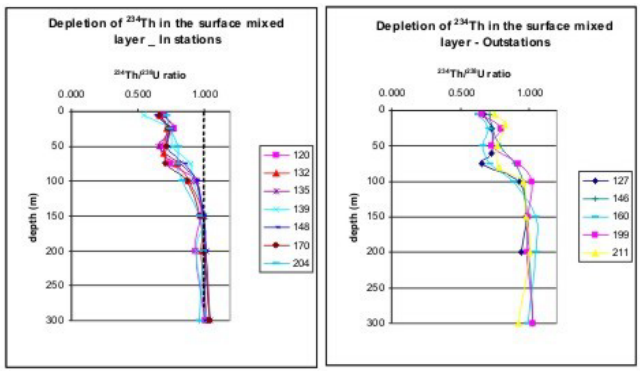

Fig. 35 Seawater total ^{234}Th (dissolved + particulate) profiles from the In and Out stations from the patch location after iron fertilization. The vertical dashed line represents ^{234}Th:^{238}U radioactive equilibrium.

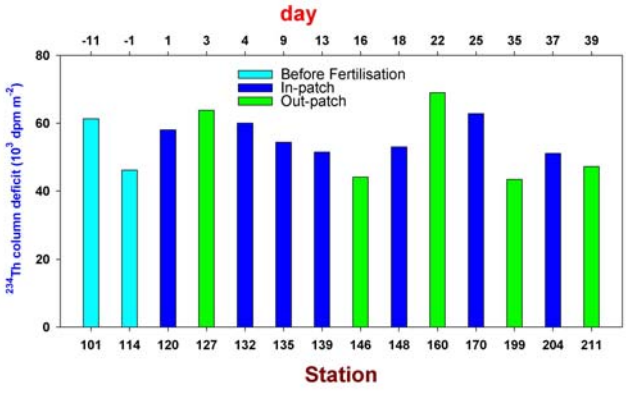

Fig. 36 Measured ^{234}Th deficit in the water column (0-100 m) from the stations in and out of the fertilized patch in the South Atlantic Ocean. The days indicated above are the elapsed days from the first iron fertilization.

downward flux of particulate ^{234}Th out of the surface water. In order to convert this flux to a carbon flux we determined the POC/^{234}Th ratio of large suspended and of sinking particles. Preliminary, uncorrected, on-board results do not show any change in the ^{234}Th depletion with time and no difference between in and outstations was seen (Figure 35). The ^{234}Th depletion in the upper 100 m remained at ~ 5.7 dpm cm^{-2} (Figure 36) implying a steady state ^{234}Th export flux of 1600 dpm m^{-2} d^{-1}. With a POC/^{234}Th ratio of 5 μmol dpm^{-1}, this amounts to carbon export of 100 mg m^{-2} d^{-1}.

The experiment has provided new insights on how ocean ecosystem functions has dampened the hopes on the potential of the Southern Ocean to sequester significant amounts of carbon dioxide from the atmosphere and thus help mitigate global warming. As expected, addition of iron stimulated growth of the phytoplankton whose biomass was doubled within the first two weeks, by taking up CO_2 from the water. However, contrary to expectations, further growth of the phytoplankton bloom ceased due to increasing grazing pressure of abundant, small crustacean zooplankton (copepods), after which the planktonic ecosystem entered a recycling mode. As a result, further CO_2 uptake declined and only a modest amount of carbon sank out of the surface layer by the end of the experiment. Hence, the transfer of CO_2 from the atmosphere to the ocean to compensate the deficit caused by the LOHAFEX bloom was smaller than in most previous experiments. The iron-fertilized patch attracted large numbers of zooplankton predators belonging to the crustacean group known as amphipods.

This work is done in collaboration with S W A Naqvi (National Institute of Oceanography, Goa) and Michiel Rutgers van der Loeff (Alfred Wegener Institute for Polar and Marine Research, Bremerhaven, Germany).

(R. Rangarajan)

Temporal variations in isotopic signatures of cave drip water

Climate reconstruction using speleothems requires knowledge of how oxygen isotopes vary seasonally in water dripping in cave galleries. We have been collecting seasonal samples of drip waters from Kotumsar cave (19°00'N, 82°00'E) in Chhattisgarh and Belum cave (15°06'N, 78°06'E) in Andhra Pradesh. Results (Figure 37) indicate that: (i) during the monsoon season, dripping waters have significantly depleted oxygen isotopic composition in Belum cave. Therefore, speleothems from

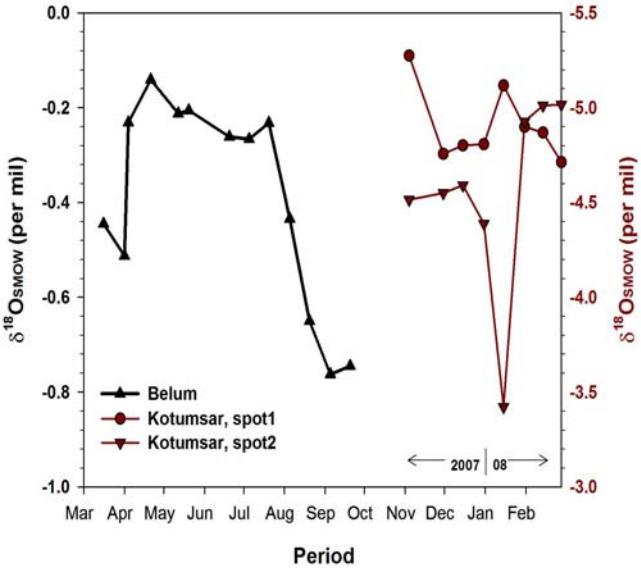

Fig. 37 Oxygen isotope ratios in the seepage water collperiodically during 2007 and 2008 from the tip of wet spots in Belum and Kotumsar caves.

this cave would show a clear signal of past rainfall variations. Drip water during winter months from two spots in the deeper parts of Kotumsar cave gave opposite trends in isotopic variations, indicating internal coupling between micro-reservoirs which needs further investigations.

This work is in collaboration with the University of Hyderabad, Hyderabad.

(R. A. Jani, R. Ramesh, M. G. Yadava)

Dripping durations and their seasonal behaviour in a limestone cave

Hydrological pathways in a cavern need investigation to understand water residence time and holding its capacity. Observing the dripping duration is a simplest way to address these.

Three spots, dripping all the time, in a cave in the Kanger Valley National Park (KVNP, 19°00'N, 82°00'E), Chhattisgarh, were monitored for a year-long variations in drip durations (time between two consecutive drips). Their temporal variations (Figure 38) indicate that during rainy months dripping is slow whereas during lean seasons it is fast, behavior opposite to what is generally expected. This suggests that during wet seasons when soil pores are filled with water, their cohesive nature suppresses drainage of stored water.

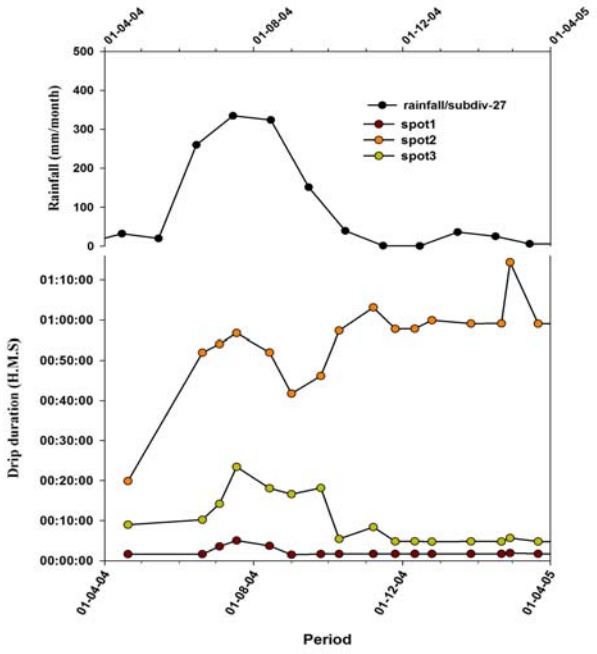

Fig. 38 Seasonal variations in the drip duration during 2004-05 under three wet spots of a cave area which is part of sub division-21, is shown at the top.

(R. Ramesh, M. G. Yadava)

Upwelling rate estimates for the Arabian Sea and the Equatorial Indian Ocean based on bomb radiocarbon

Radiocarbon measurements in water column of the Arabian Sea and the equatorial Indian Ocean during 1994, 1995 and 1997 was carried out to assess the temporal variations in bomb ^{14}C distribution and its inventory in the region with respect to GEOSECS measurements of 1977—78. Four GEOSECS stations were reoccupied (three in the Arabian Sea and one in the equatorial Indian Ocean) during this study, with all of them showing increased bomb ^{14}C penetration along with decrease in its surface water activity (Figure 39). The upwelling rates derived by model simulation of bomb ^{14}C depth profile using the calculated exchange rates ranged from 3—9 m yr^{-1}.

The western region of the Arabian Sea experiencing high wind-speed has higher estimated upwelling rates. However, lower upwelling rates obtained for the stations occupied during this study could be due to reduced ^{14}C gradient compared to that during GEOSECS sampling.

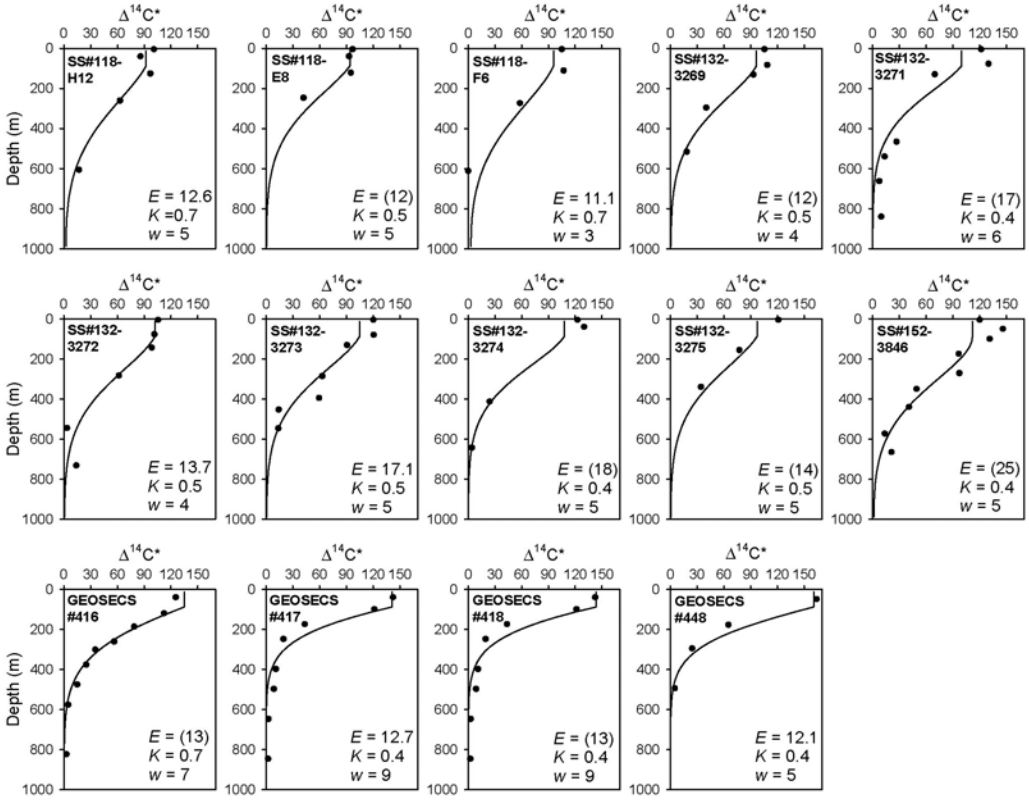

Fig. 39 Distribution of $\Delta^{14}C^*$ (excess bomb ^{14}C) versus depth for different stations. The solid line represents the simulated curve based on 1-D model for the exchange rate (E), eddy diffusivity (K) and upwelling velocity (w).

This work was carried out in collaboration with Dr. K. Dutta, IOP, Bhubneshwar.

(R. Bhushan)

Paleo-productivity variations in the Bay of Bengal during the last 40kyrs

Bay of Bengal sediments provide unique records of erosion of the Himalayas as the Ganga-Brahmaputra river system discharge huge loads of sediments to the Bay of Bengal. However, there have been changes and variation in the discharge fluxes of the sediments due to the climatic changes during the past. Also, it is reasonably established that the SW monsoon was weaker during the Last Glacial Maximum (LGM). Intensification or weakening of the SW Monsoon has modified the surface productivity in the region. Two sediment cores, from the central Bay of Bengal (4032) and the southern Bay of Bengal (4040) were analysed. These cores were ^{14}C dated using AMS on planktonic foraminiferal separates at NSF-AMS Facility, the University of Arizona, USA. Both cores show enhanced sedimentation after LGM. A constant increase in the $CaCO_3$ concentration is observed in both the cores since LGM indicating increase in surface productivity due to intensification of the SW Monsoon. The variations in organic carbon (C_{org}) can be interpreted in terms of its preservation as a function of changes in sedimentation rate and partially to the variation in the overhead productivity. Higher values of $\delta^{13}C$ for all the C_{org} in the core 4032 are indicative of enhanced detrital flux post LGM. All the productivity proxies viz. Ba, Ca and Sr show increase in productivity since LGM attesting to the intensification of the SW monsoon since LGM.

In collaboration with Drs. A.J.T Jull and G.S. Burr of NSF-AMS Facility, University of Arizona, Tucson, USA for the AMS radiocarbon dates and with Dr. R. Agnihotri, NIO, Goa for isotopic analyses.

(R. Bhushan)

High Resolution Reconstruction of Monsoon Variability from the lake sediments in Central Himalaya

A study on the reconstruction of monsoon variability during the Holocene was initiated in the Central Himalaya using shallow lake sediments located in the south of the Main Central Thrust (MCT) also known as the Southern Mountain Front (SMF). SMF is an orographic barrier for the northward penetration of the southwest summer monsoon. The lake is located on a saddle at 2200 m at Benital in the Pinder river basin. The lake developed on the anticline hollow carved by periglacial process in which a 350 cm deep trench was dug for sedimentology, geochemistry, stable isotope, mineral magnetism and radiocarbon dating. Radiocarbon dating of organic rich layer shows that the samples at depth 270 m was deposited at ~10050 cal yr BP and the sample at 70 cm deposited at ~1320 cal yr BP. Based on the age-depth model the sedimentation rate varied between 1.1 mm/yr to 5.3 mm/yr (during 1320 to 9050 cal yr BP) and between 5.3 to 15.3 mm/yr 9050 cal yrs BP beyond). Work on environmental magnetism and other geochemical parameters is in progress.

This work was carried out In collaboration with Dr. S.P. Sati of H.N.B. Garhwal University, Srinagar.

(R. Bhushan, Navin Juyal and A. D. Shukla)

IWIN National Programme

The Hydrology Group is coordinating the National Programme on Isotope Fingerprinting of Waters of India (IWIN). This is a multi-institutional collaborative research programme in which 10 Research Institutions and 4 Central Agencies are participating.

The IWIN programme aims to obtain isotope fingerprints of all water sources (Groundwater, river water, rainwater, atmospheric moisture and, surface waters of Bay of Bengal and Arabian Sea), representing the entire hydrological cycle over India. IWIN Sampling Network comprising 149 stations across the country has been established and is operational. More than 3000 samples of water and atmospheric water vapour have so far been collected and nearly half of these have already been analysed for their oxygen and hydrogen isotopic composition ($\delta^{18}O$ and δD) at IWIN partner institution's laboratory. A new Stable Isotope Ratio Mass

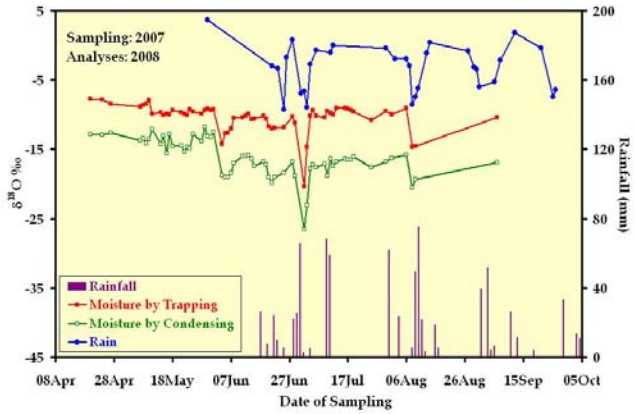

Fig. 40 Time series of $\delta^{18}O$ of daily rain and ground level atmospheric moisture samples collected both by trapping and condensing.

Spectrometer laboratory hasbeen established recently in Hydrology Group at PRL where 500 samples have been analysed for their $\delta^{18}O$. A Sample Repository Cell has also been set up at PRL where samples collected from IWIN Network Stations are being stored for later analyses.

Following information is derived from the time series (Figure-40) of $\delta^{18}O$ of rain and moisture samples collected at PRL during 2007 and analysed at NIH during 2008. (i) During large rainfall events isotopic composition of both rain and atmospheric moisture is progressively depleted in heavier isotopes (^{18}O). This signifies the rainout effect. (ii) Immediately after each large rainfall event the $\delta^{18}O$ of both subsequent rain and atmospheric moisture return to their typical baseline values for the season. (iii) Excepting significant depletion associated with large rain events, $\delta^{18}O$ of atmospheric moisture at ground level maintains a typical baseline value, which is about 2‰ lower at Ahmedabad during monsoon months compared to pre-monsoon months. The lower baseline value of atmospheric moisture during monsoon months, possibly, indicates the continental effect as well as contribution from evapo-transpiration. (iv)The $\delta^{18}O$ and δD values of both rain and atmospheric moisture have a large range of intra-seasonal variation (Rain: $\delta^{18}O$ 13‰ and δD 96‰; Atmospheric Moisture: $\delta^{18}O$ 12.6‰ and δD 76‰). (v) The liquid condensate collected by condensation on a surface cooled at 0 ºC, has $\delta^{18}O$ values lower than that of atmospheric vapour collected by complete trapping. This signifies non-equilibrium fractionation effects involved during condensation.

Collaborators

(R. D. Deshpande, A. S. Maurya, Miral Shah, S. K. Gupta)

Noble Gas Investigation of Groundwater from North Gujarat

The regional aquifer system of North Gujarat-Cambay Region is well suited for palaeoclimatic studies spanning the covering the past 30—100 kyr., Estimation of regional palaeotemperature via analyses of dissolved noble gases and stable isotopes, while using multiple tracers such as SF_6, Radon, ^4He, ^{14}C and ^3H-^3He for dating was initiated with the help of Heidelberg University.

Analysis of water samples on a transect along the flow path in the northern part of the North Gujarat-Cambay Region indicated that, 1) a linear increase of He- basedage with flow distance., 2) Unexpectedly high concentrations of SF_6 throughout the aquifer, (which precluded the use of this tracer for dating), 3) High concentrations of SF_6 suggested a that in may be of a natural origin, 4) noble gas temperatures (NGTs) from wells in the recharge area are close to 29°C similar to, recent groundwater temperatures, 5) Samples with groundwater ages ranging from 20 to 30 are ~3°C cooler. This is being ascertained.

This work with Werner Aeschbach Hertig and Martin Wieser from IUP, Uni. of Heidelberg, Germany.

(R. D. Deshpande)

Identification of the source of now-extinct ^{60}Fe in the early solar system

The presence of about a dozen short-lived nuclides in the early solar system, including ^{60}Fe and ^{26}Al, has been established from isotopic studies of meteorite samples. An accurate estimation of solar system initial abundance of ^{60}Fe, a distinct product of stellar nucleosynthesis, is important to infer the stellar source of this nuclide. Previous studies in this regard suffered from the lack of exact knowledge of the time of formation of the analyzed meteorite samples. We have carried out a combined study of the fossil records of the decay products of the two now-extinct nuclides, ^{60}Fe and ^{26}Al, in chondrules, one of the early formed solar system objects, to remove this ambiguity. We use the ^{26}Al records to infer the time

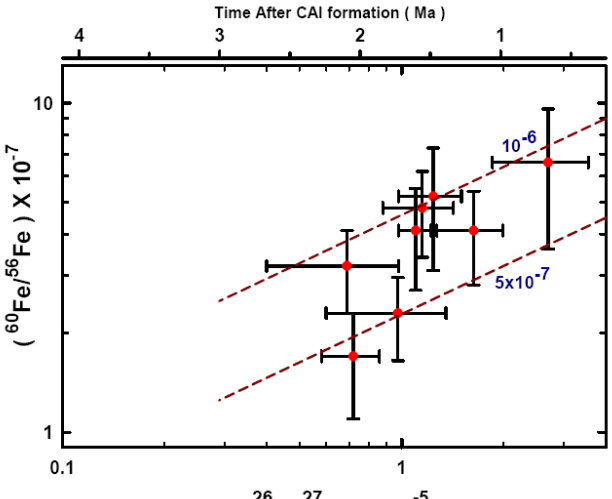

Fig. 41 A plot of initial $^{60}Fe/^{56}Fe$ at the time of formation of the UOC chondrules, as a function of their initial $^{26}Al/^{27}Al$. The time of formation of the chondrules, relative to the first solar system solids, the Ca-Al-rich refractory Inclusions (CAIs) is shown on top, based on the canonical initial $^{26}Al/^{27}Al$ value of 5×10^{-5} established for CAIs. The expected trends for two values of solar system initial $^{60}Fe/^{56}Fe$ are also shown.

of formation of the chondrules, relative to the first solar system solids, the Ca-Al-rich Inclusions. Our initial results based on a few chondrules, reported last year, suggested that both these nuclides were co-injected to the early

solar system from a single stellar source. We have now completed a study of mineralogy and petrography of more than a hundred chondrules from several unequilibrated ordinary chondrites (UOCs), belonging to low petrologic grades, and identified more than a dozen chodnrules suitable for combined study of Fe-Ni and Al-Mg isotope systematics. The selected UOCs have experienced only low temperature thermal environment during their evolution on their parent bodies (asteroids) and the chondrules in them will retain pristine isotope records. Isotopic data obtained using ion microprobe techniques yielded a weighted average mean value of $(7 \pm 1)\times10^{-7}$ (2σ) for solar system initial $^{60}Fe/^{56}Fe$. This rules out a TP-AGB star as a plausible source for ^{60}Fe and argues for a high mass (³30 solar mass) supernova as the source of ^{60}Fe along with ^{26}Al and several other short-lived nuclides present in the early solar system (Figure 41).

(R. K. Mishra and J. N. Goswami)

Calcium Aluminum Inclusions and short-lived nuclide ^{36}Cl

For long it has been suggested that the short-lived radionuclide ^{36}Cl with half life of 0.3 Myrs. was present in the early solar system. Sodalite, the Chlorine rich phase in calcium aluminum inclusions (CAIs), is an alteration product of primary phases. ^{36}Cl decays to highly volatile ^{36}Ar (98.1%), and to ^{36}S.(1.9%). ^{36}S excesses correlating with Cl/S in sodalite were reported from a CAI in the meteorites Ningqiang and in Allende (in the Pink Angel inclusion). No evidence for extinct ^{36}Cl in the study has so far been reported in fine-grained Allende CAI. Search for Cl-rich phases using X-ray imaging on CAIs from CV meteorite of petrographic grade 3.0 from the PRL collection is being carried out. Ion probe analyses of these phases for excess ^{36}S might indicate presence of short lived ^{36}Cl nuclide. Preliminary work initiated by X-ray imaging on ALL-CAI-2 (from Allende) CAI indicates a few Cl (~4%) rich phases.

(K. K. Marhas)

Source of short-lived nuclides in light of Li-Be-B systematic in CAIs

Presence of now-extinct short-lived nuclide ^{10}Be (half life ~1.5 Ma) in refractory meteoritic phases suggest energetic particle interactions as one of the sources of the short lived nuclides in the early solar system. The inferred solar system initial $^{10}Be/^{9}Be$ ratio of $\sim10^{-3}$ can be explained either by the interaction of galactic cosmic ray produced ^{10}Be trapped within the proto-solar molecular cloud or irradiation of gas and dust in the solar nebula by solar energetic particles. Possible presence of the very short-lived nuclide ^{7}Be (half life ~53 days) in Allende CAI, if confirmed, would support the local irradiation model. We have analysed three CAIs from CV3 meteorites, Efremovka (E40, EF3) and Leoville (USNM 3536-3b) for their Li-Be-B systematics using a Cameca ion microprobe (ims-4f) to further address this

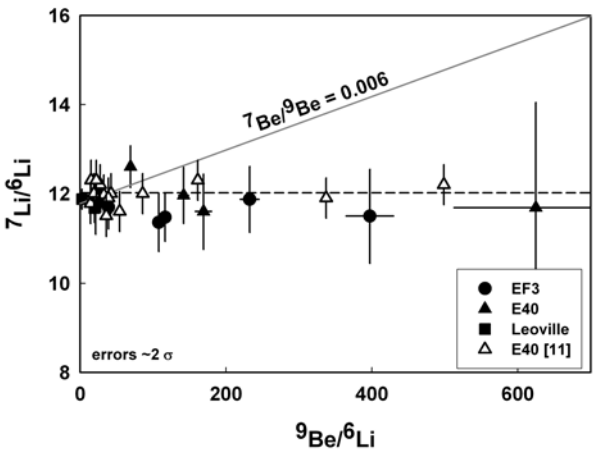

Fig. 42 Li-Be isotope data from CV3 CAIs

issue. Data for Li-Be isotope systematics obtained so far do not reveal presence of radiogenic ^{7}Be; the weighted average value from about a dozen analyses yielded initial $^{7}Li/^{6}Li$ ratio of 11.84 ± 0.10. Li isotope data obtained in this study, along with data obtained earlier in E-40, are shown in Figure 42. The low initial $^{7}Li/^{6}Li$ compared to the solar system value suggests possible heterogeneity in Li isotopic composition in the proto—solar molecular cloud.

(K. K. Marhas, J. N. Goswami, A. Singh)

NanoSIMS and Quasi-simultaneous arrival effect

PRL nanoSIMS has been successfully installed. In Nano SIMS, the production of multiple secondary ions from impact of a single primary ion, is possible. Near simultaneous arrival of these secondary ions (called quasi-simultaneous arrival or QSA) at the first dynode of the electron multiplier is detected as a single event due to an electronically fixed dead time of the electron multiplier. Thus, counts recorded by the electron multiplier for the major isotope is lower than actual/true number and this leads to erroneous ratios. This effect is clearly observed in case of elements with high ioniztaion efficiencies (for e.g. C, N, Si, O, S). Knowing secondary to primary ion ratio (k) and measured isotopic ratio, the true isotopic ratio can be calculated (based on Poisson statistics) as :

$$R_{meas} = R_{true} * (1 + \beta * k)$$

The "β" value for SiC standard, to be set as correction factor for QSA on the sample for Si, C and N varies from 0.6 to 0.7, 1.2—1.4 and 0.6—0.7 respectively.

(K. K. Marhas and Y. Kadlag)

Monitoring unit for SIMS Lab

A project to provide a remote monitoring system for real time monitoring of the status of ion probe (Cameca, ims 4F) was carried out. Seventeen parameters were identified for monitoring. For implementation, the project was divided into two phases (1) development of Backbone Systems, and (2) development of Sensor System. The backbone systems consists of the master data acquisition hardware, the interface to PC (using USB2.0), front end data logging solution, data storage solution & the dashboard web service. The Front End Data Logger (SIMS Monitoring System) was developed as a windows console application using Visual Studio 2005 in VB language. The Data storage solution has been implemented in Microsoft Access Database and a Dashboard website (SIMS Monitoring Site) has been developed as an ASP.NET web service using Visual Studio 2005 in C# (C sharp) language. The central data acquisition hardware currently operates on the PIC 18f4550 evaluation board. The PCB (Printed Circuit board) design and all required components being assembled for implementation. Future work will be on development of sensors & integration with the whole system. A few changes have to be made in the firmware, data logger & the web service to accommodate the new hardware.

This work was done in collaboration with BE student (trainee) Mr. Sunil Pillai from Govt. Engineering Collage, Gandhinagar.

(M. P. Deomurari and K. K. Marhas)

NanoSIMS Image Reduction Program

A user friendly data reduction program in IDL (interactive data language) was designed and implemented for extracting isotopic data from nanoSIMS images. These images are accumulation of various cycles of accumulation by given pixel size acquired over a given period. Any change of primary current leading to a shift of image is recorded in the consequent image. PRL_NSIRP (NanoSIMS Image Reducation Program), extracts individual cycles from the main ' *.im' file (nanoSIMS format) with an option of aligning these individual cycles in either automatic (uses F.F.T.) or manual mode (using cross correlation). All images along with ratio images can be edited for colour/contrast/ brightness and can be corrected for bad pixel or masked to a particular threshold. Apart from this, zoom option allows choosing a particular region of interest (ROI) by freehand or polygon tool which is especially useful in case of small anomalous grain within a section. Another option of dividing whole image to a chosen number of grid sizes and saving the averaged data over the subgroup is also very helpful in finding the anomalous grains. Final isotopic ratio and delta values averaged for whole image, from ROI or grid, after deadtime and quasi-simultaneous arrival corrections can be saved in an Excel sheet. Useful results in ratio or delta value for all data points can also be viewed as a plot

This work was done in collaboration with BE students Saburi Pandey, Shradda Panchamiya from Dharmsinh Desai university, Nadiad.

(K. K. Marhas)

Primordial compositions of refractory inclusions

In order to calculate the primordial composition of refractory inclusions, 17 Type A and B inclusions from CV3 chondrites were analyzed for bulk chemical and O-, Mg- and Si-isotopic compositions. After the correction for non-representative sampling, the Mg- and Si-isotopic compositions were used to calculate the original chemical composition assuming that the heavy-isotope enrichments of these elements was due to kinetic fractionation during evaporation from CaO-MgO-Al_2O_3-SiO_2 (CMAS) liquids. The resulting pre-evaporation chemical compositions are consistent with those predicted by equilibrium thermodynamic calculations for high-temperature nebular condensates at the total pressure from 10^{-6} to 10^{-1} bar. These are independent of whether they formed in a nebular region of solar composition or similar composition but 10 times enriched in dust (of ordinary chondrite composition). This is consistent with the pressure ranges predicted by dynamic models of the solar nebula for regions where temperatures are in the range of silicate condensation temperatures. Alternatively, if departure from equilibrium condensation and/or non-representative sampling of condensates in the nebula occurred, the inferred pressure range could be smaller. Simple kinetic modelling of evaporation successfully reproduces observed chemical compositions of most inclusions from their inferred pre-evaporation compositions, suggesting that closed-system isotopic exchange processes did not have a significant effect on their isotopic compositions. Comparison of pre-evaporation compositions with observed ones indicates that 80% of the enrichment in refractory $CaO + Al_2O_3$ relative to more volatile $MgO + SiO_2$ is due to initial condensation

and 20% due to subsequent evaporation for both Type A and B inclusions.

This work was done in collaboration with L. Grossman, S. B. Simon, R. N. Clayton, T. K. Mayeda, A. V. Fedkin (The University of Chicago, IL, USA), M. H. Thiemens (University of California San Diego, USA), I. D. Hutcheon, R. W. Williams (Lawrence Livermore National Laboratory, USA), A Galy (University of Cambridge, Cambridge, UK), T Ding (Institute of Mineral Resources, Chinese Academy of Geological Sciences, Beijing, China).

(Vinai K. Rai)

Shisr 007, a ureilite from hot Desert

Shisr 007, a find from Dhofar, Oman, has been classified as an moderately shocked.ureilite. As a part of our continuing effort to understand the role of desert weathering on the noble gases and nitrogen inventories of ureilites we investigated Shisr 007 for all the noble gases and N by stepwise combustion (up to 1000°C) and subsequent pyrolysis (up to 1800°C). Peak release of all the noble gases and nitrogen occurred at 800°C combustion, wherein the maximum CO_2 due to combustion of C phases was observed, clearly suggesting C phases as the principal carriers of noble gases and N in Shisr 007. This is typical of ureilites. Elemental ratios $^{36}Ar/^{132}Xe$ = 357 and $^{84}Kr/^{132}Xe$ = 0.89 are the typical of ureilites, but some isotopic ratios, particularly at low temperature combustions show features, unlike normal ureilites. These are, excess of radiogenic (^{40}Ar, ^{129}Xe) and fissiogenic (^{86}Kr, ^{134}Xe, ^{136}Xe) isotopes and (n,γ) produced isotopes from Br (^{82}Kr) and I (^{128}Xe), and cosmogenic excess at ^{83}Kr, ^{124}Xe, ^{126}Xe. In addition, a sizable excess ^{129}Xe (accompanied by excesses at ^{128}Xe and ^{82}Kr) is also present at 1800°C pyrolysis step. Excess ^{84}Kr, usually seen in the stone meteorites from hot deserts is not observed here. Desert weathering effects are not apparent in the N data. Observed anomalous noble gas isotopic features provide the first such evidence from Urelites and the results demand that the meteoroid radius should be greater than 22 cm to fecilitate generation of secondary n-flux. It also demands the presence of a labile phase which is rich in K, U, Halogens and REE (targets for spallation Kr, Xe) in Shisr 007. It is suggested that this could be a phosphate (apatite?).

This work was done in collaboration with Dr. R. Bartoschewitz, Germany.

(S. V. S. Murty and R. R. Mahajan)

A Martian crustal component of nitrogen and noble gases in MIL 03346

Martian meteorites have provided information on the composition of noble gases and nitrogen in the atmosphere and interior of planet Mars. So far, two interior components (Chass-S, Chass-E) in Chassigny; a mixture of interior (Chass-S) and modern Mars atmosphere in Shergottites, elementally fractionated atmosphere in Nakhlites and ancient Mars atmosphere in ALH84001, have been identified. Noble gas and nitrogen studies on Nakhla, Y000593 and MIL03346 using vacuum crushing (VC) and/or step-wise pyrolysis (P) were carried out to evaluate the martian interior components. The low temperature (up to 400°C) steps of two bulk samples of Nakhla (NK-30, NK-34) released N (26%, 41%) with $\delta^{15}N$ of ~20‰, ^{36}Ar (2.3%, 6.5%) with $^{40}Ar/^{36}Ar$ ~ 3000 and negligible amounts of Kr and Xe. For MIL 03346 the low T (upto 400°C) release accounts for 85% of N (+30‰) and is accompanied by only =10% of Ar, Kr, Xe having $^{129}Xe/^{132}Xe$ = 1.989, $^{136}Xe/^{132}Xe$ = 0.3695 and $^{40}Ar/^{36}Ar$ = 135000.

Composition of gases released at low temperature in the three nakhlites are different and cannot be explained as being due to terrestrial contamination or as a mixture of previously identified components The low temperature component in MIL03346 has high $^{40}Ar/^{36}Ar$ ratio. It is neither Martian atmosphere (modern or ancient) nor interior (mantle) component, as both ^{129}Xe and ^{136}Xe are in excess. Such high $^{40}Ar/^{36}Ar$ has not been observed in the low temperature release for any nakhlite. This high ^{40}Ar is not due to in situ decay of ^{40}K (peak radiogenic ^{40}Ar release in nakhlites is observed at = 800°C) and is excess ^{40}Ar (from a trapped component), which is accompanied by excesses in ^{129}Xe and ^{136}Xe. This suggests a source where the parent isotopes ^{40}K, ^{129}I and ^{244}Pu are concentrated by chemical differentiation, pointing to the early crust that contributed to the Mars atmosphere by degassing. Preservation of diverse trapped components in nakhlites suggests a heterogeneous magma source.

(S. V. S. Murty and R. R. Mahajan)

Space and Atmospheric Sciences

The activities of Space and Atmospheric Sciences Division encompass research investigations involving neutral and plasma species of the atmospheres of Earth and other planets. The main emphasis is to investigate the alterations in the ionosphere due to solar disturbances and the changes in the Earth's atmosphere due to natural and/or man-made sources. These investigations are carried out by measurements of various parameters and substantiated with suitable models in conjunction with the lab-based experiments. Experiments on-board satellites with a host of ground-based observational support are being planned.

Vertical distribution of ozone over marine regions

As a part of the Integrated Campaign for Aerosols, gases and Radiation Budget (ICARB), balloon launches were made from 18 March to 11 May 2006, to study the vertical distribution of ozone over the Bay of Bengal (BoB) and the Arabian Sea (AS). A set of 29 ozone soundings were made on alternate days. Higher ozone levels were observed up to 3 km over the BoB than over the AS. This is due to transport from the polluted Indo-Gangetic plain to the BoB. In the free troposphere, however, the ozone levels were lower over the BoB as compared to AS (Figure 43).

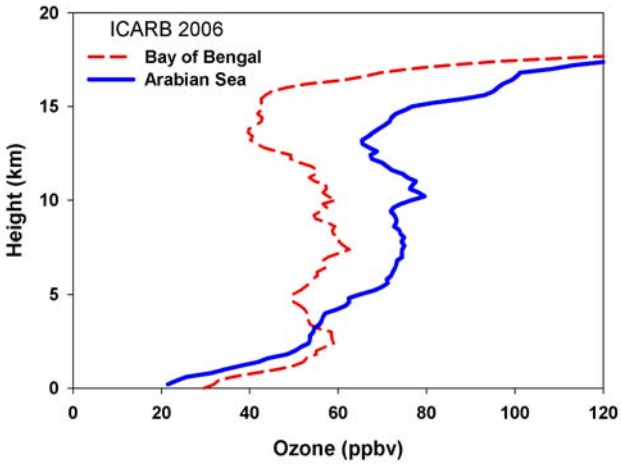

Fig. 43 Altitude profiles of ozone over Bay of Bengal and Arabian Sea measured during ICARB 2006 campaign.

Such changes in ozone concentrations arise due to convective activities in the atmosphere over the BoB which vertically transport ozone-poor air from the marine boundary layer to the free troposphere. In contrast, ozone-rich air is transported downward over the northern AS. Thus, these results suggest that the two marine regions across the Indian continent have contrasting vertical transports, which

result in different ozone distributions during pre-monsoon season.

(S. Lal, Shilpy, S. Srivastava, S. Venkataramani, T. A. Rajesh and Y. B. Acharya)

Study of boundary layer effects on the vertical distribution of trace gases

The air segment of Winter ICARB campaign was conducted during 2-20 January, 2009. About 250 air samples were collected, onboard an aircraft, for the analysis of CO, CH_4, CO_2 and non-methane hydrocarbons over Hyderabad, Visakhapatnam, Port Blair, Chennai and Mangalore. In addition, insitu measurements of ozone using an UV based analyzer were made. The preliminary results show higher levels of these gases within the boundary layer up to about 1.5 km.

(S. Srivastava, I. Guha, S. Venkataramani, K. S. Modh, T. K. Sunilkumar and S. Lal)

Seasonal variability and long term trends in NO_2

Nitrogen dioxide (NO_2), which plays a key role in atmospheric chemistry, is increasing over different parts of the world. Data from the Global Ozone Monitoring Experiment (GOME) were used to evaluate the capabilities of the global chemical transport model, Model of Ozone and Related Tracers (MOZART), in simulating the columnar abundance of tropospheric NO_2 over Delhi, Ahmedabad, Pune and Bangalore. The model was installed and rigorously tested at PRL. The model qualitatively reproduced the seasonal behaviour (Figure 44). However, absolute values of the columnar NO_2 simulated by MOZART were consistently higher compared to GOME data. This could be due to higher emission and seasonally invariant estimates in the Precursor of Ozone and their effects in the Troposphere (POET) inventory used as input in MOZART.

The GOME data show an increasing trend of NO_2 at the selected Indian sites but at times the rate of increase is not as high as expected from the rate of industrial and economic growth in these regions. Compared to India, similar polluted regions of China show higher rate of increase in the satellite observed NO_2 column abundances.

(Varun Sheel and S. Lal)

Weighting functions for CO in the 4.7 μm absorption band

An Indian satellite I-STAG (Indian Satellite for Aerosols and Gases) has been proposed to study aerosols and trace gases in the lower atmosphere. Carbon monoxide and other trace gases using a high resolution grating spectrometer named MAGIS (Measurement of Atmospheric Gases by Infrared Spectrometer) are planned to be measured. In order to obtain the critical parameters needed for the design of the payload, the radiance, transmittance and weighting

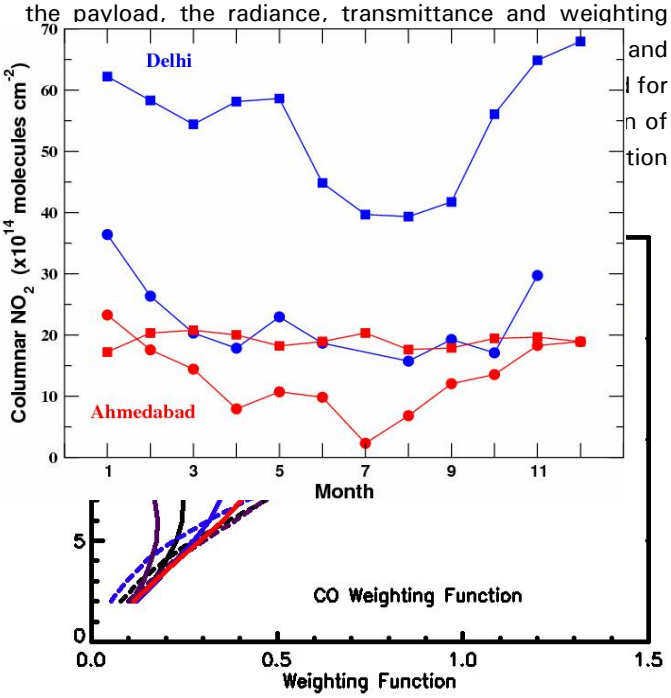

Fig. 44 Tropospheric columnar NO_2 over Delhi and Ahmedabad from model simulations (square) and GOME data (circle).

Fig. 45 Altitude profiles of weighting functions for CO for the 4.7μm band.

parameters for these gases were taken from the HITRAN (High Resolution Transmission) database. Tropical atmosphere and nadir viewing geometry were assumed with radiance at top of atmosphere at the 4.7 μm band center (2143 cm^{-1}) as 266 $nW/(cm^2\ sr\ cm^{-1})$. Typical profiles of weighting function are depicted in Figure 45.

(Amit Misra, Varun Sheel and Y. B. Acharya)

Regional and seasonal variations in aerosol optical characteristics over India

Regional and temporal variations in aerosol optical characteristics over seven different regions in India were studied for the period 2001-2005 from the daily mean MODIS Terra aerosol optical depth (AOD) and fine mode fraction (FMF) data. Northeast India has the lowest annual mean AOD of 0.28 while southern India has an AOD of 0.35. High altitude locations have lower AODs and densely populated, urban and industrialised locations have high AODs. Regions dominated by pollution have high FMF and high AODs, while high FMF and AODs over a wide range are found in the regions dominated by natural aerosols. In Northeast and East regions, FMFs are >0.8 throughout the year indicating the dominance of fine mode aerosols. Results indicate that in addition to AOD variations, knowledge on aerosol source s is essential to understand FMF variations. Frequency distribution of AODs and FMFs confirm the seasonal and spatial variations in aerosol sources over India.

This work was done in collaboration with R. Cherian, IITB.

(S. Ramachandran)

Physical and optical characteristics of aerosols over Bay of Bengal and Arabian Sea

Examination of spectral AODs over Bay of Bengal and Arabian Sea during pre-monsoon season of 2006 using polynomial fits showed that the aerosol size distribution is of mixed type or bimodal with contributions from fine and coarse modes. Model results suggest that the relationship between Angstrom exponent (α) and AOD depends on aerosol size distribution analogous to the measured AOD spectra. The second order polynomial coefficients (α_2 and α_1) are obtained for these measured AOD spectra. Over Bay of Bengal, for 76% of AOD spectra, α_2–α_1 is > 1 suggesting the presence of fine mode aerosols from a wide variety of fine mode fractions, while over the Arabian Sea α_2–α_1 is < 1 for 84% of AOD spectra, clearly indicating the dominance of coarse mode aerosols.

These result (Figure 46) for the first time have brought out the spatial variability in the dominant aerosol types that contribute to the spectral distribution of AODs over these oceanic regions.

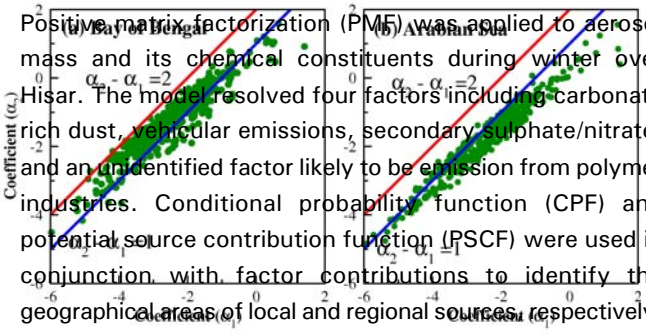

Fig. 46 Correlation between the second order polynomial fit coefficients α_1 and α_2 computed in the spectral range of 0.4—0.875 μm over the (a) Bay of Bengal and the (b) Arabian Sea.

(S. Kedia and S. Ramachandran)

Source specific aerosol radiative forcing over an urban region in India

A novel approach of combining source apportionment results for aerosol mass concentrations with AODs, enabled estimation of source specific aerosol radiative forcing. Positive matrix factorization (PMF) was applied to aerosol mass and its chemical constituents during winter over Hisar. The model resolved four factors including carbonate rich dust, vehicular emissions, secondary sulphate/nitrate, and an unidentified factor likely to be emission from polymer industries. Conditional probability function (CPF) and potential source contribution function (PSCF) were used in conjunction with factor contributions to identify the geographical areas of local and regional sources, respectively. Model apportioned species concentrations were used to determine factor specific optical and radiative aerosol properties, which were then used as inputs in a radiative transfer model to estimate aerosol radiative forcing. The results suggested that the aerosol radiative forcing was primarily governed by the aerosol optical and radiative properties, while the mass concentrations played a secondary role.

(R. Sunder Raman, S. Ramachandran and S. Kedia)

Measurements of surface aerosol radiative forcing over Ahmedabad

The global, direct and diffuse solar fluxes in the wavelength range of 0.3 to 2.8 μm have been measured during 2008 using a set of pyranometers. Aerosol optical depths (AOD)

at five wavelengths (0.38, 0.44, 0.5, 0.675, and 0.87 μm) were simultaneously measured using a sun photometer. The global, direct and diffuse fluxes were correlated with 0.5 μm AODs to estimate aerosol surface forcing. Regression between the direct solar flux at the surface and the AOD indicated that the direct solar flux decreases by ~100 Wm^{-2} during winter and by 150 Wm^{-2} in pre-monsoon with every 0.1 increase in AOD. The global flux decreases by ~30 and 45 Wm^{-2} during winter and pre-monsoon respectively. The intra annual variations in solar flux are consistent with the variations in the aerosol columnar concentration over Ahmedabad.

(R. Srivastava, S. Ramachandran and T. A. Rajesh)

Long term temperature changes in the middle atmosphere over Mt. Abu

Analaysis of 11 year LIDAR data of the middle atmospheric temperature over Mt. Abu revealed a decreasing temperature trend. The observed trend is -4.8 ± 2.5°K/decade in the altitude range of 35-45 km. The trend in winter is stronger than that of summer. Trend obtained using LIDAR was found to agree qualitatively with the satellite (HALOE onboard UARS) observations. Observed decrease in temperature is attributed to the increase in CO_2 concentration in the middle atmosphere due to anthropogenic activities.

(Som Sharma, Y. B. Acharya , H. Chandra and S. Lal)

Mesospheric temperature inversions over Mt. Abu

Two episodes of Mesospheric Temperature Inversions (MTIs) during 8—11 March 2000 and 23—26 December 2000 were examined using data from the Rayleigh Lidar at Mt. Abu. The magnitude of upper level (red arrow, Figure 47) MTIs increased gradually from 10 to 20 K during 8-11 March 2000.

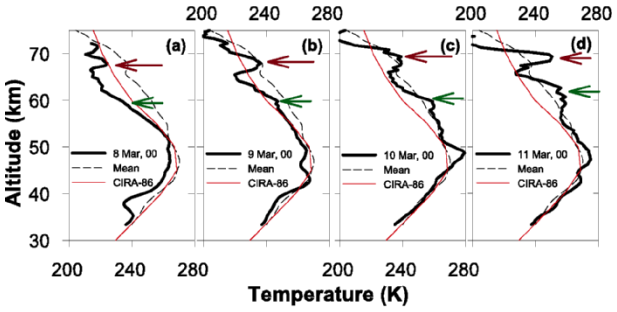

Fig. 47 A sequence of nocturnal mean height profiles of temperature illustrating mesospheric temperature inversions observed over Mt. Abu during 8-11 March 2000. Monthly climatological mean profile of March and CIRA-86 model temperature profiles are also shown.

Decrease in temperature just below MTIs and the sudden warming in the stratosphere are also observed. The separation between the upper and lower levels of MTIs is higher in March than during December. This study reveals that, every MTI event has unique characteristics and hence their formation mechanism could be complex over sub-tropical region.

(Som Sharma, Y. B. Acharya, H. Chandra and S. Lal)

Mesospheric gravity wave modes using sodium airglow intensity fluctuations

In order to identify the dominant modes of mesospheric gravity waves, sodium (Na) airglow measurements were carried out in the months of November to February during 2006-2009 over Mt. Abu (24.6°N, 72.7°E) and Gadanki (13.5°N, 79.2°E). Altitude profiles of upper mesospheric temperatures over both the sites obtained from SABER instrument onboard TIMED satellite were used. Spectral analyses of Na airglow intensity variations reveal that 15-30 min periods are dominant whenever the height of mesopause is below 94 km while the 30-45 min component was significant when the height of mesopause exceeded 97 km.

(S. Sarkhel, R. Sekar and D. Chakrabarty)

Long-term variations in oxygen green line emission over Kiso, Japan

Continuous wavelet transform analysis of 16 years long ground based photometric data of the oxygen green line (557.7 nm) at Kiso (35.8ºN, 137.6ºE) indicated semiannual, annual, and quasi-biennial variations in the airglow emission, along with nocturnal variations. The semiannual component was observed during certain epochs and was statistically significant at 2000 hours LT. This weakened as the night progressed. The annual component was present during the entire epoch, but its amplitude showed a minimum at midnight. In addition, a strong quasi-biennial component was also seen at 2000 and 0200 hours LT, the amplitude of which exceeds the semiannual component during certain epochs. This component was not detected by earlier studies using the same data. These variations in the oxygen airglow show the effect of tidal dynamics in the mesosphere and the lower thermosphere.

(Uma Das and H. S. S. Sinha)

Fine structures of mesospheric turbulence

Fine structures of mesospheric neutral turbulence are investigated using rocket-borne electron density

measurements at Sriharikota (13.7°N, 80.2°E). Spectra of electron density fluctuations were obtained using the continuous wavelet transform and from this the turbulence parameters were estimated. Analysis suggested that the turbulence was not continuously present in the mesosphere but existed in layers of different thicknesses varying from 0.1 km to 3 km, interspersed by regions of stability. Some of the important inferences are: (a) the identification of thin layers of turbulence with 100-200 m thickness over low latitude which were found to lie on the edges of the thick layers of turbulence, (b) sharp gradients in turbulence parameters at the edge regions were detected from experimental observations for the first time (Figure 48), and (c) the source of the turbulence was inferred to be the gravity waves in the lower atmosphere.

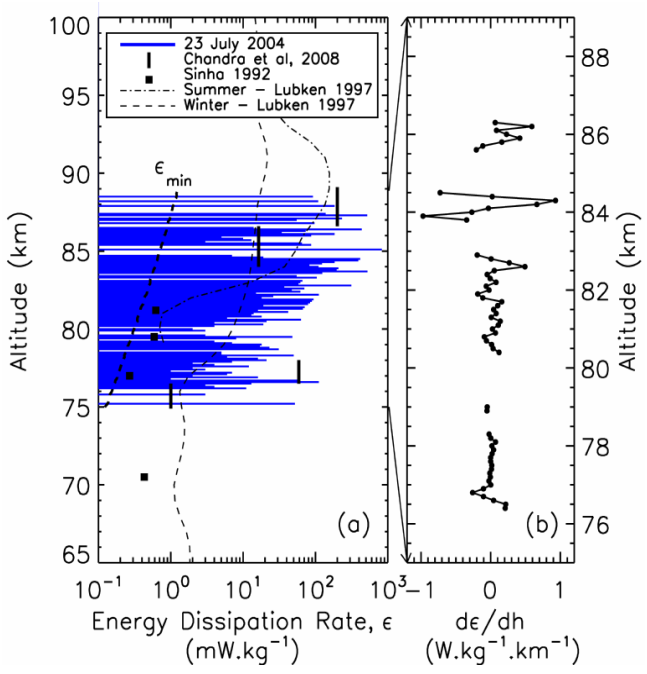

Fig. 48 (a) Energy dissipation rates estimated from the wavelet power spectra of electron density. (b) The gradient in the energy dissipation rate where turbulence was observed in layers of thickness greater than 500 m.

(Uma Das, H. S. S. Sinha, Som Sharma, H. Chandra and Sanat K. Das)

Effect of an X-class flare seen in the neutral oxygen dayglow emissions

A X6.2/3B class solar flare occurred on 13 December 2001 at 1424 UT. It peaked at 1430 UT and lasted for about half an hour. The peak-flare to pre-flare intensity ratio in the X-ray flux was greater than 300. EUV flux, as observed by the Solar EUV Monitor increased by 60% over the pre-flare background level. The effects of this flare on the low-latitude neutral OI 630.0 nm dayglow emission brightness were obtained from Carmen Alto (23.16°S, 70.66°W; 10.6° Mag. Lat.), Chile. The analysis revealed a prompt increase of 25 to 53% in emission brightness over a large spatial region (Figure 49). This period was devoid of any energetic particle fluxes.

This study, therefore, suggests that the prompt increase in the dayglow is a direct signature of an increase in the photoelectrons in response to a sudden change in the solar flux.

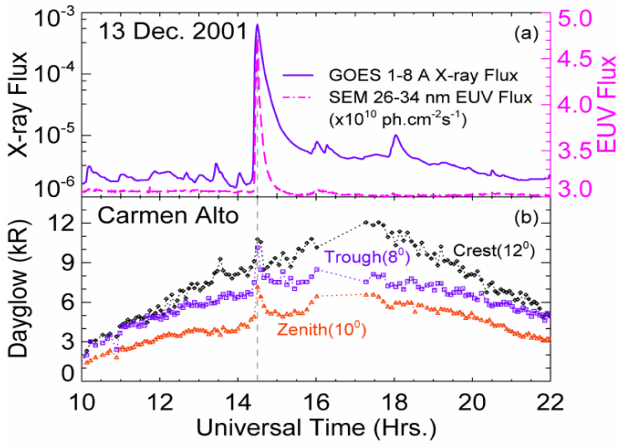

Fig. 49 (a) X-ray flux (1-8 Å) in Wm^{-2} observed by GOES-10 and EUV flux in 26 – 34 nm wavelength range in photons $cm^{-2}\ s^{-1}$ by SEM/CELIAS/SOHO on 13 December 2001 showing a sharp increase in the solar flux at 1424 UT (0924 LT). (b) Observed OI 630.0 nm dayglow emission brightness (in kilo Rayleighs) in the same time duration shows a prompt enhancement in the neutral optical emissions concurrent with the solar EUV variation.

(Uma Das and D. Pallamraju)

Dynamics of the low-latitude upper atmosphere

Spectral analysis of variations in the OI 630.0 nm dayglow emissions from Carmen Alto, (23.16°S, 70.66°W; 10.6°S Mag. Lat.), Chile, suggest the presence of gravity wave with dominant periodicities of 2-hours and 20-12 min. The variability in the equatorial electrojet was compared with that of the dayglow brightness to assess the contribution of the plasma dynamics on the neutrals. The results show that the variation in the neutral dayglow emissions displays dynamical signatures of both the neutrals and of the plasmas in the IT (Ionosphere-Thermosphere) system. The behaviour of lower latitude neutral dynamics shows greater influence

of plasma dynamics as compared to those from regions away from the magnetic equator. Further, the availability of an extended database of over 70 days of near continuous measurements of dayglow emission brightness permitted an assessment of the influence of the solar and the atmospheric sources from below into the IT system. The analysis indicates that the long-term variability is predominantly influenced by the variation in the solar flux with varying strengths of middle-atmospheric wave modes into the IT system.

(D. Pallamraju and Uma Das)

Signature of mangetospheric sub-storm in OI 630.0 nm dayglow

Observations of OI 630.0 nm dayglow intensity in bi-directional mode from Gurushikhar, Mt. Abu revealed distinct fluctuations in the dayglow intensity in both the directions at ~1130 IST for about half an hour during the geomagnetic storm of on 02 February, 2002. This dayglow intensity fluctuation was concomitant with the similar fluctuations in Equatorial Electrojet (EEJ) strength and the deviatins in the north-south component (H) of magnetic field, observed from several low latitude stations in the Indian sub-continent. Variations in H over the low latitude stations indicate that the fluctuations in the dayglow intensity on this day are possibly due to electric fields associated with sub-storm. The investigation provides an explicit evidence for the effects of sub-storm on OI 630.0 nm dayglow.

This work was done in collaboration with B. M. Pathan, Indian Institute of Geomagnetism and J. H. Sastri, Indian Institute of Astrophysics.

(D. Chakrabarty, R. Sekar and R. Narayanan)

Role of the equatorial ionization anomaly in the development of the evening pre-reversal enhancement of the equatorial zonal electric field

A model to account for the characteristic features of the evening pre-reversal enhancement (EPRE) of the zonal electric field was developed. This model elucidated the importance of the F region equatorial ionization anomaly (EIA) in the development of the EPRE for the first time. Simultaneous presence of EIA and a strong EPRE is a necessary pre-requisite for the development of the equatorial spread F (ESF). This study thus established a close relationship between the occurrence of the EIA and the ESF. During the EPRE, which begins at around 1700 LT when the F region neutral winds turn eastward and continue till the post sunset zonal electric field reversal time, an overall positive feedback occurs between the eastward electric field (in the lower side of the flux tube integrated F region), and the increased flux tube integrated Pedersen conductivity (FTIC) of the tropical F region. The increase in FTIC can occur because of the increase in electron density through the increase in solar flux and thereby the intensification of the EIA. While the influence of the EIA on the EPRE is immediate, the growth time for the EIA is 2 to 3 hours. Therefore, for a strong EPRE to occur, a fairly strong EIA is required at 1700 LT which is then sustained by the electric field associated with the EPRE during its growth period. This study suggested that the currents responsible for EPRE are an extension of the daytime Sq current system.

(Satya Prakash, D. Pallamraju and H. S. S. Sinha)

Evidence for TEC enhancement associated with ESF using multi-technique observations

An event of Vertical Total Electron Content (VTEC) enhancement associated Equatorial Spread F (ESF) was identified based on GPS TEC, VHF radar (53 MHz), thermospheric airglow (630.0 nm and 777.4 nm) observations from Gadanki (13.5°N, 79.2°E, dip latitude 4.5°N), a station close to dip equator and ionosonde observations from Thumba, a dip equatorial station. The TEC observations correspond to 2° west of Gadanki and therefore, the VTEC values were shifted in time. The time shift was calculated using the spatial separation of the longitude of measured TEC with that of Gadanki and using the derived eastward drift of the plasma structures of ~80 m/s. This eastward drift was derived on the basis of the bi-directional (zenith and 45°E) 777.4 nm airglow observations from Gadanki.

The Doppler velocities inside the plasma structure were predominantly downward during the interval (21.9—22.1 IST)when the TEC enhancement occurred. High altitude (300—350 km) descending ESF structure observed by VHF radar was concomitant with enhancement in 777.4 nm intensity. This result provides an evidence of TEC enhancement due to the plasma enhancement structures (Figure 50) associated with ESF from a location close to dip equator. This confirms earlier predictions by ESF model.

This work was done in collaboration with K. N. Iyer's group at Saurashtra University, Rajkot, A. K. Patra of National Atmospheric Research Laboratory and Sudha Ravindran of Space Physics Laboratory.

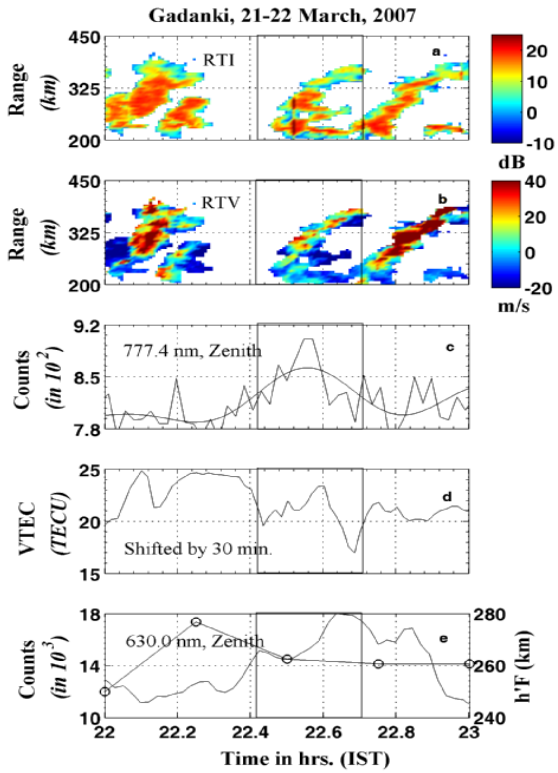

Fig. 50 (a) Range-Time-Intensity and (b) the Range-Time Velocity maps of the ESF structure on 21—22 March, 2007. Note the (c) increase in 777.4 nm airglow intensity, (d) enhancement in VTEC, (e) increase in 630.0 nm airglow intensity and relatively stable base of the F layer during the interval marked by rectangular box.

(R.Sekar, S. Sarkhel, and D. Chakrabarty)

Ionospheric response of solar flares

The effects of solar flares on the ionosphere at low latitudes that include the changes in lower ionosphere, ionospheric current system, ionospheric drifts and sudden changes in f_{min} are examined Both E- and F-region drifts at Thumba show a decrease following the solar flares. Temporal variations of solar X-ray intensity, as observed by GOES and f_{min} during few solar flare events for 1999 showed good agreement between f_{min} and X-ray flux intensities from the Sun. The delayed effects of various solar flares, sudden commencements and magnetic storms are examined in detail.

(H. Chandra, Som Sharma and H. O. Vats)

Vertical drifts over Ahmedabad from HF Doppler technique

High Frequency (2.5 MHz) Doppler radar observations over Ahmedabad provided high resolution vertical movement of F region. As the phase of the transmitted wave is affected by the vertical movement of the F layer, the phase height variations were measured digitally with a sampling frequency of 50 Hz and a velocity resolution of 1 m/s. Vertical velocity up to 25 m/s with a mean value of 9.2 m/s were observed. The measured vertical velocity showed good agreement with the vertical velocity estimated from the time variation of the minimum virtual height of F-layer.

The work was done in collaboration with R Raghava Rao and S.R. Das.

(H. Chandra and Som Sharma)

Ionospheric effects of the space weather event

The space weather event of 24-26 September 1998 was studied using solar wind, Interplanetary Magnetic Field (IMF) and ground magnetic data. The response to equatorial ionosphere was studied from quarter hourly ionograms from Thumba. Geomagnetic storm on 25 September with sudden commencements at 0445h local time resulted in the late appearance of E_{sq} at Thumba. The IMF turned southward on the morning of 25 September 1998 and solar wind velocity exceeded 850 km/s. It is inferred that the disappearance of sporadic-E was associated with the counter electrojet caused by prompt penetration of electric field.

(R. G. Rastogi and H. Chandra)

Equatorial electrojet over Brazilian sector

Based on the data from a closely spaced network of magnetometers, those were deployed for the International Electrojet Year (1993—94) the morphology of the electrojet in the Central American sector was studied with higher spatial resolution for the first time. Diurnal and latitudinal variations in the horizontal and vertical components are shown to obey Chapman's model of EEJ. The center of EEJ was around 0.25°S of dip equator in the morning and it shifted gradually to 1.5°S of dip equator in the evening. The electrojet current during mid-day hour was along the magnetic equator.

The work was done in collaboration with M E James of Gujarat University and K Kitamura and K Yumoto of Japan.

(R. G. Rastogi and H. Chandra)

High latitude ionosphere over Mars: Comparison with Earth's ionosphere

The electron density was calculated using a model and compared with the radio occultation measurements made on Mars by Mars Global Surveyor (MGS) and Mars 4/5, and on Earth by Constellation Observing System for Meteorology, Ionosphere and Climate (COSMIC). The results

from the present calculation are also compared with other models (Figure 38). The present model suggests that the dayside ionosphere of Mars has D, E, and F layers at height ranges 25—35 km, 100—112 km and 125—145 km due to the impact of galactic cosmic rays, X-rays and solar EUV radiation respectively. The water cluster ions $H_3O^+(H_2O)_n$, $NO_2^-(H_2O)_n$ and $CO_3^-(H_2O)_n$ dominate the D region, while NO^+, CO_2^+ and O_2^+ are the major ions in E and F regions. The calculated peak heights of E and F regions are in good agreement with MGS observations (Figure 51).

It is seen that D region peak density on Mars was one or two orders of magnitude less compared to the D region peak density corresponding to the Earth. The height of F layer peak in the Martian ionosphere is lower by factor of 1.8 as compared to the ionosphere of Earth. E regions are created at nearly the same height in the ionospheres of both planets, but the layer thickness is considerably less on Mars than on Earth. This implies that solar EUV energy is deposited within smaller altitude range in the upper ionosphere of Mars as compared to Earth.

This work was carried out in collaboration with M.A. Abdu and his group at INPE, Brazil.

(S. A. Haider)

Solar X-ray flare and Coronal Mass Ejection in the Ionospheres of Mars and Earth

The radio occultation data obtained from the Mars Global Surveyor (MGS) are used for the period 12-18 May, 2005 to understand the response of X-ray flare and CME in the Total Electron Content (TEC) of E region ionosphere of Mars during a violent solar event that occurred on 13 May, 2005. Modeling of this flare-induced TEC is also carried out in the E region ionosphere of Mars. This is done using observed X-ray flux during the flare. Observations and modeling studies reveal that during this flare the E region ionosphere of Mars caused enhancements in TEC by factors of 6 to 10. This effect is also observed in the E region plasma frequency (f_{OE}) of Earth's ionosphere at nearly same latitude to the MGS observations on Mars. The response of mass ejections from the solar corona is registered in the E region ionosphere of Mars after 38 hours, while its effect was recorded in the E region of Earth's ionosphere after 7 hours. The present investigation reveals that plasma frequency corresponding to sporadic E layer (f_{OEs}) increases by factors of ~ 3.2 to 6 on Earth and ~3.5 to 4.5 on Mars during the arrival of CME. TEC is also found to increase proportionately.

This work was carried out in collaboration with M. A. Abdu and his group at INPE, Brazil.

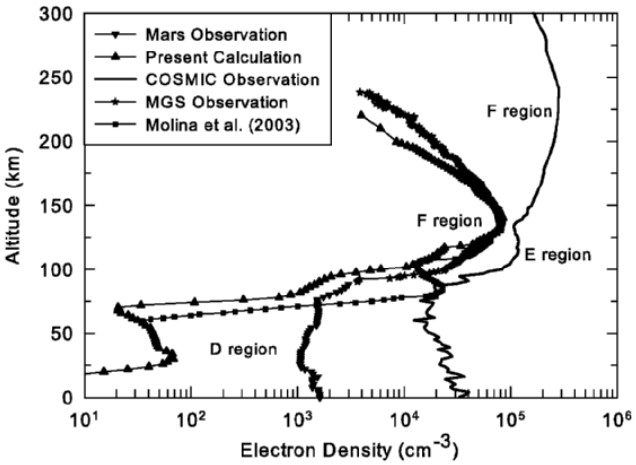

Fig. 51 Simulated and observed altitude profiles of electron density over ionospheres of Mars and Earth.

(S. A. Haider)

Zonal wave structures in the lower atmosphere of Mars during nighttime

Modeling investigations on zonal wind perturbations in the night-time D region ionosphere of Mars during winter and summer seasons for latitudes 60°- 64°S and 64.7°- 67.3°N were carried out. The production rates of ion and electron densities were calculated over different longitude sectors due to impact of galactic cosmic rays on the lower atmosphere of Mars during nighttime at these latitudes. In these calculations, temperature and air density were used from the measurements made by radio occultation experiment onboard Mars Global Surveyor. The spectral analysis suggests that the mode of wave number 2 in northern and wave numbers 3 and 8 in southern high latitudes respectively are dominant. It is found that nighttime ionosphere of Mars consists of a permanent D region peak, which varies with longitudes in both hemispheres.

(S. A. Haider and Varun Sheel)

Effect of dust on ions in the Martian lower atmosphere

The ion—aerosol interaction model developed earlier at PRL was used to study the effect of dust on ions in the troposphere of Mars. It is observed that with an average dust concentration profile, the positive hydrated ions, $H_3O^+(H_2O)_n$ where n = *1,2,3,4* decrease by two orders of magnitude. The reduction is maximum at the surface where the dust concentration is highest and decreases with height up to an altitude of 40km. Above 40km, effect of dust on the ions is not seen. The reduction in density due to dust is also seen for other positive and negative ions, but

the effect is not as pronounced as the hydrated ions. The study indicates that during massive dust storms on Mars, the lower ionosphere could be significantly perturbed.

(Varun Sheel and S. A. Haider)

Projectile charge state dependence of dissociative ionization

In an experiment done at the Inter-University Accelerator Centre (IUAC), dissociative ionization of SF_6 under the impact of fast carbon and oxygen ions was studied. Fully correlated momentum distributions of fragment ions were obtained using a multi-particle momentum spectrometer developed at PRL and stationed at IUAC. The focus was on understanding the dissociation sequences of multiply charged SF_6 ions and the dependence of these sequences on the nature of the projectile. It is expected that the momentum correlations should be independent of the projectile and be only governed by the intermediate state of the SF_6 ion.

This work was done in collaboration with C.P. Safvan at IUAC.

(B. Bapat, R. K. Kushawaha, and I. A. Prajapati)

Structural changes observed in dissociating di-cations

The observation of associative processes (*e.g.* formation of H_2^+ and H_3^+) in di-cations of organic molecules implies that their geometric structure is different from that of the parent molecule. By observing the fragmentation of doubly charged methanol $(CH_3—OH)^{2+}$ using an ion momentum spectrometer, the bond angles and hence the structure of the unstable methanol di-cation are deduced. Similar investigation on chloro-methane ($CH_3—Cl$) shows that the structural changes are largely the same as in methanol and are primarily driven by the presence of electronegative radicals ($—OH$ and $—Cl$) on one of the bonding sites of carbon.

(R. K. Kushawaha, and B. Bapat)

Photochemistry of carbon clusters

The study of photochemical reactions of small clusters is the first step for understanding the chemistry of particulate matter in the atmosphere. An apparatus for producing clusters of carbon and for mass spectrometric analysis of carbon clusters seeded with other gases and exposed to UV radiation has been designed and is being fabricated. Laser ablation and low pressure discharge methods of cluster generation will be employed, while analysis will be carried out by a high-resolution reflectron time-of-flight mass spectrometer.

(A. K. Saxena, S. B. Banerjee and B. Bapat)

Theoretical Physics

Scaling and mu-tau Symmetry

A special Ansatz called scaling has been proposed for the neutrino mass matrix with a view to constraining neutrino masses and mixing angles. We demonstrated that this Ansatz can follow from a symmetry called generalized mu-tau symmetry imposed in the type-I seesaw model. Consequences of this Ansatz for leptogenesis were worked out in detail. It was shown that the scaling form of neutrino mass matrix can generate non-zero lepton asymmetry in a simple model with two right-handed neutrinos. In contrast, similar model with mu-tau symmetry leads to vanishing asymmetry.

This work was done in collaboration with W. Rodejohann from University of Heidelberg.

(A. S. Joshipura)

Fermion Masses in mu-tau Symmetric SO(10)

A symmetry exchanging the mu and tau neutrino states has been postulated to understand large atmospheric neutrino mixing angle. The mixing angles in the quark sector are however small. It was shown that it is possible to simultaneously understand large neutrino and small quark mixing from a mu-tau symmetry. This was demonstrated through a concrete model based on SO(10) gauge group. Detailed fits to fermion masses and mixing angles were performed in this model using both type-I and type-II seesaw mechanisms. Predictions of these schemes were worked out and it was shown that such models predict very small CP violation in neutrino oscillations.

(A. S. Joshipura, K. M. Patel and B. Kodrani)

Constraining R-Parity Violation in Supersymmetry using Transverse Polarization at Linear Collider

Supersymmetry offers an elegant solution to the gauge hierarchy problem. Here, radiative corrections to the mass of the Higgs bosons needed to implement spontaneous gauge symmetry breaking are naturally small. Supersymmetric theories, unless artificially constrained, do not conserve a multiplicative quantum number, known as R parity. Experiments to constrain couplings which violate R parity are suggested at linear colliders, making use of transverse beam polarization. Azimuthal asymmetries in b-quark pair production through annihilation of transversely polarized electron and positron beams are suggested as sensitive tests of R-parity violation. These asymmetries also allow this theory to be distinguished from others that involve exchange of massive spin-1 or spin-2 particles. The measurements proposed would

considerably improve the existing experimental bounds on *R*-parity violating couplings.

This work was done in collaboration with Rohini M. Godbole from CHEP, Indian Institute of Science, Bangalore and Santosh Rai from University of Helsinki.

(S. D. Rindani)

Anomalous Higgs Couplings to Neutral Gauge Bosons in Associated HZ Production at Linear Collider

In an earlier study, angular distributions and angular asymmetries of the *Z* boson in associated Higgs and *Z* production in polarized electron-positron annihilation were calculated with a view to placing simultaneous constraints on possible anomalous Higgs couplings to the neutral gauge bosons, the photon and the *Z*. As an extension the present work examined angular distributions and correlations of charged leptons arising from the decay of the *Z* produced in the above process. Not only is this a natural extension because the detection of the *Z* needs the measurement of a decay channel, but it also affords additional variables which help constrain couplings that are not accessible to measurement through only *Z* angular variables. A number of different variables are proposed, which now enable constraining even the real parts of CP-violating couplings of the Higgs to two *Z* bosons or a photon and a *Z* boson. Sensitivity of the experiment to various coupling measurements is evaluated.

(Pankaj Sharma and S. D. Rindani)

Top Polarization and Its Measurement at LHC as Tool to Constrain New Physics

Being the heaviest quark, the top quark is expected to play a special role in the understanding of the mechanism of spontaneous gauge symmetry breaking, which occurs at a scale similar to the mass of the top quark. At the same time, since the top quark decays before it hadronizes, it provides a unique platform to study top polarization mechanisms. This is because spin information is maintained in the decay products of the top quark. While numerous studies have suggested the measurement of top and anti-top spin correlations at hadron and lepton colliders to obtain information on top-quark interactions, it is not generally realized that single top polarization can provide better statistical significance and yet enable better constraints on new physics.

The azimuthal distribution of charged leptons arising from the decay of a top (or anti-top) sensitively depends on the transverse polarization of the top quark. This in turn reflects the structure of the theory. Using the little Higgs model as an example, it is shown how the azimuthal distributions of charged leptons arising from the decay of a top quark at hadron colliders like the Tevatron and the LHC can be used to constrain the couplings of the extra *Z* boson in the model.

This work was done in collaboration with Rohini M. Godbole from CHEP, Indian Institute of Science, Bangalore and Ritesh K. Singh frm Würzburg University).

(Kumar Rao and S. D. Rindani)

GUT Baryogenesis

Grand unified theories (GUTs) were proposed to unify the strong, the weak and the electromagnetic interactions. As quarks and leptons are treated on the same footing in this theory, an interesting outcome was the prediction of baryon number violation and the explanation of the presence of more matter compared to antimatter in the universe. It was later pointed out that due to a quantum effect known as anomaly, which exists in the standard model, the universe would again have equal amount of matter and antimatter before the electroweak phase transition. We pointed out that in some GUTs, the produced baryon number remains unaffected by the anomaly and no new ingredients are required to explain why there is more matter compared to antimatter in the universe.

This work was done in collaboration with Dr. P. Gu from ASICTP, Trieste, Italy.

(U. Sarkar)

Leptogenesis, Dark Matter and LHC

We proposed an extension of the standard model to understand the observed neutrino masses and to simultaneously explain the baryon asymmetry of the universe. The most interesting feature of the model is that the scale of lepton number violation is very low, and hence, the model is testable in the next generation accelerators like the Large Hadron Collider. The model also predicts a stable scalar particle that could be the candidate for dark matter, whose slow decay could produce the 511 keV gamma rays from our galactic centre, as observed by INTEGRAL.

This work was done in collaboration with Prof. J. McDonald and Dr. N. Sahu from University of Lancaster, UK.

(U. Sarkar)

Quark-Gluon Plasma

Emission of thermal photons from the possible quark-gluon plasma state was analyzed to understand the role of

viscosity of the plasma state. In this Israel-Stewart theory of causal hydrodynamics was used. This is in contrast to the earlier approaches where the acausal hydrodynamics was used. In particular it was seen that photon production rates can be enhanced by several factors due to the viscous effect in chemically nonequilibrated plasma.The implication of this in LHC and RHIC experiments was then examined.

(Jitesh Bhatt and V. Sreekanth)

Neutrino Dark Energy in Grand Unified Theories

A left-right symmetric model that accommodates the neutrino dark energy proposal was developed. In this model, Type III seesaw mechanism was implemented to give masses to the neutrinos. The consistency of the model was determined by minimizing the scalar potential and by obtaining the conditions for the required vacuum expectation values of the different scalar fields. This model was then embedded in an SO(10) grand unified theory and the allowed symmetry breaking energy scales were determined by the condition of the gauge coupling unification. Although $SU(2)_R$ breaking is required to be high, its abelian subgroup $U(1)_R$ is broken in the TeV range. This can then give the required neutrino masses and predict new gauge bosons that could be detected at LHC. The neutrino masses are studied in detail in this model, which shows that at least 3 singlet fermions are required.

(Jitesh Bhatt, Utpal Sarkar and Santosh Kumar Singh)

Majorana Neutrino Superfluidity and Stability of Neutrino Dark Energy

One of the major problems in cosmology with mass varying neutrino model of dark energy is that the instability inherent in the models would eventually evolve to a system that is not the dark energy type. In this work it was demonstrated that if the neutrino becomes superfluid, then its dynamics will become stable, and hence, the mass varying neutrino models can be revived. We demonstrate that due to long-range attractive forces in a class of mass varying neutrino dark energy models, Majorana neutrinos can form Cooper pairs and show BCS superfluidity. We describe the condensates for Majorana neutrinos and estimate the value of the gap, critical temperature and Pippard coherence length for a simple neutrino dark energy model. In the strong coupling regime bosonic degree of freedom can become important and Bose-Einstein condensate may govern the dynamics for the mass varying neutrino models. Formation of the condensates can significantly alter the instability scenario in the mass varying neutrino models.

(Jitesh Bhatt and Utpal Sarkar)

CP Asymmetry in $B^+ \to K^+\pi^0$ and Implications for New Physics

The CP asymmetry in $B^0 \to K^+\pi^-$ is expected to be similar to that in $B^+ \to K^+\pi^0$. The experimental data however show $\sim 5\sigma$ difference between the two, leading to the so called $\Delta A_{K\pi}$ puzzle. This is taken as a hint of new physics, physics beyond the standard model, and has led to phenomenological investigations within specific models. However, it is known that often sub-leading terms that are neglected in numerical estimates can affect the CP asymmetries while preserving the predictions for the branching ratios. Employing specific sum rule(s) following from (approximate) flavour symmetry, we show that it is possible to accommodate the observed experimental values within the standard model. Sub-leading terms can improve the concordance of theoretical predictions with the data. This observation is in agreement with recent QCD based estimates within the standard model. It is shown that resolution of this puzzle via modified electroweak penguin contributions is possible for a large CP violating phase generated by the new physics. However, it is pointed out that the data on polarization in $B \to VV(T)$, B_S mixing (and large CP phase), and $B^+ \to \tau^+\nu_\tau$ rate cannot be simultaneously accommodated within SM or new physics with only enhanced electroweak penguins. A plausible resolution of these (while maintaining the $B \to K\pi$ rates and asymmetries), could be a general two Higgs doublet model. Further, we argue that if the recent exclusive determination of V_{ub} is included in the fit, the theoretical expectations tend to be in better agreement with the experimental data. Therefore, inclusion of the sub-leading terms and a precise determination of input parameters may resolve this puzzling issue. However, it is perhaps premature to ascribe the effect to new physics.

(Namit Mahajan)

Possible Interpretations for the State Y(4140)

The CDF collaboration has recently reported an evidence of a new narrow structure in $J/\psi\varphi$ invariant mass distribution in the decay $B^+ \to K^+ J/\psi\varphi$ with a mass of $\sim$4143 MeV and width $\sim$11.6 MeV. The state is above the open charm threshold and therefore the conventional charmonium interpretation is immediately ruled out. The width of the state is far too small to fit in the tetraquark picture. It is therefore possible that the newly observed state is a molecular state with $D_S^+ - D_S^-$ peripheral structure, though a large binding energy ($\sim$80 MeV) will make the core structure

to contribute significantly to the decay properties. If the molecular interpretation is correct, then more states in the vicinity with similar decay pattern are expected. Also, a measurable two photon partial width is expected for such a molecular state. Another possibility is that this state could be an exotic hybrid charmonium state with quantum numbers $J^{PC}=1^{-+}$. Hybrid mesons are mesons with a glue component. There has been a proposal that another state, Y(4260), is a hybrid charmonium with $J^{PC}=1^{--}$. The masses and widths of the two states (and the mass ordering) seem to follow the expectations from both the flux-tube model calculations and lattice studies. If true, this would open up a new era in hadron spectroscopy. The best discriminator would be the two photon final state. For hybrid mesons, such a decay is forbidden. For the present case, this is easy to see due to Yang's theorem. Also, if the hybrid interpretation is correct, the decay will be dominated by light hadron final states and also decay to $J/\Psi\omega$ is possible. Further, we propose that the state to be searched in e^+e^- collisions in association with an ISR photon and pion(s), and also at hadron colliders in association with J/Ψ. More information is needed to pin point all the properties and hence the quantum numbers of the newly observed state.

(Namit Mahajan)

Kinetics of Chiral Phase Transition in Hot and Dense Quark Matter

We studied the kinetics of chiral phase transition in dense matter in the context of looking for QCD critical point in relativistic heavy ion collision experiments. While most of the theoretical investigations have so far been based on equilibrium properties, the experimental situation is actually a nonequlibrium process. In this context we study the phase transition kinetics for chiral transition in dense quark matter. Using a variational method we calculated the thermodynamic potential for two-flavor quark matter in Nambu-Jona-Lasinio model. We then used a Ginzburg—Landau expansion of free energy near the transition. We then discuss the dynamics of phase transition by solving time-dependent Ginzburg—Landau (TDGL) equation to calculate various correlation functions, growth laws for dynamical scaling, bubble dynamics and spinodial transitions.

This work was done in collaboration with A. Singh and S. Puri from School of Physical Sciences, Jawaharlal Nehru University, New Delhi.

(H. Mishra)

R-Mode Instability of Neutron Star and Quark Hadron Phase Transition

A rapidly rotating neutron star will quickly slow down if it is unstable with respect to bulk flows, known as the r-modes, which transfer the star's angular momentum to gravitational radiation. This phenomena occurs if damping is sufficiently small and hence it provides a probe for the viscosity of the matter in the interior of the star. Instability of r-modes could limit neutron star rotational frequencies. We continued our work on r-mode oscillations using a chiral model for hadrons as well as different effective models for quark matter including the color superconducting phase for quark matter.

(H. Mishra, T. K. Jha and V. Sreekanth)

BCS-BEC Crossover in Quark Matter

Although quark matter at very high baryon densities is expected to be in a superconducting phase due to color interaction at densities relevant for neutron star interior, the situation is not so clear. This is due to the fact that the strong coupling dynamics is unclear in these density regimes. As the coupling increases, the coherence length of the cooper pair of the quarks starts decreasing and can become of the order of interparticle separation. Under these conditions, it is appropriate to describe the Cooper pairs as a localized bound state. At low enough temperatures, the ground state then can be a Bose condensate of such diquark molecule. The variational calculation that we have developed for a simple four fermion interaction mode is now being implemented for a more realistic model like Nambu-Jona-Lasinio model as well as chiral sigma model.

This work was done in collaboration with Amruta Mishra from Indian Institute of Technology, New Delhi.

(H. Mishra and B. Chatterjee)

Renormalization Group Evolution of Neutrino Masses and Mixing in the Type-III Seesaw Mechanism

In the type III seesaw mechanism, neutrino masses are generated by extending the standard model to include new fermions transforming as triplets under the $SU(2)_L$ group. At energies below their respective mass scales, the heavy fields get sequentially decoupled to give an effective dimension-5 operator. Above their mass thresholds, these fields also participate in the renormalization of the wave functions, masses and coupling constants. We computed the renormalization group evolution of the effective neutrino mass matrix in this model, with particular emphasis on the threshold effects. The evolution equations are obtained in a basis of neutrino parameters where all the quantities are

well-defined everywhere, including at $\theta_{13} = 0$. We also pointed out the important role of the threshold effects and Majorana phases in the evolution of mixing angles through illustrative examples.

This work was done in collaboration with J. Chakrabortty from Harish Chandra Research Institute, Allahabad and A. Dighe and S. Ray from Tata Institute of Fundamental Research, Mumbai.

(Srubabati Goswami)

Renormalization Group Evolution of Neutrino Mixing Parameters Near $\theta_{13} = 0$ and Models with Vanishing θ_{13} at the High Scale

Renormalization group (RG) evolution of the neutrino mass matrix may take the value of the third leptonic mixing angle θ_{13} very close to zero. On the other hand, starting from $\theta_{13} = 0$ at the high scale it may be possible to generate a non-zero θ_{13} radiatively. In the most general scenario with non-vanishing CP violating Dirac and Majorana phases, we explored the evolution in the vicinity of $\theta_{13} = 0$, in terms of its structure in the complex U_{e3} plane. This allows us to explain the apparent singularity in the evolution of the Dirac CP phase δ at $\theta_{13} = 0$. We also introduced a formalism for calculating the RG evolution of neutrino parameters that uses the Jarlskog invariant and naturally avoids this singular behaviour. It was seen that the parameters needed extreme fine-tuning in order to provide exactly vanishing θ_{13} during evolution. For the class of neutrino mass models with $\theta_{13} = 0$ at the high scale, we calculated the extent to which RG evolution could generate a nonzero θ_{13} when the low energy effective theory is the standard model or its minimal supersymmetric extension. We find correlated constraints on θ_{13}, the lightest neutrino mass m_0, the effective Majorana mass m_{ee} measured in the neutrinoless double beta decay, and the supersymmetric parameter $\tan\beta$.

This work was done in collaboration with A. Dighe and S. Ray from Tata Institute of Fundamental Research, Mumbai.

(Srubabati Goswami)

Hybrid Textures in Minimal Seesaw Mass Matrices

In the context of minimal seesaw framework, the implications of Dirac and Majorana mass matrices in which two rigid properties co-exist, (namely, equalities among mass matrix elements and texture zeros) were examined. In the first part of the study, we discussed general possibilities of the Dirac and Majorana mass matrices for neutrinos with such hybrid structures. We then classified the mass matrices into realistic textures (which are compatible with global neutrino oscillation data) and unrealistic ones (which do not comply with the data). Among the large number of general possibilities, we find that only 3 patterns were consistent with the observations at the level of the minimum number of free parameters. These solutions have only 2 adjustable parameters, so that all the mixing angles can be described in terms of the two mass differences or pure numbers. We analyzed these textures in detail and assessed their impacts for future neutrino experiments and for leptogenesis.

This work was done in collaboration with Atsushi Watanabe from Harish Chandra Research Institute, Allahabad.

(Srubabati Goswami and Subrata Khan)

Minimal Seesaw Textures with Two Heavy Neutrinos

Systematic analysis of Dirac and Majorana mass matrices in seesaw models with two heavy right-handed neutrinos, was carried out. We performed thorough classification of the vanishing matrix elements that are compatible with the results from the current neutrino oscillation experiments. We included the possibility of a non-diagonal Majorana mass matrix, which leads to new solutions that are consistent with the data. In a basis where the Majorana mass matrix is diagonal, these solutions imply a Dirac matrix with specific relationships amongst its elements. It was seen that at the level of total 4 zeros together in the Dirac and the Majorana sectors, the mass matrices are almost consistent with the data but one mixing angle is predicted to be unsuitable. At the next level, i.e. with total 3 zeros, only seven patterns of mass matrices can describe the experimental data well. The seven solutions have testable predictions for the future neutrino experiments. In particular, each solution has definite predictions about the observation of the 1-3 leptonic mixing angle and the effective mass measured in neutrino-less double beta decay. The solutions of the mass matrices contain novel texture forms and provide new insights into the lepton-generation structure. We also examined possible connections between these textures and the tri-bimaximal mixing to search for symmetry principles behind the mass matrix structure.

This work was done in collaboration with Atsushi Watanabe from Harish Chandra Research Institute, Allahabad.

(Srubabati Goswami)

Resolving the Mass Hierarchy with Atmospheric Neutrinos using a Liquid Argon Detector

We explored the potential offered by large-mass Liquid Argon detectors for determination of the sign of Δm^2_{31} or the neutrino mass hierarchy, through interactions of atmospheric neutrinos. Results for a 100 kT sized magnetized detector which provides separate sensitivity to

ν_e, and, over a limited energy range, to ν_μ, were presented. We also examined the sensitivity for the unmagnetized version of such a detector. After including the effect of smearing in the neutrino energy and direction, and incorporating the relevant errors (statistical, theoretical and systematic) we performed a binned χ^2 analysis of simulated data. The χ^2 is marginalized over the presently allowed ranges of neutrino parameters and determined as a function of θ_{13}. We find that such a detector offers superior capabilities for hierarchy resolution, allowing a $>4\sigma$ determination for a 100 kT detector over a 10 year running period for values of $\sin^2 2\theta_{13} > 0.05$. For an unmagnetized detector, a 2.5σ hierarchy sensitivity is possible for $\sin^2 2\theta_{13} = 0.04$.

This work was done in collaboration with Raj Gandhi from Harish Chandra Research Institute, Allahabad, Pomita Ghoshal from Tata Institute of Fundamental Research and S. Umasankar from Indian Institute of Technology, Mumbai.

(Srubabati Goswami)

Very Special Relativity is Incompatible with Thomas Precession

Glashow and Cohen shown that proper subgroups of the Lorentz group like HOM(2) or SIM(2) can explain several results of special relativity like time dilation, relativistic velocity addition and a maximal isotropic speed of light. We demonstrated that that such SIM(2) and HOM(2) based VSR theories predict null Thomas precession and are therefore ruled out by observations of the fine-structure splitting of atomic spectra.

(Suratna Das and Subhendra Mohanty)

Signature of Short Distance Physics on Inflation Power Spectrum and CMB Anisotropy

The two-point correlation function of the interacting field in terms of the two-point function of the free-field in a quasi-de Sitter space using the □ all □n-Lehmann representation, were computed. This enabled computation of two-point correlation function of the inflatons for the case of (a) decaying inflaton (b) inflaton as a composite particle and (c) inflaton as an unparticle using the KL spectral function that depends on the short distance physics. In all these cases, it was observed that the short distance interactions suppresses the power spectrum at large scales. If an inflaton is considered as a composite of fermions then the inflaton power spectrum should display oscillations and suppression at large scale. This may be indicated in the WMAP data and can be confirmed by future observations with PLANCK.

(Suratna Das and Subhendra Mohanty)

Perturbative Reheating and Gravitino Production in Inflationary Models

The low reheat temperature at the end of inflation from the gravitino bound constrains the creation of heavy Majorana neutrinos associated with models of leptogenesis. However, a detailed view of the reheating of the Universe at the end of inflation implies that the maximum temperature during reheating can be orders of magnitude higher than the final reheat temperature. This then permits the production of the heavy Majorana neutrinos needed for leptogenesis. We carried out the complementary calculation of the gravitino production during reheating and its dependence on the maximum temperature. We found that the gravitino abundance generated during reheating for a quartic potential is comparable to the standard estimate of the abundance generated after reheating and studied its consequences for leptogenesis.

This work was done in collaboration with N. Sahu from Lancaster University.

(R. Rangarajan)

$\bar{v}_\varphi$Fluctuations of the Inflaton and Non-gaussianities in the Cosmic Microwave Background Radiation

Non-gaussian fluctuations in the curvature of the Universe and in the cosmic microwave background radiation due to self interactions of the inflaton field are usually treated as negligible compared to those arising from non-linearities in cosmological perturbation theory. We have presented arguments as to why it would not be correct to outrightly ignore such contributions in models of inflation such as new inflation, natural inflation and running mass inflation. We have then calculated the 3-point function of the inflaton fluctuations using the canonical formalism and further obtained the 3-point function of the curvature perturbations. Issues related to the constancy of curvature perturbations outside the horizon have also been examined.

(N. Mahajan and R. Rangarajan)

Estimating Parameters of a Dynamical System

Recently, there has been considerable interest in determining parameters of a nonlinear dynamical system from the chaotic time series data given in the form of the equations. Most of these studies use the synchronization property of coupled dynamical systems. Though the methods based on

synchronization have proved useful in estimating the parameters of nonlinear dynamical systems, two limitations of these methods may be noted. First, variables used in the estimation must be synchronizing variables in the sense that with a suitable coupling between two identical dynamical systems they should lead to synchronization. Second, the total time must be larger then the synchronizing time scale. We have proposed a new method of parameter estimation which addresses these limitations. The method is based on a modification of the Newton-Raphson method to include dynamics and is able to remove the above two problems associated with synchronization based methods and also the accuracy of parameter estimation is better. It works in the presence of noise. Also, for a three dimensional system with quadratic nonlinearity it is able to determine the exact form of dynamical equations by determining all possible parameters of such a system.

(R. E. Amritkar)

One- Plus Two-body Random Matrix Ensembles with Spin: Results for Pairing Correlations

For the embedded Gaussian orthogonal ensemble of random matrices generated by random interactions in presence of a mean-field for fermions with spin degree of freedom [denoted by EGOE(1 + 2)-s], in the strong coupling region, it is demonstrated that the partial densities over pairing subspaces follow Gaussian form and propagation formulas for their centroids and variances are derived. Similarly for this ensemble, the present study demonstrated that: (i) the pair transfer strength sums, a statistic for chaos, follows the form of ratio of two Gaussians (a law known for spinless fermion systems); (ii) a quantity used in conductance peak spacings analysis (for small metallic grains) exhibits bimodal form when pairing is stronger than the exchange interaction.

This work was done in collaboration with N.D. Chavda from M.S. University, Baroda.

(V. K. B. Kota and Manan Vyas)

Random Matrix Ensembles with Random Two-body Interactions Carrying SU(4) Symmetry

We introduced and analyzed the embedded Gaussian unitary ensemble of random matrices, for *m* fermions in Ω number of single particle orbits, generated by random two-body interactions that carry *SU*(4) symmetry and termed EGUE(2)-*SU*(4). Here the *SU*(4) algebra corresponds to Wigner's super-multiplet *SU*(4) symmetry in nuclei. Formulation based on Wigner-Racah algebra of the embedding algebra $\cup(4\Omega)\supset\cup(\Omega)\otimes SU(4)$ is developed for analytical treatment of this ensemble. Using this, analytical formulas were derived for the covariances in energy centroids and spectral variances. It is found that these covariances increase in magnitude as we go from EGUE(2) to EGUE(2)-s to EGUE(2)-*SU*(4) implying that symmetries may be responsible for chaos in finite interacting quantum systems.

(V. K. B. Kota and Manan Vyas)

Statistical Law for Multiplicities of SU(3) Irreps for *m* Boson Systems in a Oscillator Shell

Statistical law for the multiplicities of the *SU* (3) irreps in the reduction of a totally symmetric irreducible representations $\{m\}$ (i.e. for m bosons) of $U(\mathrm{N}), \mathrm{N}=(\eta+1)(\eta+2)/2$ with η being the 3 dimensional oscillator major shell quantum number, is derived in terms of the quadratic and cubic invariants of *SU* (3), by determining the first three terms of an asymptotic expansion for the multiplicities. To this end, the bivariate Edgeworth expansion was used. Simple formulas, in terms of *m* and η, for all the parameters in the expansion were derived. Numerical tests with large *m* and η = 4, 5 and 6 exhibited good agreements with the statistical formula for the *SU* (3) multiplicities. This work was first successful extension of the Bethe's spin decomposition formula (derived nearly 60 years back) to a (λ,μ) non-trivial group symmetry.

This work was done in collaboration with J.A. Castilho Alcaras from Instituto de Fisica Teorica, UNESP, Sao Paulo, Brazil.

(V. K. B. Kota and K. B. K. Mayya)

Deformed Shell Model Results for Two Neutrino Positron Double Beta Decay of ^{74}Se

Half-lives $T^{2\nu}_{1/2}$ for two neutrino positron double beta decay modes β^+EC/ *EC EC* were calculated for ^{74}Se (a nucleus of current experimental interest), using deformed shell model based on Hartree-Fock states employing a modified Kuo interaction in $(^2p_{3/2}, ^1f_{5/2}, ^2p_{1/2}, ^1g_{9/2})$space. The calculated half-life for the EC EC mode is $\sim 10^{26}$yrs and it may be possible to observe this decay in the near future with improved sensitivity of experiments.

This work was done in collaboration with R. Sahu from Berhampur University, Berhampur.

(V. K. B. Kota and A. Shukla)

Pairing in Spin Polarized Two-Species Fermionic Mixtures with Mass Asymmetry

We examined the pairing mechanism of fermions with

mismatch in their Fermi momenta due to a mass asymmetry. Using a variational ansatz for the ground state, we additionally examined the BCS - BEC crossover of this system. It was shown that the breached pairing solution with a single fermi surface is stable. We also included the temperature effects on the fermion pairing within an approximation that is valid for temperatures below the critical temperatures.

This work was done in collaboration with A. Mishra from Indian Institute of Technology, New Delhi.

(S. A. Silotri, D. Angom and H. Mishra)

Controlling the Flow of Microscopic Particles – The Role of Beam Size

We used a diode laser emitting at 785 nm (maximum power 46 mW) and an inverted Nikon microscope (TE2000U) to develop an optical trapping set-up. Using the traditional method for optical trapping that utilizes the full aperture of the microscope objective with a beam expander, we could trap the particles that were stable in an optical trap. However, in contrast to the usual scheme of trapping when we did not use the beam expander and instead took the original laser beam through the microscope objective and focussed it over the sample volume, a directional flow of the particles towards the centre of the trap was observed. It was seen that the flow velocity depended on the size and the power of the laser beam at the sample. This flow can be understood by the range of the trap force or the shape of the potential well created by the trapping beam at the sample. We suggest controlling the motion of microscopic particles in a fluid by varying a simple parameter like beam size for micro-fluidics applications.

(Jitendra Bhatt, Ashok Kumar, R. P. Singh)

Second Order Coherence Properties of Optical Vortices

We have been generating optical vortices and studying their properties for some time. However, most of the properties examined till now, utilized first order coherence of light i.e. correlations of electric fields. We examined photon correlation spectroscopy of optical vortices that deals with second order coherence or intensity correlations. Intensity correlation experiment for a randomized optical vortex as well as for a plane laser beam was conducted by passing these beams through a rotating ground glass plate. It was observed that intensity autocorrelation for an optical vortex decreases faster than that for a plane laser beam.

(Ashok Kumar and R. P. Singh)

Quasi-Gaussian Output from Dual Case I Waveguide Resonators with Mirrors of Step-Index Reflectivity Profiles

For waveguide laser resonators, three recognized low loss configurations exist, in which the waveguide is either closed at each end by a plane mirror (dual Case I design), or one of the plane mirrors is replaced by a curved mirror at some distance from the guide exit. Earlier, we proposed a variant of the latter design by exploiting the self-imaging properties of multi-mode waveguides. It was predicted that the resonator will produce a quasi-Gaussian output with

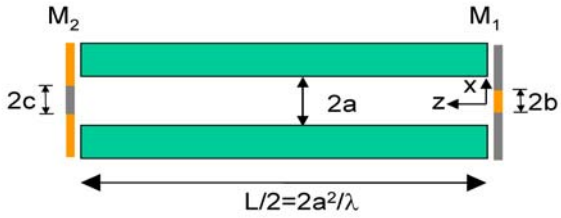

Fig. 52 Schematic of a self-imaging resonator in which a waveguide of cross section 2a × 2a and length L/2 (where $L = 4a^2/\lambda$) is closed at each end by a plane mirror with step-reflectance profiles. The reflectivity of the mirror M_1 at the $z=0$ plane is r_1 on a square block 2b × 2b centered at the origin and r_2 elsewhere with $r_1 \approx 1$ and $r_2 \approx 0$. The reflectivity of the mirror M_2 at the $z=L/2$ plane, on the other hand, is taken to be r_2 on a square block 2c × 2c centered at the origin and r_1 elsewhere.

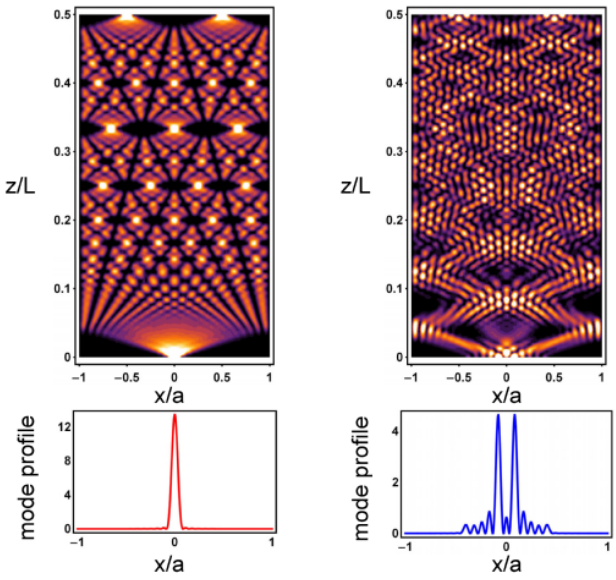

Fig. 53 The transverse intensity profiles in the x-z plane, for the lowest loss resonator mode (left column) and the next mode (right column) when $b=c=0.44a$. In each column, the top figure displays the contour plot of the intensity profile inside the waveguide and the bottom figure shows the mode profile at the output end ($z=0$) of the resonator.

low round trip loss and excellent mode discrimination. This was so, even though the curved mirror was placed much nearer to the guide exit (making the resonator more compact) than was conventional for achieving those results.

Recently, we used a dual Case I configuration with end mirrors of suitable reflectivity profiles (Figure 52) to achieve the desirable features (Figure 53) of the previous design. Since there is no free space region between the waveguide and the mirrors, the resonator has the additional advantages of being compact and portable. Furthermore, the design affords easy fabrication even for semiconductor integrated optics technology, where curved reflecting mirrors are prohibitively difficult to implement whereas plane mirrors can be mimicked by cleaved facets.

This work was done in collaboration with R.M. Jenkins from QinetiQ (U.K.) and A.R. Davies from Royal Holloway, University of London (U.K.).

(J. Banerji and Subimal Deb)

Formulation of a New Quantum Entity—The "Transition Amplitude Wave"

Based on the work carried out over the years, a new quantum entity has been identified which arises as an excitation in the centre of mass trajectory of a bound system (charged particle in a magnetic field, atoms and molecules). It is demonstrated that the entity termed as the "transition amplitude wave" or equivalently a quasi-particle—the "transiton", exhibits wave manifestations on the macro-scale, which have been demonstrated through a number of experiments.

(R. K. Varma)

Observation of Curl-free Vector Potential on the Macro-scale for Charged Particles in a Magnetic Field

Contrary to the well-known micro-scale quantum effect — the Aharonov-Bohm effect relating to the observation of curl-free vector potential—we have made observations of a curl-free vector potential on the macro-scale. Such an observation would be regarded as "impermissible" because macro-scale electro-dynamic phenomena are supposed to be governed by classical electro-dynamics. It does not recognize a curl-free vector potential, but only the magnetic field, which alone is regarded as an observable.

Figure 54 (left) demonstrates the detector response function for various electron energies. Presence of undulations in the detector current as a function of the current in a toroidal solenoid produces the curl-free vector potential in the space around. This is in contrast to the "flat" response expected

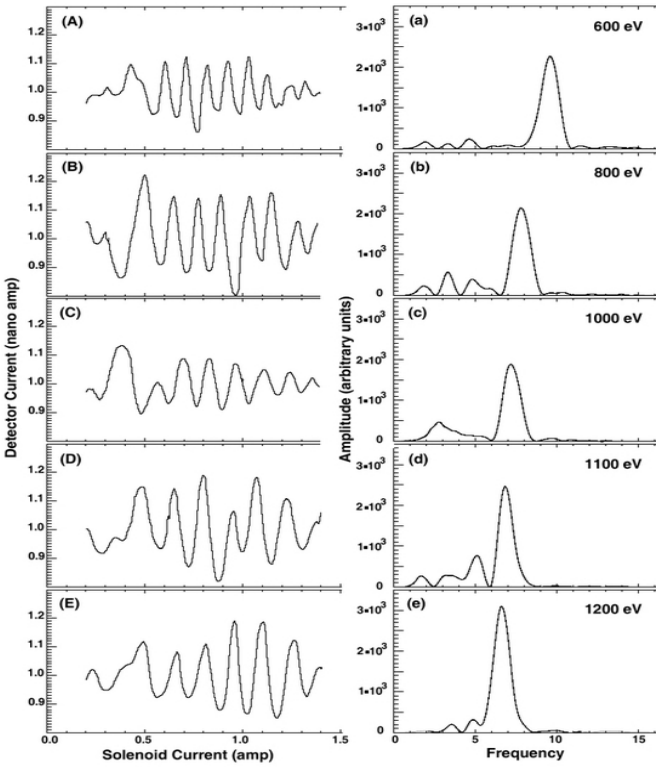

Fig. 54 Left: Detector current response for various electron energies (as shown in the right panel), as a function of the $\sqrt{\varepsilon}$ current in a toroidal solenoid producing the vector potential. Right: Fourier plots of the respective frames in the left panel.

as per the classical electrodynamics, which thereby signals the detection of the curl-free vector potential on the macro-scale. The increasing inter-peak separation with increasing energy is clearly seen in the left panel. Figure 54 (right panel) represents Fourier plots of the respective figures on the left which give a dominant frequency peak, which shifts to lower frequency side with increasing energy. This is in consonance with the theoretically predicted dependence.

(R. K. Varma, S. B. Banerjee and A. Ambastha)

The Concept of a Macro-quantized Atom

The concept of a new kind of atom is proposed which has quantized energy levels, but which does not involve the Planck quantum. It consists of a charged atom itself as the circulating body and another charged body as the nucleus. The circulating atom carries the "transition amplitude wave" excitation in its centre of mass trajectory. This accounts for the matter wave attribute, which results in the quantization. However, the quantization itself is related to the quantized energy levels of the circulating atom.

(R. K. Varma)

Observation of Curl-free Vector Potential using the "Transiton" Excited Ionized Atom or Molecule

A prediction on the observability of curl-free vector potential on the macro-scale using a charged atom or a molecule with a "transiton" excitation in its centre of mass trajectory was made. This idea is similar to the one invoked for the charged particle dynamics in a magnetic field. With the atom (or molecule) it will be a free space detection, similar to the Aharonov-Bohm effect, but would be on the macro-scale.

(R. K. Varma)

Publications in journals

Astrophysics and Astronomy

1. Anandarao, B.G., Venkata Raman, V., Ghosh, S.K., Ojha, D.K., and Kumar, M.S.N., 2008, *"Near-infrared photometry and radio continuum study of the massive star-forming regions IRAS 21413 + 5442 and IRAS 21407 + 5441"*, MNRAS, v. 390, p. 1185–1194.

2. Bhatt, Nipa, J., Jain, Rajmal, and Aggarwal, Malini, 2009, *"Predicting maximum sunspot number in solar cycle-24",* Journal of Astronomy and Astrophysics, v. 30, p. 71-77.

3. Chesneau, O., Banerjee, D.P.K., Millour, F., Nardetto, N., Sacuto, S., Spang, A., Ashok, N.M., Das, R.K., Hummel, C., Karus, S., Morel, S., Petr Gotzens, M., Rantakyro, F., Rivinius, T., Scholler, M., and Wittkowski, M., 2008, *"VLTI monitoring of the dust formation event of the Nova V1280 Sco"* Astronomy and Astrophysics, v. 487, p. 223–235.

4. Das, R.K., Banerjee, D.P.K., Ashok, N.M., and Chesneau, O., 2008, *"Near Infrared studies of V1280 Sco (Nova Scorpii 2007)"*, MNRAS, v. 391, p. 1874–1886.

5. Fan, J.H., Rieger, F.M., Hua, T.X., Joshi, U.C., Li, J., Wang, Y.X., Zhou, J.L., Yuan, Y.H., Su, J.B., and Zhang, Y.W., 2008, "*A possible disk mechanism for the 23-day QPO in Mkn 501",* Astroparticle Physics, v. 28, p. 508-515.

6. Ganesh, S., Joshi, U.C., and Baliyan, K.S., 2009, *"Optical Polarimetry of Comet NEAT C/2001 Q4"*, ICARUS, v. 201, p. 666-673.

7. Ganesh, S., Omont, A., Joshi, U.C., Baliyan, K.S., Schultheis, M., Schuller, F., and Simon, G., 2009, *"Stellar populations in a standard ISOGAL field in the Galactic disk"*, Astronomy and Astrophysics, v. 493, p. 785-807.

8. Goldman, B., and 23 colleagues (including Baliyan, K.S., Ganesh, S., Joshi, U.C.), 2008, *"CLOUDS search for variability in brown dwarf atmospheres",* Astronomy and Astrophysics, v. 487, p. 277-292.

9. Gupta, A.C., Deng, W.G., Joshi, U.C., Bai, J.M., and Lee, M.G., 2008, "*Multi-color optical variability of the TeV blazar Mrk 501 in the low-state",* New Astronomy, v. 13, p. 375-384.

10. Jadeja, A.K., Iyer, K.N., Vats, H.O., and Manoharan, P.K., 2008, *"Geo-effectiveness of CMEs"*, Journal of Astronomy and Astrophysics, v. 29, p. 287-291.

11. Janardhan, P., Tripathi, D., and Mason, H., 2008, *"The Solar Wind Disappearance Event of 11 May 1999: Source Region Evolution"*, Astronomy and Astrophysics Letters, v. 488, L1"L4.

12. John, Kohl, Jain, Rajmal, Steven, R., Crammer, Larry, Gardner, D., Anil, K., Pradhan, John, C., Raymond, and Leonard, Strachen, 2008, *"Next Generation UV Coronagraph Instrumentation for Solar Cycle-24"*, Journal of Astronomy and Astrophysics, v. 29, p. 321-327.

13. Kamath, U.S., Ashok, N.M., and Anupama, G.C., 2008, *"Nova V4444 Sagittarii 1999 in the early decline and quiescent phases"*, Bulletin of Astronomical Society of India, v. 36, p. 141–150.

14. Lokesh, Bharti, Joshi, Chandan, Jaaffrey, S.N.A., and Jain, Rajmal, 2009, *"Spectropolarimetery of umbral fine structures from Hinode: Evidence for magnetoconvection*", MNRAS, v. 393, p. 65-70.

15. Naik, Sachindra, Banerjee, D.P.K., and Ashok, N. M., 2009, "*Near-infrared observations of the novae V2491 Cygni and V597 Puppis*", MNRAS, v. 394, p. 1551-1558.

16. Naik, Sachindra, Mukherjee, U., Paul, B., and Choi, C.S., 2009, "*Orbital phase spectroscopy of four high mass X-ray binary pulsars to study the stellar wind of the companion",* Advance Space Research, v. 43, p. 900-904.

17. Richichi, A., Fors, O., Mason, E., Stegmeier, J., and Chandrasekhar, T., 2008, *"Milliarcsecond angular resolution of reddened stellar sources in the vicinity of the Galactic Center"*, Astronomy and Astrophysics, v. 489, p. 1399–1408.

18. Schultheis, M., Sellgren, K., Ramirez, S., Stolovy, S., Ganesh, S., Glass, I.S., and Girardi, L., 2009, *"Interstellar extinction and long-period variables in the Galactic centre",* Astronomy and Astrophysics, v. 495, p. 157-168.

19. Shuo Wang, Yuanyong, Deng, Rajmal, Jain, Vasyl Yurchyshyn, Haimin, Wang, Yuanyuan, Liu, and Zhiliang, Yang, 2008, *"The Evolution of Vector Magnetic Field Associated with Major Flares in NOAA AR10656"*, Journal of Astronomy and Astrophysics, v. 29, p. 57-61.

20. Thompson, L.A., Scott, T., Xiong, Yao-Heng, Castle, R.M., Chakraborty, A., Gruendl, R.A., and Rich, R.W., 2009, *"Un ISI S: Laser guide Star and Neutral Guide Star Adaptive Optics System"*, PASP, v. 121, p. 498-511.

21. Vats, H.O., and Baliyan, K.S., 2008, *"Observations of WD1524 at MIRO and participation in WET observing program",* Communications in Asteroseismology, v. 154, p. 71-82.

Solar Physics

22. Louis, R.E., Bayanna, A.R., Mathew, S.K., Venkatakrishnan, P., 2008, *"Dynamics of Sunspot Light Bridges as Revealed by High-Resolution Images from Hinode",* Solar Physics, v. 252, p. 43-54.

23. Mierla, M., Davila, J., Thompson, W., Inhester, B., Srivastava, N., Kramer, M. St. Cyr O. C., Stenborg, G., Howard, R., 2008, *"A Quick Method for Estimating the Propagation Direction of Coronal Mass Ejections using STEREO-COR1 Images"*, Solar Physics, v. 252, p. 385-396.

24. Shibu, K., Mathew, 2008, *"Enhanced p-mode Absorption Seen Near the Sunspot Umbral-Penumbral Boundary"*, Solar Physics, v. 251, p. 515–522.

25. Srivastava, N., Mathew, S.K., Louis, R.E., Wigelmann, T. *"Source region of the 2003 November 18 CME that led to the strongest magnetic storm of cycle 23"*, 2009, Journal of Geophysical Research, 114, A03107, doi:10.1029/2008JA013845.

PLANEX

26. Banerjee, D., 2009, *"Reply to Comments on :Thermoluminescence and optically stimulated luminescence signals from volcanic ash: Hostory of volcanism in Barren Island, Andaman Sea"* by M.A. Alam and Chandrashekaram, D., Quaternary Geochronology,doi:10.1016/j.quageo.2009.05.007

27. Banerjee, D., 2009, *"Thermoluminescence and optically stimulated luminescence signals from*

volcanic ash: History of volcanism in Barren Island, Andaman Sea", Quaternary Geochronology, doi:10.1016/j.quageo.2009.01.011.

28. Bhandari, N., Murty, S.V.S., Shukla, P.N., Mahajan, R.R., Shukla, A.D., Lashkari, G., Sisodia, M.S., Tripathi, R.P., Parthasarathy, G., Verma, H.C., and Franchi, A.I., 2008, *"Ararki (L5) chondrite : The first meteorite find in Thar Desert of India"*, Meteoritics & Planetary Science, v. 43, p. 761-770.

29. Crawford, L.A., Joy, K.H., Kellett, B.J., Grande, M., Anand, M., Bhandari, N., Cook, A.C., d'Uston, L., Fernandes, V.A., Gasnault, O., Goswami, J.N., Howe, C.J., Juovelin, J., Koschny, D., Lawrence, D.J., Maddison, B.J., Maurice, S., Narendranath, S., Pieter, C., Okada, T., Rothery, D.A., Russell, S.S., Sreekumar, P., Swinyard, B., Wieczorek, M., Wilding, M., 2009, "*The scientific rationale for the CIXS X-ray spectrometer on India's Chandrayaan-1 mission to the moon*", Planetary and Space Science, v. 57, p. 725-734.

30. Dhingra, D., 2008, *"Planetary Impacts in Focus"*, Current Science, v. 95, No. 10, p. 1394-1395.

31. Grande, M., Maddison, B.J., Howe, C.J., Kellett, B.J., Sreekumar, P., Huovelin, J., Crawford, L.A., Duston, C.L., Smith, D., Anand, M., Bhandari, N., Cook, A., Fernandes, V., Foing, B., Gasnault, O., Goswami, J.N., Holland, A., Joy, K.H., Kochney, D., Lawrence, D., Maurise, S., Okada, T., Narendranath, S., Pieters, C., Rothery, D., Russell, S.S., Shrivastava, A., Swinard, B., Wilding, M., Wieczorek, M., 2009, "*The CIXS X-ray spectrometer on Chandrayaan-1"*, Planetary and Space Science, v. 57, p. 717-724.

32. Pabari, J.P., 2008, "*Efficient extension of conventional low frequency filter bank spectrometer by implementation of high resolution Chirp Z signal processing"*, International Journal of Electronics, v. 95, No.10, p. 1073-1081.

33. Pabari, J.P., Shah, A.B., Vadher, N.M., Shah, V.M., and Dubey, A., 2008, "*Investigations on groove design for modulating frequency response of SAW RAC chirp filter"*, International Journal of Electronics, v. 95, No.11, p. 1201-1208.

34. Sreekumar, P., Acharya, Y.B., Umapathy, C.N., Ramakrishna, Sharma, Shanmugam, Tyagi, A., Kumar, Vadawale, S., Sudhakar, M., Abraham, L., Kulkarni, R., Purohit, S., Premlatha, R.L., Banerjee, D., Bug, M., and Goswami, J.N., 2009, "*High Energy X-ray Spectrometer on Chandrayaan-1*, Current Science, v. 96, p. 320-325.

Planetary and Geosciences

35. Ashwini Kumar, Sarin, M.M., and Sudheer, A.K., 2008, "*Mineral and anthropogenic aerosols in Arabian Sea-atmospheric boundary layer: Sources and Spatial Variability",* Atmospheric Environment, v. 42, p. 5169-5181.

36. Ashwini Kumar, Sudheer, A.K., and Sarin, M.M., 2008, "*Chemical Characteristics of aerosols in MABL of Bay of Bengal and Arabian Sea during spring inter-monsoom : A comparative study",* Journal of Earth System Sciences*,* v. 117, p. 325-332.

37. Baroni, M., Cole-Dai, J., Rai, V.K., Thiemens, M.H., Savarino, J., 2008, "*Mass-independent sulfur isotopic compositions of volcanic sulfate recorded in Antarctic ice cores over the last millennium",* Journal of Geophysical Research-Atmospheres, v. 113, D20112, doi:10.1029/2008JD010185.

38. Bhushan, R., Dutta, K., and Somayajulu, B.L.K., 2008, "*Estimates of Upwelling rates in the Arabian Sea and the Equatorial Indian Ocean based on bomb radiocarbon*", Journal of Environmental Radioactivity, v. 99, p. 1566-1571.

39. Das, J.P., and Murty, S.V.S., 2009, *"Trapped nitrogen in individual chondrules: Nature of chondrule precursors and clues to formation mechanisms",* Journal of Geophysical Research, 114, E01008, doi:10.1029/2008JE003232.

40. Fernandes L., Bhosle, N.B., Prabhu Matondkar, S.G., and Bhushan, R., 2009, *"Seasonal and spatial distribution of particulate organic matter in the Bay of Bengal",* Journal of Marine Systems, v. 77(1-2), p. 137-147.

41. Goswami, J.N., Annadurai Mylswamy, 2008, *"Chandrayaan-1 mission to the Moon"*, Acta Astronautica, v. 63, p. 1215-1220.

42. Goswami, J.N., and Annadurai, M., 2009, *"Chandrayaan-1: India's first planetary mission to the moon"*, Current Science, v. 96, No.4, p. 486-491.

43. Grossman, L., Simon, S.B., Rai, V.K., Thiemens, M.H., Hutcheon, I.D., Williams, R.W., Galy A., Ding T., Fedkin A.V., Clayton R.N., Mayeda T.K., 2008. "*Primordial compositions of refractory inclusions",* Geochimica et Cosmochimica Acta, v. 72, p. 3001–3021.

44. Jadhav, M., Amari, S., Marhas, K.K., Zinner, E., Maruoka, T., Gallino, R. 2008, "*New stellar sources for high-density, presolar graphite grains",* Astrophysical Journal v. 682, p. 1479-1485.

45. Juyal, N., Pant, R.K., Basavaiah, N., Bhushan, R., Jain M., Saini, N.K., Yadava, M.G., and Singhvi, A.K., 2009, "*Reconstruction of Last Glacial to early Holocene monsoon variability from relict lake sediments of the Higher central Himalaya, Uttarakhand, India*", Journal of Earth System Sciences, v. 34, p. 437-449.

46. Kirpa, Ram, Sarin, M.M., and Hegde, P., 2008, "*Atmospheric abundances of primary and secondary carbonaceous species over two high-altitude sites in India: Sources and temporal variability",* Atmospheric Environment, v. 42, p. 6785-6796, doi:10.1016/j.atmosenv.2008.05.031.

47. Madhavan, B.L., Niranjan, K., Sreekanth, V., Sarin, M.M., and Sudheer, A.K., 2008, "*Aerosol characterization during summer monsoon period over a tropical coastal Indian station, Visakhapatnam",* Journal of Geophysical Research - Atmospheres, v. 113, D21208, doi: 10.1029/2008JD010272.

48. Marhas, K.K., Amari, S., Gyngard, F., Zinner, E., and Gallino, R., 2008, "*Iron and nickel isotopic ratios in presolar SiC grains",* Astrophysical letters, v. 689, p. 622-645.

49. Murugan, M., Mukund, V., Ramesh, R., Hiremath, M.B., Josephrajkumar, A. and Shetty, P.K., 2009, *"Centennial rainfall variation in semiarid and tropical humid environments in the cardamom hill slopes, southern western Ghats, India*", Caspian Journal of Enviornment Science, v. 6, no.1, p. 31-39.

50. Prakash, S., Ramesh, R., Sheshshayee, M.S., Dwivedi, R.M., and Raman, M., 2008, *"Quantification of new production using winter Noctiluca scintillans bloom in the Arabian Sea",* Geophysical Research Letters, v. 35, L 08604, doi:10.1029/2008GL033819.

51. Rao, T.R., Radhakrishna, B., Srivastava, R., Satyanarayana, T.M., Rao, D.N., and Ramesh, R., 2008, *"Inferring microphysical Processes occurring in mesoscale convective systems from Radar measurements and isotopic analysis*", Geophysical Research Letters, v. 35, L09813, doi:10.1029/2008GL033495.

52. Rastogi, N., and Sarin, M.M., 2008, **"***Atmospheric ^{210}Pb and ^{7}Be in ambient aerosols over low- and high-altitude sites in semiarid region: Temporal variability and transport processes",* Journal of Geophysical Research–Atmosphere, v. 113, D11103, doi: 10.1029/2007JD009298.

53. Ratan, K., Mohapatra, Susanne, P., Schwenzer, Siegfried, Herrmann, Murty, S.V.S., Ulrich, Ott, and Jamie, D., Gilmour, 2008, "*Noble gases and nitrogen in Martian meteorites Dar al Gani 476, Sayh al Uhaymir 005 and Lewis Cliff 88516: EFA and extra neon",* Geochim. Cosmochim. Acta., v. 73, p. 1505-1522.

54. Ray, J.S., 2009, "*Carbon Isotopic Variations in Fluid-deposited Graphite: Evidence for multicomponent Rayleigh isotopic fractionation"*, International Geology Review, v. 51, p. 45-57.

55. Rengarajan, R., Singh, S.K., Sarin, M.M., Krishnaswami, S., 2009, "*Strontium isotopes and Major ion chemistry in the Chambal River System, India: Implications to Silicate Erosion Rates of the Ganga",* Chemical Geology, v. 260, p. 87-101, doi:10.1016/j.chemgeo.2008.12.013.

56. Roy, P.D., Nagar, Y.C., Juyal, N., Smykatz Kloss, W., Singhvi, A.K., 2009, "*Geochemical Signatures of Late Holocene paleohydrological changes from Phulera and Pokaran saline playas near the eastern and the western margins of Thar Desert, India".* Journal Asian Earth Science, v. 34, p. 275-286.

57. Roy, P.D., Sinha, R., Smykatz-kloss, W., Singhvi, A.K., and Nagar, Y.C., 2009, "*Playas of the Thar Desert: Mineralogical and Geochmeical Archives of Late Holocene Climate"*, Journal of Asian Earth Science, v. 1(2), p. 43-61.

58. Rudraswami, N.G., Goswami, J.N., Chattopadhyay, B., Sengupta, S.K., and Thapliyal, A.P., 2008, *"^{26}Al records in chondrules from unequilibrated ordinary chondrites: II. Duration of chondrule formation and*

parent body thermal metamorphism", Earth and Planetary Science Letters, v. 274, p. 93-102.

59. Sheth, H.C., Ray, J.S., Bhutani, R., Kumar, A., and Smitha, R.S., 2009, "*Volcanology and eruptive styles of Barren Island: an active mafic stratovolcano in the Andaman Sea, NE Indian Ocean"*, Bulletin of Volcanology doi:10.1007/s00445-009-0280-z.

60. Sheth, H.C., Ray, J.S., Ray, R., Vanderkluysen, L., Mahoney, J.J., Kumar, A., Shukla, A.D., Das, P., Adhikari, S., Jana, B., 2009, "*Geology and geochemistry of Pachmarhi dykes and sills, Satpura Gondwana Basin, central India: problems of dyke-sill flow correlations in the Deccan Traps",* Contributions to Mineralogy and Petrology, doi:10.1007/s00410-009-0387-4, v. 158, p. 357-380.

61. Singh, S.K., Rai, S.K., and Krishnaswami, S., 2008, "*Sr and Nd isotopes in river sediments from the Ganga Basin: Sediment provenance and spatial variability in physical erosion"*, Journal of Geophysical Research, v. 113, F03006, doi:10.1029/2007JF000909.

62. Singhvi, A.K., and Porat, N., 2008, "*Impact of luminescence dating on Geomorphological and Paleoclimatic research in drylands".* Bores, v. 37, p. 536-558.

63. Tiwari, M., and Ramesh, R., 2008, *"Problems and prospects of stable isotope applications to marine microfossils for paleoceanography and paleoclimate reconstruction*", The Palaeobotanist, v. 57, p. 303-309.

64. Vadawale, S.V., Purohit, S., Shanmugam, M., Acharya, Y.B., Goswami, J.N., Sudhakar, M., Sreekumar, P., 2008, *Characterization and selection of CZT detector modules for HEX experiment onboard Chandrayaan-1,* Nuclear Instruments and Methods, Part A, doi:10.1016/j.nima.2008.09.036, v. 598, 2009, p. 485-495.

65. Weinman, B., Goodbred, S.L., Jr., Zheng, Y., Aziz, Z., Singhvi, A.K., Nagar, Y.C., Steckler, M., 2008, "*Controls of Floodplain Evolution on Shallow Aquifer Development and the Distribution of Groundwater Arsenic: Araihazar, Bangladesh*", A-v. Geen. Bull. Geol. Soc. Am., v. 120 (11/12), p. 1567-1580.

66. Yadav, D.N., and Sarin, M.M., 2009, "*Ra-Po-Pb isotope systematics in waters of Sambhar Salt Lake, Rajasthan (India) : Geochemical characterization and particulate Reactivity"*, Journal of Environmental Radioactivity, v. 100, p. 17-22.

Space and Atmospheric Sciences

67. Bapat, B., Vandana, Sharma, and Kumar, S.V.K., 2008, "*Dissociative states of SF_4^{2+} probed by fragment momentum spectroscopy*", Physical Review A, v. 78, p. 042503.

68. Chakrabarty, D., Sekar, R., Sastri, J.H., and Sudha Ravindran, 2008, *"Distinctive effects of interplanetary electric field and substorm on nighttime equatorial F layer: a case study",* Geophysical Research Letters, v. 35, L19108, doi:10.1029/2008GL035415.

69. Chandra, H., Sharma, Som, Das, S.R., and Rao, R.R., 2008, *"Vertical drift from HF Doppler Measurements over Ahmedabad",* Journal of Indian Geophysical Union, v. 12, p. 173-178.

70. Chandra, H., Sinha, H.S.S., Das, U., Misra, R.N., Das, S.R., Datta, J., Chakravarty, S.C., Patra, A.K., Rao, V., and Rao, D.N., 2008, "*First mesospheric turbulence study using coordinated rocket and MST radar measurements over Indian low latitude region"*, Annales Geophysicae, v. 26, p. 2725-2738.

71. Chandra, H., Vats, H.O., and Sharma, Som, 2008, "*Effects of solar flares on the interplanetary medium and terrestrial environment",* Asian Journal of Physics, v. 17, p. 365-383.

72. Cherian, R., Venkataraman, C., and Ramachandran, S., 2009, *"Temporal variability in emission category influence on organic matter aerosols in the Indian region",* Geophysical Research Letters, v. 36, L06809, doi:10.1029/2008GL036311.

73. Das, S.K., Jayaraman, A., and Misra, A., 2008, *"Fog-induced variations in aerosol optical and physical properties over the Indo-Gangetic Basin and impact to aerosol radiative forcing",* Annales Geophysicae, v. 26, p. 1345-1354.

74. Das, U., and Sinha, H.S.S., 2008, "*Long term variations in oxygen green line emission over Kiso, Japan from ground photometric observations using continuous wavelet transform"*, Journal of Geophysical Research, doi:10.1029/2007JD009516.

75. Haider, S.A., Abdu, M.A., Batista, I.S., Sobral, J.H., Xiaoli Luan, Esa Kallio, Maguire, W.C., Verigin, M.I., and Singh, V., 2009, *"D, E, and F layers in the daytime at high latitude terminator ionosphere of Mars: Comparison with Earth's ionosphere using COSMIC data*, Journal of Geophysical Research, v. 114, A03311,doi:101029/2008JA013709.

76. Haider, S.A., Varun, Sheel, Singh, V., Maguire, W.C., and Molina-Cuberos, J., 2008, *"Model calculation of production rates, ion and electron densities in the evening troposphere of Mars at latitudes 67°N and 62°S: Seasonal variability"*, Journal of Geophysical Research, v. 113, A08320, doi:10.1029/2007JA012980.

77. Kedia, S., and Ramachandran, S., 2008, *"Features of aerosol optical depths over the Bay of Bengal and the Arabian Sea during premonsoon season:Variabilities and anthropogenic influence",* Journal of Geophysical Research, v. 113, D11201, doi:10.1029/2007JD009070.

78. Kedia, S., and Ramachandran, S., 2008, *"Latitudinal and longitudinal variation in aerosol characteristics from Sun photometer and MODIS over the Bay of Bengal and Arabian Sea during ICARB",* Journal of Earth System Science, v. 117, p. 375-387.

79. Kulkarni, P., Ramachandran, S., Bhavani Kumar, Y., Rao, D.N., and Krishnaiah, M., 2008, *"Features of upper troposphere and lower stratosphere aerosols observed by lidar over Gadanki, a tropical Indian station",* Journal of Geophysics Research, v. 113, D17207, doi:10.1029/2007JD009411.

80. Kushawaha, R.K., and Bhas, Bapat, 2008 "*Dissociation dynamics of the methanol dication"*, Chemical Physics Letters, v. 463, p. 42-46.

81. Lal, S., Sahu, L.K., Venkataramani, S., Rajesh, T.A., and Modh, K.S., 2008 Distributions of O_3, CO and NMHCs over the rural sites in centralIndia, Journal of Atmospheric Chemistry, v. 61, p. 7384, doi:10.1007/s10874-009-9126-5.

82. Lal, S., Sahu, L.K., Gupta, S., Srivastava, K.S., Modh, K.S., Venkataramani, S., Rajesh, T.A., 2008, *"Emission characteristic of ozone related trace gases at a semi-urban site in the Indo-Gangetic plain using inter-correlations",* Journal of Atmospheric Chemistry, v. 60, doi:10.1007/s10874-008-9115-0, p.189-204.

83. Prakash, S., Pallamraju, D., and Sinha, H.S.S., 2009, "*Role of the Equatorial Ionization Anomaly in the Development of the Evening Pre-Reversal Enhancement of the Equatorial Zonal Electric Field"*, Journal of Geophysical Research, v. 114, A02301, doi:10.1029/2007JA012808.

84. Ramachandran, S., and Cherian, R., 2008, *"Regional and seasonal variations in aerosol optical characteristics and their frequency distributions over India during 2001-2005"*, Journal of Geophysical Research, v. 113, D08207, doi:10.1029/2007JD008560.

85. Ramachandran, S., and Rajesh, T.A., 2008*, "Asymmetry parameters in the lower troposphere derived from aircraft measurements of aerosol scattering coefficients over tropical India",* Journal of Geophysical Research, v. 113, D16212, doi:10.1029/2008JD009795.

86. Rastogi, R.G., and Chandra, H., 2008, *"A new phenomenon on IMF and geomagnetic field",* Indian Journal of Physics, v. 82, p. 1247-1254.

87. Rastogi, R.G., Chandra, H., James, M.E., Kitamura, K., and Yumoto, K., 2008, "*Characteristics of the equatorial electrojet in Central America"*, Earth Planet and Space, v. 60, p. 623-632.

88. Sekar, R., and Chakrabarty, D., 2008, *"Role of over-shielding electric field on the development of pre-midnight plume event: simulation results",* Journal of Atmospheric and Solar Terrestrial Physics, v. 70, p. 2212-2221.

89. Sekar, R., Chakrabarty, D., Narayanan, R., and Patra, A.K., 2008, *"Thermospheric airglow intensity variations corresponding to various ESF structures revealed by VHF radar maps",* Annales Geophysicae, v. 26, p. 3863-3873.

90. Sunil Kumar, S., Deshmukh, P.C., Kushawaha, R.K., Sharma, V., Prajapati, I.A., Subramanian, K.P., and Bapat, B., 2008, "*Breakup of the SF_6^{3+} photoion revealed by momentum correlation between fragments"*, Physical Review A, v. 78, p. 062706.

Theoretical Physics

91. Agarwal, R., and Santhanam, M.S., 2008, *"Digital watermarking in the singular vector domain"*, International Journal of Image and Graphics, v. 8, p. 351-368.

92. Ahalpara, D.P., Verma, A., Parikh, J.C., and Panigrahi, P.K., 2008, *"Characterizing and modeling cyclic behavior in non-stationary time series through multi-resolution analysis"*, Pramana, v. 71, p. 459-485.

93. Ananthanarayan, B., and Rindani, S.D., 2008, "*Two-particle kinematic distributions from new physics at an electron–positron collider with polarized beams"*, European Physical Journal C, v. 56, p. 171-179.

94. Banerji, J., Deb, S., Jenkins, R.M., and Davies, A. R., 2009, "*Quasi-Gaussian output from dual case I waveguide resonators with mirrors of step-index reflectivity profiles*", Applied Optics, v. 48, p. 539-544.

95. Bhatt, J., Panigrahi, P.K., and Vyas, M., 2008, *"Entanglement-induced sub-Planck phase-space structures",* Physical Review A, v. 78, p. 03410 (1-4). (Highlighted in Virtual Journal of Quantum Information).

96. Bhatt, J.R., Gu, P., Sarkar, U., and Singh, S., 2008, *"Left-right symmetric model of neutrino dark energy",* Physics Letters B, v. 663, p. 83-85.

97. Chatterjee, B., Mishra, H., and Mishra, A., 2009, *"Relativistic BCS-BEC crossover: a variational approach"*, Physical Review D, v. 79, p. 014003 (1-11).

98. Choudhury, S., Muralidharan, S., and Panigrahi, P.K., 2009, *"Quantum teleportation and state sharing using a genuinely entangled six-qubit state"*, Journal of Physics A, v. 42, p. 115303 (1-8).

99. Das, P., Raju, T.S., Roy, U., and Panigrahi, P.K., 2009, *"Sinusoidal excitations in two-component Bose-Einstein condensates in a trap"*, Physical Review A, v. 79, p. 015601 (1-4).

100. Gandhi, R., Ghoshal, P., Goswami, S., and Sankar, S.U., 2008, *"Resolving the Mass Hierarchy with Atmospheric Neutrinos using a Liquid Argon Detector",* Physical Review D, v. 78, p. 073001 (1-6).

101. Goswami, S., and Watanabe, A., 2009, *"Minimal Seesaw Textures with Two Heavy Neutrinos",* Physical Review D, v. 79, p. 033004 (1-13).

102. Gu, P., and Sarkar, U., 2008, *"B-L Conserved Baryogenesis",* Modern Physics Letter A, v. 23, p. 2047-2051.

103. Gu, P., and Sarkar, U., 2008, *"Radiative Neutrino Mass, Dark Matter and Leptogenesis",* Physical Review D, v. 77, p. 105031 (1-4).

104. Gu, P., and Sarkar, U., 2008, *"Radiative seesaw in left-right symmetric model",* Physical Review D, v. 78, p. 073012 (1-5).

105. Gu, P., and Sarkar, U., 2008, *"SO(10) GUT Baryogenesis"*, Physics Letters B, v. 663, p. 80-82.

106. Gu, P., Hirsch, M., Sarkar, U., and Valle, J.W.F., 2009, *"Neutrino masses, leptogenesis, and dark matter in hybrid seesaw",* Physical Review D, v. 79, p. 033010 (1-4).

107. Jenkins, R.M., Blockley, A.F., Banerji, J., and Davies, A.R., 2008, "*Fibre coupled dual-mode waveguide interferometer with $\lambda/130$ fringe spacing*", Physical Review Letters, v. 100, p. 163901 (1-4).

108. Jha, T.K., and Mishra, H., 2008, *"Constraints on nuclear matter parameters in an effective chiral model"*, Physical Review C, v. 78, p. 065802 (1-9).

109. Jha, T.K., Mishra, H., and Sreekanth, V., 2008, "*On attributes of a rotating neutron star with a hyperon core"*, Physical Review C, v. 77, p. 045801 (1-11).

110. Joshipura, A.S., and Kodrani, B.P., 2009, *"Complex CKM matrix, spontaneous CP violation and generalized mu– tau symmetry"*, Physics Letters B, v. 670, p. 369-373.

111. Kota, V.K.B., 2008, *"Eigenvalue Density for Random Covariance Matrices from a 2x2 Partitioned GOE",* Advanced Studies in Theoretical Physics v. 2, p. 845-854.

112. Kota, V.K.B., Mayya, K.B.K. and Castilho Alcaras, J.A., 2009, *"Statistical law for multiplicities of SU(3) irreps (λ,μ) in the plethysm $\{\eta\}\otimes^3\{m\}\rightarrow(\lambda,\mu)$"*, Journal of Physics A, v. 42, p. 145201 (1-20).

113. Lambiase,G., Mohanty, S., and Scarpetta, G., 2008, *"Magnetic field amplification in f(R) theories of gravity",* Journal of Cosmology and Astroparticle Physics, v. 0807, p. 019 (1-24).

114. Leclair, R.J., Haq, R.U., Kota, V.K.B., and Chavda, N.D., 2008, *"Power Spectrum Analysis of the Average-Fluctuation Density Separation in Interacting Particle Systems"*, Physics Letters A, v. 372, p. 4373-4378.

115. Manimaran, P., Panigrahi, P.K., Parikh, J.C., 2008, *"Difference in nature of correlation between NASDAQ and BSE indices"*, Physica A, v. 387, p. 5810-5817.

116. Manimaran, P., Panigrahi, P.K., Parikh, J.C., 2009, "*Multiresolution analysis of fluctuations in non-stationary time series through discrete wavelets*", Physica A, v. 388, p. 2306-2314.

117. Masso, E., Mohanty, S., Nautiyal, A., and Zsembinszki, G., 2008, *"Imprint of spatial curvature on in flation power spectrum",* Physical Review D, v. 78, p. 043534 (1-8).

118. McDonald, J., Sahu, N., and Sarkar, U., 2008, *"Type-II Seesaw at Collider, Lepton Asymmetry and Singlet Scalar Dark Matter"*, Journal of Cosmology and Astroparticle Physics, v. 0804, p. 037 (1-14).

119. Mishra, A., and Mishra, H., 2009, *"LOFF and breached pairing with cold fermionic atoms"*, European Physical Journal D, v. 53, p. 75-87

120. Mishra, S., Shukla, A., Sahu, R., and Kota, V.K.B., 2008, *"Deformed shell model for* β^+/EC *and* $2\nu\beta^+\beta^+/\beta^+EC/ECEC$ *and decay half lives of medium heavy* $N \sim Z$ *nuclei"*, Physical Review C, v. 78, p. 024307 (1-7).

121. Mohanty, S., and Nautiyal, A., 2008, *"Natural inflation at the GUT scale"*, Physical Review D, v. 78, p. 123515 (1-5).

122. Muralidharan, S., and Panigrahi, P.K., 2008, *"Quantum-information splitting using multipartite cluster states"*, Physical Review A, v. 78, p. 062333 (1-5). (Highlighted in Virtual Journal of Quantum Information).

123. Prasanna, A.R., and Mohanty, S., 2009, *"Photon propagation in torsion background"*, General Relativity and Gravitation, doi:10.1007/s10714-009-0790 1.

124. Rao, D.D.B., Ghosh, S., and Panigrahi, P.K., 2008, *"Generation of entangled channels for perfect teleportation using multielectron quantum dots"*, Physical Review A, v. 78, p. 042328 (1-6).

125. Rao, D.D.B., Panigrahi, P.K., and Mitra, C., 2008, *"Teleportation in the presence of common bath decoherence at the transmitting station"*, Physical Review A, v. 78, p. 022336 (1-5). (Highlighted in Virtual Journal of Quantum Information).

126. Sahu, N., and Sarkar, U., 2008, *"Extended Zee model for neutrino mass, leptogenesis, and sterile-neutrino-like dark matter",* Physical Review D, v. 78, p. 115013 (1-6).

127. Santhanam, M.S., and Kantz, H., 2008, *"Return interval distribution of extreme events and long term memory"*, Physical Review E, v. 78, 051113 (1-9).

128. Silotri, S., Angom, D., Mishra, H., and Mishra, A., 2008, *"Pairing in spin polarised two species fermionic mixtures with mass asymmetry",* European Physical Journal D, v. 49, p. 383-390.

129. Sree Ranjani, S., Kapoor, A.K., and Panigrahi, P.K., 2008, *"Normalizable states through deformation of Lam and the associated Lam potentials"*, Journal of Physics A, v. 41, p. 285302 (1-11).

130. Sree Ranjani, S., Panigrahi, P.K., Kapoor, A.K., and Khare, A., 2009, *"An explicit realization of fractional statistics in one dimension",* Annals of Physics, v. 324, p. 1176-1183.

131. Sree Ranjani, S., Roy, U., Panigrahi, P.K., and Kapoor, A.K., 2008, *"Soliton response to transient trap variations",* Journal of Physics B, Atomic Molecular and Optical Physics, v. 41, p. 235301 (1-8).

132. Vyas, M., Kota, V.K.B., and Chavda, N.D., 2009, *"One- plus two-body random matrix ensembles with spin: Results for pairing correlations",* Physics Letters A, v. 373, p. 1434-1443.

133. Vyas, V.M., Patel, P., and Panigrahi, P.K., Kumar, C.N., and Greiner, W., 2008, *"Chirped chiral solitons in the nonlinear Schrdinger equation with self-steepening and self-frequency shift",* Physical Review A, v. 78,p. 021803 (R) (1-4).

Publications in Proceedings of Symposia

Astronomy and Astrophysics

1. Ashok, N.M., Banerjee, D.P.K., Joshi, V., Naik, Sachindra, 2008, *"V2491 Cygni"*, Published by Central Bureau Electronic Telegrams (CBET), 1354.

2. Anandarao, B.G., Richardson, E.H., Chakraborty, A., and Epps, H., 2008, *"A wide-field near-infrared camera and spectrograph for the Mt. Abu I.2 m telescope"*, Proceeding of SPIE., v. 7014, p. 70142-70148.

3. Chakraborty, A., Richardson, E.H., and Mahadevan, S., 2008, *"PRL advanced radial velocity all sky search (PARAS), An efficient fibre-fed spectrograph for planet searches"*, Proceeding of SPIE, v. 7014E, p. 146-151.

4. Janardhan, P., Fujiki, K., Kojima, M., and Tokumaru, M., 2007, *"Locating the Solar Source of the Extremely Low-density, Low-velocity Solar Wind Flows of 11 May 1999"*, Proceeding of the ILWS Workshop, Goa, India, ISBN: 81-87099-40-2, 132-138.

5. Provencal, J., Thompson, S., Baliyan, K.S., Vats, H.O., 2008, *"Preliminary XCOV26 Results for EC14012-1446",* Proceedings of the White Dwarf Meeting, Barcelona, doi:10.1088/1742-6596/172/1/012061, 30 June, - 4 July, 2008, 101.

7. Schultheis, M., Ganesh, S., Omont, A., Aringer, B., Robin, A.C., 2008, *"Stellar Populations in the Galactic Bulge" in* Proceedings of the conference *"Mapping the Galaxy and Nearby Galaxies",* Astrophysics and Space Science Proceedings, published by ISBN 978-0-387-72767-7. Springer Science, Business Media, LLC, 376.

6. Schultheis, M., Ramirez, S., Sellgren, K., Stolovy, S., and Ganesh, S., 2009, "*Interstellar extinction in the Galactic Center and its impact on the study of AGB stars",* Proceedings of conference - The Evolving ISM in the Milky Way and Nearby Galaxies, Pasadena, USA, 2-5 December, 2007, E59, p. 1-7.

Solar Physics

8. Bayanna, A.R., Kumar, B., Louis, R.E., Venkatakrishnan, P., and Mathew, S.K., *"Development*

of a Low-order Adaptive Optics System for Udaipur Solar Observatory", 2008, in Proceedings of *Challenges for Solar Cycle- 24*, Eds. R. Jain, P. Venkatakrishnan and J. Karpen, Journal Astrophysics and Astronomy, 29, p. 353-358.

9. Denis, S.P., Coucke, E., Gabriel, C., Delrez and Venkatakrishnan, P., *"Optomechanical and Thermal design of the Multi-Application Solar Telescope for USO"*, 2008, in *Ground Based and Airborne Telescopes II,* Eds. Larry M. Stepp and Ro berto Gilmozzi, Proceedings of SPIE 7012, 701235-8.

10. Gosain, S., Sanjay, Tiwari, S., Joshi, J., Venkatakrishnan, P., *"Software for interactively visualizing solar vector magnetograms of Udaipur Solar Observatory"*, in Proceedings of *Challenges for Solar Cycle- 24*, Eds. R. Jain, P. Venkatakrishnan and J. Karpen,Journal of Astrophysics and Astronomy, 29, p. 107-113.

11. Gosain, S., and Venkatakrishnan, P., *"A 2-dimensional Scanning Solar Vector Magnetograph at Udaipur Solar Observatory"* in *Solar Polarization 5: In Honor of Jan Stenflo,* Eds. Svetlana V. Berdyugina, K. N. Nagendra, and Renzo Ramelli, ASP Conf. Ser. 405, 467-472.

12. Mathew, S.K., *"A New 0.5m Telescope (MAST) for Solar Imaging and Polarimetry"*, 2008, in *Solar Polarization 5: In Honor of Jan Stenflo,* Eds. Svetlana V. Berdyugina, K. N. Nagendra, and Renzo Ramelli, ASP Conf. Ser. 405, p. 461-466.

13. Maurya, R.A., and Ambastha, A., *"H_α Intensity Oscillations in Large Flares"*, in Proceedings of *Challenges for Solar Cycle- 24*, Eds. R. Jain, P. Venkatakrishnan and J. Karpen, Journal Astrophysics and Astronomy, 29, p. 249-252.

14. Maurya, R.A., and Ambastha, A., *"Magnetic and Velocity Fields in Active Regions"*, in Proceedings of *Challenges for Solar Cycle- 24*, Eds. R. Jain, P. Venkatakrishnan and J. Karpen, J. Astrophysics and Astronomy, 29, p. 103-105.

15. Tiwari, S., Joshi, J., Gosain, S., and Venkatakrishnan, P., *"Evolution of Magnetic Helicity in NOAA 10923 Over Three Consecutive Solar Rotations"*, 2008, Astrophysics and Astronomy Proceedings, DOI 10.1007/978-1-4020-8868-1_22, p. 329-335.

Planetary and Geosciences

16. Deshpande, R.D., and Gupta, S.K., 2009, *"An Insight into the Origin and Distribution of High Fluoride in Groundwaters of North Gujarat-Cambay Region",* Proceedings of the Seminar on Water for Future-Issues and Options, Central Water Commission, p. 1-16.

17. Deshpande, R.D., and Gupta, S.K., 2009, *"Application of Isotopic Tracers for Efficient Water Resource Management", Proceedings of the Regional Workshop on Issues related Ground Water Management and Water use Efficiency in the State of Gujarat and U.T. of Daman and Diu",* Central Ground Water Board, p. 156-169.

18. Deshpande, R.D., and Gupta, S.K., 2009, *"Dissolved Noble Gases in Groundwater Hydrology",* Proceedings of the International Conference on Water, Environment, Energy and Society (WEES-2009), Allied Publishers, v. 3, p. 1249-1259.

19. Dhingra, D., 2009, *"Lithological Mapping of Lunar Terranes Using Hybrid Classification Approach"*, 40th Lunar & Planetary Science Conference, Texas, USA, Abstract # 1456.

20. Durga Prasad K., and Murty, S.V.S., 2008, *"Characterization of water sensors for lunar water probing sensor network. Proc. Int. Conf. on Emerging Scenarios in Space Technology and Applications (ESSTA2008),* Sathyabama University, Jeppiaar Nagar, Chennai, India, 13-15, November, p. 377-384.

21. Murty, S.V.S., Mahajan, R.R., Shukla, A.D., Mazumdar, A.C., Shukla, P.N., Durga, K., Prasad, Rai, V.K., Panda, D., Ghevaria, Z.G., and Goswami, J.N., JODIA (L5) and Mahadevpur (H4/5): Two recent ordinary chondrite falls in India, 72nd Annual Meeting of Meteoritical Society, 13-18 July, 2009, Abstract No#5058.

22. Shanmugam, M., Acharya, Y.B., Santhosh Vadawale, Banerjee, D., Umapathy, C.N., Sharma, M.R., Lalitha, Abraham, Anurag, Tyagi, Ravi, Kulkarni, Sudhakar, M., and Premalatha, 2008, *"High Energy X-ray (HEX) Spectrometer instrumentation for Chandrayaan-1 and its developmental challenges",* Proceeding Int. Conf. On Emerging Scenarios in Space Technology and Applications (ESSTA2008), Sathyabama University, Jeppiaar Nagar, Chennai, India, 13-15, November, p. 371-376.

23. Sreekumar, P., Umapathy, C.N., Ramakrishna Sharma, M., Sreekantha, C.V., Tyagi, A., Kumar, M., Sudhakar, L., Abraham, R., Kulkarni, R.L., Premlatha, A.K., Srivastava, S., Neeraj Kumar, Bug, M., Acharya, Y.B., Vadawale, S., Shanmugam, M., Banerjee, D., Purohit, S., Patel, H., Goswami, J.N., 2009, High-Energy X-ray Spectrometer (HEX) on Chandrayaan-1: Studies of volatile transport on moon and mapping of U, Th-rich terrain, Lunar and Planetary Science Conference, 40, # 2572.

24. Srivastava, N., 2009, *"Spectral Reflectance studies for maturation trends in a mare and highland swirl"*, 40th Lunar & Planetary Science Conference, Texas, USA, Abstract # 1577.

25. Zinner, E., Amari, S., Gyngard, F., and Marhas, K.K., 2008, *"Iron and nickel isotopic compositions of presolar SiC grains from supernovae"*, Proceeding *10th Symposium on Nuclei in the Cosmos,* p. 201-026.

Theoretical Physics

26. Gharekhan, A., Rath, D., Ojha, A.N., Pradhan, A., Sureshkumar, M.B., and Panigrahi, P.K., 2009, *"Comparative study of laser and lamp fluorescence of cancer and normal tissues through wavelet transform and singular value decomposition"*, Proceedings of SPIE, v. 7176, p. 717608 (1-8).

27. Jenkins, R.M., Perrett, B.J., McNie, M.E., Finlayson, E.D., Davies, R.R., Banerji, J., and Davies, A.R., 2008, *"Hollow optical waveguide devices and systems",* Conference on Electro-Optical and Infrared Systems: Technology and Applications V, Cardiff, U.K., 16-18 September, 2008, Proceedings of SPIE, v.7113, p.71130E (1-8).

28. Kota, V.K.B., Shukla, A., and Sahu, R., 2008, *"Shell Model Based SDM and DSM Methods for Double Beta Decay",* Proceedings of the Workshop on Neutrinoless Double Beta Decay, Edited by V. Nanal, Tata Institute of Fundamental Research, Mumbai, p. 47-57.

29. Kota, V.K.B., Vyas, M., and Mayya, K.B.K., 2008, *"Spectral distribution analysis of random interactions with J-symmetry and its extensions"*, International Journal of Modern Physics E, v. 17 (Supp), p. 318-333.

30. Roy, P., Mishra, H., et al., 2009, *"Working group report: Quark Gluon Plasma"*, Proceedings of WHEPP X Jan. 2008, Institute of Mathematical Science, Chennai, Pramana, v. 72, p. 285-294.

31. Sahu, R., Mishra, S., Shukla, A., and Kota, V.K.B., 2008, *"New Applications of Deformed Shell Model",* Proceedings of the DAE-BRNS Symposium on Nuclear Physics, Editors: R.K. Choudhury, A. Saxena and B.J. Roy, v. 53, p. 189-198.

Library and Information Services

32. Nishtha A, *"Linux for Librarians"*, 2009, Proceedings of the National Workshop on Library 2.0 : A Global Information Hub, organized by PRL, p. 180-188.

Monographs / Review Articles

1. Ahalpara, D.P., Arora, S., and Santhanam, M.S., 2009, *"Genetic programming based approach for synchronization with parameter mismatches in EEG"*, Lecture Notes in Computer Science, v. 5481, p. 13 24.

2. Ambastha, A., 2008, "*Helioseismic effects of energetic transients"*, *Journal Astrophysics Astronomy*, 29, p. 93-101.

3. Amritkar, R.E., 2008, "Synchronization of Networks", Pramana, v.71, p.195-201.

4. Das, A.C., 2008, *"Space Weather"* in Electromagnetic Phenomena Related to Earthquakes and Volcanoes, ed. Birbal Singh, Narosa Publishing House, New Delhi, p. 212-222.

5. Gupta, S.K., 2009, *"Sustaining Akshaydhara, Pristine Perennial Flow of Water, for Growing India",* in Sustainable Management of Water Resources – Emerging Science and Technology Issues in South Asia. XII General Assembly of Scope, India, (eds. M.G.K. Menon and V.P. Sharma), INSA, p. 161-168.

6. Gupta, S.K., and Deshpande, R.D., 2009, "*Contributions of the Water Isotope Studies to Hydrology of India",* in Sustainable Management of Water Resources – Emerging Science and Technology Issues in South Asia. XII General Assembly of Scope, India, (eds. M.G.K. Menon and V.P. Sharma), INSA, p. 284-294.

7. Jain, R., Venkatakrishnan, P., and Karpen, J., (eds.) Proceedings of *Challenges for Solar Cycle 24, 2008,* Journal Astrophysics Astronomy.

8. Juyal, N., and Sundriyal, Y.P., 2008, Late "*Quaternary climatic studies in Himalaya"*, in Glimpses of Geoscience Research in India. The Indian Report to IUGS 2004-2008. (eds. A.K. Singhvi, A. Bhattacharya and S. Guha). Indian National Science Academy publication, p. 51-55.

9. Lal, D., and Krishnaswami, S., 2009, "*Cosmic Ray Geophysics and its Evolution*. "India in the World of Physics: Then and Now" (eds. A.N. Mitra) PHISPC Centre for Studies in Civilizations, Pearson Longman, p. 461-480.

10. Krishnaswami, S., and Lal, D., 2008, "*Cosmogenic Nuclides in the Environment: A Brief Review of their Applications",* in "Recent Advances in Earth System Sciences" (eds. H. Gupta and Fareeduddin) Geol. Soc. India, Golden Jubilee Memoir, p. 559-600.

11. Krishnaswami, S., and Singh, S.K., 2008, "*Erosion in River Basins of India",* in "Glimpses of Geoscience Research" in India (eds. A.K.Singhvi, A.Bhattacharya and S.Guha) Indian National Science Academy, p. 32-40.

12. Krishnaswami, S., and Cochran, J.K., (eds.), 2008, U-Th Series Nuclides in Aquatic Systems, Elsevier, Amsterdam, p. 1-458.

13. Rajmal, Jain, and Lokesh, Bharti, 2008, "Genesis of Solar Flares and Associated Phenomena", Asian Journal of Physics, v.17, p. 319-334.

14. Rajmal, Jain, 2008, "X-ray Spectroscopy of the Solar Flares", Asian Journal of Physics, v. 17, p. 504-527.

15. Singh, R.P., Ashok Kumar, and Bhatt, J., 2008, *"Vortices of Light: Generation, Characterization and Applications",* Progress in Nonlinear Optics Research, Miyu Takahashi and Hina Gotô (eds.), Nova Science Publishers, NY., p. 359-381.

16. Singh, R.P., 2009, *"Aerosols in a controlled environment: a study using static and dynamic light scattering"*, Light Scattering Review, v.4, Kokhanovsky, Alexander A. (eds.), Springer, p. 469-509.

17. Singhvi, A.K., 2008, "*Luminescence and Electron Spin Resonance studies in India",* "Glimpses of Geoscience Research" in India. The Indian Report to IUGS 2004-2008. (eds. A.K. Singhvi, A. Bhattacharya and S. Guha). Indian National Science Academy publication, p. 193-198.

18. Singhvi, A.K., Bhattacharya, A., and Guha, S., (editors), 2008, Indian Report to IUGS, Indian National Science Academy, p. 337.

19. Srivastava, N., 2008, "*Coronal mass ejections and associated phenomena*" in *Recent Advances in Solar Physics*, Editors: B.N. Dwivedi and Udit Narain, Publisher: World Scientific, Singapore, p. 193-214.

20. Venkatakrishnan, P., and Gosain, S., 2008, "Solar Magnetic Fields", in *Recent Advances in Solar Physics* , Editors : B.N. Dwivedi and Udit Narain, Publisher: World Scientific, Singapore, p. 193-214

Technical Reports

1. Bhavsar. K.,*"Power Factor",* PRL-TN-2008-90, Physical Research Laboratary, Ahmedabad.

2. Ganesh, S., Joshi, U.C., Baliyan, K.S., Mathur, S. N., Patwal, P.S., and Shah, R.R., "*Automation of PRL's Astronomical Optical Polarimeter with a GNU/ Linux based distributed control system",* PRL-TN-2008-93, Physical Research Laboratory, Ahmedabad March, 2009.

3. Pabari, J.P., *"Backend Electronics and Quasi-Optics for Submillimeter Heterodyne Spectroscopy of NO_2"*, PRL-TN-2008-91, Physical Research Laboratory, Ahmedabad, September, 2008.

4. Rajesh T.A., *"Graphical User Interface for Stepper Motor based Filter Wheel control",* PRL-TN-2008-92, Physical Research Laboratory, Ahmedabad, July, 2008.

Publications for Education

1. Goel, Suruchi, Mahajan, R.R., and Murty, S.V.S., 2009, *"Meteorites: Archives of Solar System History". Virat Surya*, Indian Planetary Society, v. 6, p. 27-30.

2. Rao, K., Sahu, N., and Panigrahi, P.K., 2008, *"Fermion Number Fractionization"*, Resonance, v. 13, p. 738-751.

3. Hari Om Vats

As a part of public outreach the following five space science Cartoon books were translated into Hindi for school and college students:

a. What is Global warming?
b. What is Geomagnetism?
c. What is Ozone Hole?
d. What is Polar Region?
e. What is Upper atmosphere?

Facilities and Services

Administrative

Activities on the Promotion of National Language

As a part of implementation and progressive use of Hindi in PRL,the Hindi Pakhwada was celebrated at PRL from September 14 - 28, 2008. Thehighlights of the celebrations included word quiz, essay, elocution,Hamara Karya, self written poetry competitions. A Technical Seminar in Hindi on Various Scentific Programs in PRLwas held at PRL on 19 March, 2009. 21 members participated and presentedtheir papers in this Seminar.Papers were also presented from SAC and IPR.Vishwa Hindi Divas was organised in PRL on 12.1.2008.

Shri R.S. Gupta, Hindi Officer-II delivered lectures in Hindi workshops held by various Deptt. like Space Applications Centre, AirportAuthority, Food Corporation of India, Income Tax, Doordarshan on differenttopics including Various applications of comoputers inHindi.

Computer Centre

The Computer Centre is equipped with a IBM Power5 Machine with 4 processors and 8GB RAM to cater to the high computing needs of PRL. It also has four HP servers, each with four AMD processors, 4 GB RAM, 1.5 TB disk space, providing computing power with large disk storage of 500GB. The computing machines are connected to a high-speed (100/1000 Mbps) local area network (LAN) to provide easy, fast and reliable access to our 200 PC's and a few workstations. The Thaltej campus is connected via a 40 Mbps 5.4 GHz microwave non-line-of-sight Link and the Udaipur Solar Observatory and the Mt. Abu campuses are connected through 2 Mbps MLNNs from BSNL. This ensures the clock connectivity to users from Thaltej, USO, and Mt. Abu campuses. Our main campus is also connected to Thaltej via BSNL's 2 Mbps MLLN for voice communication, providing intercom telephone facility between the two campuses. The Centre provides centralized virus free E-mails by automatically scanning all incoming E-mails with Centrally installed Anti-Spam filter. The Center also provides web enabled email service. Internet authorizations, monitoring and reporting functions have been added to have optimal usage of Internet bandwidth.

To cater to the high end computing needs, PRL has become a resource partner of C-DAC's Grid Garuda Project. The Grid Garuda network is integrated to PRL LAN providing seamless access of Garuda resources to PRL scientists.

PRL SPACENET set up is upgraded with IP based Network Connectivity. Spacenet is installed at USO and Mt. Abu with IP based equipments. Spacenet is used for Voice, Data, and Video conferencing for interacting with USO, Mt. Abu campuses and various ISRO centers.

PRL Main Campus and PRL Dispensary are now connected by 10 Mbps Wireless link extending all computer services to PRL Dispensary.

The Thaltej Campus is connected to SAC via 2 Mbps MLLN provided by BSNL for direct data transfer for various payloads of Chandrayan – I.

Mathematical, numerical and visualization application software like IMSL, IDL, Mathematica, SigmaPlot, MATLAB, Lahey FORTARN 95, Maple, and Data Explorer etc. have also been installed to cater to the needs of the scientific community.

Library & Information Services

Library plays a crucial role in facilitating research in the laboratory by making available latest books, journals, e-journals in the respective areas. In addition to these activities, PRL Library subscribes to full-text databases like ScienceDirect, IOP Archive, PROLA, Scientific American Online Archive. As no library can be completely self-sufficient, it also provides document delivery service through ILL and commercial vendor. During 2008-09 the Library assisted the students and scientists in procuring 122 books for book grant and 88 books for personal use.

In 2008-09, 216 scientific & general books, 78 Hindi books, and 77 CDs/DVDs were added in the libraries at the Main & Thaltej campuses, 7 books were added in USO library. So the final collection stands at 18752 books, 1946 Hindi books and 1002 CDs/DVDs in Main & Thaltej libraries and 2090 books in USO library.

This year, LPS Consortium was formed consisting of members – LEOS, Bangalore, PRL, Ahmedabad and SAC, Ahmedabad to subscribe to SPIE Digital Library. The SPIE Digital Library is a very extensive resource available on optics and photonics, providing access to more than 260,000 technical papers from SPIE Journals and Conference Proceedings from 1990 to the present. More than 17,000 new research papers are added annually to this database.

The library homepage gives link to 141 online journals out of the 153 journal titles subscribed by the library. It also provides access to the institutional repository consisting of journal articles published by the PRL authors from 1995 to present using the open source digital library software – Greenstone.

During 2008-09, the number of visits to the library were 8761 and circulation count of the documents was 9673. The number of ILL requests of other institutes fulfilled by PRL Library was 219 and that of requests of PRL staff fulfilled by other libraries was 205.

The library also organized a two day national workshop on "Library2.0: A Global Information Hub" during February 5-6, 2009. Mrs Nishtha Anilkumar, Librarian, was the Workshop Co-ordinator. The workshop was attended by more than 80 participants from all over India. There were 13 invited papers for oral presentation and additional contributory papers for poster presentation. Seven poster presentations were made by the PRL Library and computer centre staff.

WORKSHOP

PRL Workshop is a general-purpose mechanical workshop that provides extensive support to scientists and engineers. The workshop has a wide range of machines such as metal cutting machines, welding machines and CNC Lathe Machine in machine shop. The workshop plays an important role in designing, developing and manufacturing precise mechanical components and helps the scientists to establish various systems for a variety of experimental set up.

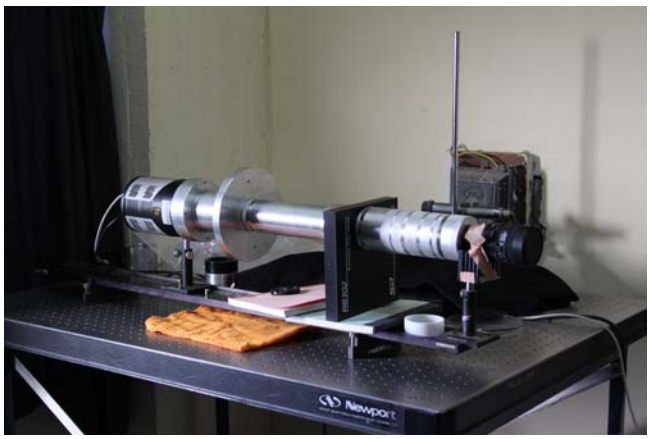

The workshop also carries out sheet and structural metal fabrication jobs. The high vacuum welding joints are also carried out by using TIG welding machine. One CNC Lathe machine carry out precise turning jobs. Various lens adaptor, optical components and mounts were fabricated at the workshop. Some of the major works carried out

during the year are listed below

A multi-wavelength airglow imager was designed to characterize the three dimensional characteristics of Atmospheric Gravity Waves. This consists of several lenses, automated filter wheel system and a high sensitive CCD detector. The whole mechanical system is fabricated in PRL workshop including mechanical coupling between the filter wheel and the CCD detector. Critical focusing of the lenses has been carried out successfully at the workshop.

High precision vacuum couplers were made from SS304 for turbo molecular pump stations for the Radiocarbon Dating Laboratory. It can be directly connected to any standard 6 inch glass or metal set u

A high-vacuum flexible metal coupling was made for the carbonate preparation system of the GEO 20-20 stable isotope mass spectrometer laboratory. This facilitates trapping of acid remains during carbon dioxide extraction.

Designed and built various components needed for the indigeneously developed system for study of the photochemical reactions of clusters and gases. These include: fabrication of mount, anode, and cathode for the hollow cathode, cusp for magnetic field carbon cluster source; mount for DC sputtering carbon cluster source and Nozzles for gas beams.

Fabricated mounting plates for a Time-of-Flight spectrometer and precision ceramic spacers for detector and spectrometer assembly.

This fabrication of a Proto-type CCD Imager & Tip/tilt assembly Fabrication for the PARAS cassegrian unit was successfully completed. The Assembly housed a peltier cooled 1kx1k CCD, a single fixed filter, a beam splitter from Newport and the tip/tilt unit with auto-guider from Star-Light Xpress. The aim of the unit was to test the concept of the tip/tilt and auto guiding for correcting the telescope tracking errors and remove hystersys associated with it.

Designed and developed the precise structure for the newly acquired instrument "Near-Infrared Camera and Spectrograph" (NICS), which is used at the cassegrain focus of the Mt Abu 1.2 m telescope. The structure was made as per requirement and successfully implemented on the existing Mt. Abu telescope.

Designed a 10 feet cubical dome for the solar optical telescope, which features heavy duty structure, rail, clamp mounting, guiding arrangement and weather proofing. This dome is successfully commissioned and installed at Thaltej Campus.

A Benthos gravity corer was replicated at PRL workshop with the required technical modification and was employed during cruise on board Sagar Sampada vessel.

Designed, developed and implemented the winch drive assembly for the Tethered balloon flight experiment conducted at the PRL main building terrace by the Space and Atmospheric Science Division.

Honorary Fellows

Professor J. E. Blamont

Academician V. I. Ginzburg

Professor A. M. J. Tom Gehrels

Professor D. Lal, FRS

Professor M. G. K. Menon, FRS

Professor U. R. Rao

Professor P. Crutzen

Professor K. Kasturirangan

Professor A. Hewish

Academic Faculty

Name	Designation	Specialisation	Academic Qualification
Goswami J. N. FNA, FASc, FNASc, FTWAS, FRAS	Director	Solar System Studies (Pre - Solar Processes)	Ph D, PRL, Gujarat Univ. (1978)
Ambastha A. K.	Professor	Solar Plasma Physics, Coronal Structure and Polarization	Ph D, PRL, Gujarat Univ. (1981)
Amritkar R. E. FASc	Professor	Nonlinear Dynamics & Chaos	Ph D, IISc, Bangalore (1978)
Ashok N. M.	Professor	Close Binary Stars, Novae IR spectroscopy	Ph D, PRL, Gujarat Univ. (1983)
Baliyan K. S.	Associate Professor	AGNs, Comets, Atomic Physics, Milky Way	Ph D, Roorkee Univ. (1986)
Banerjee D.	Reader	Thermoluminscence & Planetary Physics	Ph D, PRL Gujarat Univ. (1996)
Banerjee D. P. K.	Associate Professor	Novae, Be Stars, Planetary Nebulae, IR and Optical Studies	Ph D, PRL, Gujarat Univ. (1991)
Banerji J.	Professor	Classical Optics, Quantum Physics	Ph D, City Univ.(New York) (1982)

Name	Designation	Specialisation	Academic Qualification
Bapat B.	Associate Professor*	Atomic & Molecular Processes	Ph D, TIFR, Mumbai Univ. (1997)
Bhatt J. R.	Reader	Astrophysics	Ph D, IPR, MS Univ. (1992)
Bhushan Ravi	Scientist-SE	Oceanography and Paleoclimatology	Ph D, MS Univ.(2009)
Chakrabarty A.	Reader	Extra-solar planets, Star Formation & Instrumentation	Ph D, PRL, Gujarat Univ. (1999)
Chakrabarty D.	Scientist-SE*	Upper Atmoshere and Geomagnetic Storm	Ph.D, PRL, MLS Uni. (2008)
Chandrasekhar T.	Professor	High Angular Resolution Studies, Late type stars Solar Coronal Studies Comets	Ph D, PRL, Gujarat Univ. (1982)
Deshpande R. D.	Scientist-SE	Application of Environmental Tracers in Hydrology	Ph D, PRL, M S Univ. (2007)
Goswami S.	Associate Professor	High Energy Physics	Ph D, Calcutta Univ. (1998)
Haider S. A.	Professor*	Planetary and Cometary Atmospheres	Ph D, Banaras Univ. (1984)
Jain R.	Professor	Solar Physics	Ph D, PRL, Gujarat Univ. (1983)
Janardhan P.	Associate Professor	Solar Radio Astronomy & Space Weather	Ph D, PRL, Gujarat Univ. (1992)
Joshi B.	Scientist-SD	Solar Physics, Astronomy	Ph D, ARIES, Kumaun Univ (2007)
Joshi U. C.	Professor	AGNs, Milky way, Star Formation and Comets	Ph D, Kumaun Univ. (1981)
Joshipura A. S. FNA, FASc, FNASc	Outstanding Scientist	Particle Physics	Ph D, Bombay Univ. (1979)
Juyal N.	Scientist-SE	Quaternary Geology & Paleoclimate	Ph D, MS.Univ. (2004)
Kota V. K. B.	Senior Professor - H	Nuclear Physics	Ph D, Andhra Univ. (1977)
Lal S. FNA, FASc, FNASc	Senior Professor	Atmospheric Chemistry of Trace Gases	Ph D, PRL, Gujarat Univ. (1982)
Mahajan N.	Reader	Particle Physics	Ph D, Delhi Univ. (2003)
Marhas K. K.	Reader	Solar System studies	Ph D, PRL, DAVV Indore (2001)
Mathew S. K.	Reader	Solar Magnetic & Velocity Fields	Ph D PRL, Gujarat Univ. (1999)

Name	Designation	Specialisation	Academic Qualification
Mishra H.	Associate Professor	Strong Interaction Physics & Nuclear Astrophysics	Ph D, IOP, Utkal Univ. (1994)
Mohanty S.	Professor	Astroparticle Physics	Ph D, Wisconsin Univ. (1989)
Murty S. V. S. FASc	Professor	Isotope Cosmochemistry	Ph D, IIT, Kanpur (1981)
Naik S.	Reader*	High Energy Astro- physics, X-ray Binaries	Ph D, TIFR, Mumbai Univ. (2003)
Panigrahi P. K.	Associate Professor	Field Theory	Ph D, Rochester Univ. (1988)
Rai V.	Reader	Stable Isotope Cosmochemistry	Ph D, PRL, MS Univ. (2001)
Raju Pallam D.	Associate Professor	Space and Atmospheric Sciences	Ph D, PRL, DAVV Indore (1996)
Ramachandran S.	Associate Professor	Atmospheric Aerosols Radiative & Climate Impacts	Ph D, PRL, MS Univ. (1996)
Ramesh R. FNA, FASc, FNASc, FTWAS	Senior Professor	Paleoclimatology, Oceanography & Modelling	Ph D, PRL, Gujarat Univ. (1984)
Rangarajan R.	Associate Professor	Particle Physics & Cosmology	Ph D, Univ. of California, Santa Barbara (1994)
Rao B. G. A.	Senior Professor	Star formation, Planetary Nebulae, AGB Stars and Imaging Fabry Perot Spectroscopy	Ph D, PRL, Gujarat Univ. (1978)
Ray J. S.	Associate Professor*	Isotope Geochemistry	Ph D, PRL, MS Univ. (1997)
Rengarajan R.	Scientist-SE	Atmospheric aerosols & aqueous geochemistry	Ph D, PRL, MLS Univ. (2004)
Rindani S. D. FASc, FNA	Senior Professor	Particle Physics	Ph D, IIT, Bombay (1976)
Sarin M. M. FASc, FNA,FNASc,	Senior Professor	Atmospheric Areosol & Chemistry, Oceanography	Ph D, PRL, Gujarat Univ. (1985)
Sarkar U. FNA, FASc,FNASc,	Senior Professor	Particle Physics	Ph D, Calcutta Univ. (1984)
Sekar R.	Professor*	Upper Atmospheric & Ionospheric Physics	Ph D, PRL, Gujarat Univ. (1991)
Sheel V.	Reader	Modelling of Lower Atmosphere	Ph D, PRL, Gujarat. Univ. (1996)
Singal A. K.	Reader	Radio Astronomy & Astrophysics	Ph D, TIFR, Bombay Univ. (1986)
Singh A. D.	Reader	Atomic Physics	Ph D, IIA, Bangalore Univ. (1998)

Name	Designation	Specialisation	Academic Qualification
Singh R. P.	Scientist – SF*	Laser Physics	Ph D, JNU, New Delhi (1994)
Singh S. K.	Reader	Isotope Geochemistry	Ph D, PRL, MS Univ. (1999)
Singhvi A. K. FNA, FASc, FNASc, FTWAS	Outstanding Scientist	Palaeoclimatology and Geochronology	Ph D, IIT, Kanpur (1975)
Srivastava N.	Associate Professor*	Solar Physics	Ph D, PRL, Ravi Shankar Shukla Univ. (1994)
Subramanian K. P.	Associate Professor	Experimental Atomic and Molecular Physics	Ph D, PRL, Gujarat Univ. (1987)
Vadawale S. V.	Reader	High Energy Astrophysics and X - ray Spectroscopy	Ph D, TIFR, Mumbai Univ. (2003)
Vats H. O.	Associate Professor	Space Weather & Radio Astronomy	Ph D, PRL, Gujarat Univ. (1979)
Venkatakrishnan P.	Senior Professor	Solar Physics	Ph D, Bangalore Univ. (1984)
Yadava M. G.	Scientist-SE	Palaeoclimate, Radiocarbon dating and Stable isotopes	Ph D, PRL, DAVV Indore (2003)

* Effective from 1 July, 2009.

Technical Faculty

Name	Designation
Acharya Y. B.	Engineer-G
Adhyaru P. R.	Engineer-SE*
Dadhania M. B.	Engineer-SF*
Dholakia G. G.	Scientist-SG
Dutt N.	Engineer-SF*
Jokhakar D. H.	Engineer-SE
Modh K. S.	Engineer-SE
Narayanan R.	Scientist-SF*
Prajapati I. A.	Scientist-SE
Rao D. K.	Scientist-SE
Shah A. B.	Engineer-SF*
Shah K. J.	Scientist-SE
Shah R. R.	Engineer-SF
Singh M.	Engineer-SF
Ubale G. P.	Engineer-SE
Venkataramani S.	Scientist-SE

* Effective from 1 July, 2009.

Visiting & Honorary Faculty

Honorary & Academic Faculty

Prof. R. K. Varma, FNA, FASc, FNASc

Prof. S. Krishnaswami, FNA, FASc, FNASc, FTWAS
INSA Senior Scientist

Prof. R. G. Rastogi, FNA, FASc, FNASc
Visiting Professor

Prof. S. K. Bhattacharya, FASc, FNASc

Dr. S. K. Gupta, FNASc

Prof. A. C. Das

Prof. N. Bhandari, FNA, FASc, FNASc
INSA Honorary Scientist

Prof. D. P. Dewangan

Dr. S. P. Gupta

Prof. Harish Chandra

Prof. H. S. S. Sinha

Technical Faculty

R. N. Misra
(Director,CSSTEAP School)

D. V. Subhedar